

Republic of Iraq
Ministry of Higher Education and Scientific Research
University of Misan/College of Engineering
Department of Civil Engineering



Behavior of Reinforced Concrete Column Strengthening with HPFRC under Eccentric Loads

By

Hayder Lateef Naji

B.Sc. Civil Engineering, 2016

A Thesis

Submitted in Partial Fulfillment of the

Requirements for the Degree of

Master of Science/Master of Structural Engineering

(in Civil Engineering)

March 2025

Supervisor: Prof. Dr. Abdulkhaliq Abdulyimah Jaafer

بِسْمِ اللَّهِ الرَّحْمَنِ الرَّحِيمِ

﴿إِنَّ هَذَا كَانَ لَكُمْ جَزَاءً وَكَانَ سَعْيُكُمْ

مَشْكُورًا﴾ (22)

صدق الله العلي العظيم

Abstract

The strengthening and rehabilitation of present structures are increasingly important for construction operations. Various strengthening and rehabilitation approaches are used to enhance column strength under various loading conditions, such as eccentric loads. In the last decade, a new method used to strengthen RC structural components is high-performance fiber-reinforced concrete (HPFRC). Despite the large number of conducted studies, most of them did not consider the application of HPFRC as a jacketing material. This study aimed to investigate the effectiveness of strengthening square RC columns by applying HPFRC as a jacketing material under eccentric loaded. Especially, when there is a honeycomb as a damage in the ends of the column body. For this purpose, the experimental work included the fabrication of thirty column specimens cast from normal strength concrete (NSC) and divided into seven groups based on the honeycomb defect ratio. The cross-section area of the unstrengthening specimens was (120x120 mm) with a total height of 950 mm. Each column had two corbel heads at the ends to accommodate eccentric loads during the test. Concrete cover conducted with 15 mm for all column sides. All the column specimens have similar longitudinal and transverse reinforcement details to conduct this experimental program. The parameters of this investigation were the eccentricity (50 or 100 mm), strengthening jacket thickness (15 or 30 mm), strengthening side (full cast or laminates), and the honeycomb defect ratio (35% or 70%) of the cross-section; all of these were considered. In this research study, the honeycomb was configured in a column specimen as a ratio of the cross-section (35% and 70%) of the specimen's gross area at a constant length ($L_e/4$), represented by using foam slices 30 mm thick, divided by a sharp tool according to the required dimensions

and weak strength concrete. The effects of these parameters on load-carrying capacity, load displacement, ductility, stiffness, and toughness behaviors of the columns were studied. The research results indicated that HPFRC is a reliable strengthening method to enhance the strength, stiffness, ductility, and toughness of reinforced concrete columns subjected to eccentric loads. The increase in axial load capacity and stiffness is directly related to the thickness of the HPFRC jacket and inversely related to the eccentricity ratio. Specifically, the full casting strategy of the HPFRC jacket proved to be more effective than the laminate. Moreover, the gain in strength ranged from (73.04% to 152.17%) for the columns strengthened with 2-sides and ranged from (156.2% to 173.91%) for the columns strengthened with 4-sides.

Supervisor Certification

We certify that the preparation of this thesis entitled " **Behavior of Reinforced Concrete Columns Strengthening with High Performance Fiber Reinforced Concrete under Eccentric Loads** " was presented by "**Hayder Lateef Naji**", and prepared under my supervision at The University of Misan, Department of Civil Engineering, College of Engineering, as a partial fulfillment of the requirements for the degree of Master of Science in Civil Engineering (Structural Engineering).

Signature:

Prof. Dr. Abdulkhaliq Abdulyimah Jaafer

Date:

In view of the available recommendations, I forward this thesis for discussion by the examining committee.

Signature:

Assist Prof. Dr. Murtada Abass Abd Ali

(Head of Civil Eng. Department)

Date:

Examining Committee's Report

We certify that we, the examining committee, have read the thesis titled **(Behavior of Reinforced Concrete Columns Strengthening with HPFRC under Eccentric Loads)** which is being submitted by **(Hayder Lateef Naji)**, and examined the student in its content and in what is concerned with it, and that in our opinion, it meets the standard of a thesis for the degree of Master of Science in Civil Engineering (Structures).

Signature:

Name: Prof. Dr. Abdulkhaliq Abdulyimah Jaafar
(Supervisor)

Date: / /2025

Signature:

Name: Prof. Dr. Mohammed Salih Abd-Ali
(Chairman)

Date: / /2025

Signature:

Name: Prof. Dr. Murtada Abass Abd Ali
(Member)

Date: / /2025

Approval of the College of Engineering:

Signature:

Name: Prof. Dr. Abbas Oda Dawood
Dean, College of Engineering

Date: / /2025

Signature:

Name: Asst. Prof. Dr. Samir Mohammed
Chassib

(Member)

Date: / /2025

Dedication

The deepest words of gratitude and appreciation are the gratitude and dedication of a great person. If you are where I am today, then that is why it deserves a special mention that it is my father. I will not forget to devote the fruits of this effort to those who filled me with supplication, and what I am today God's response to her prayers for me. She is my mother.

I would like to apply My sincere appreciation to my wife. I feel very lucky that they have been in my life.

Sincerity to my family and friends goes for their love, support, guidance, and endless patience in all my endeavors.

Hayder Lateef Naji

Acknowledgements

First of all, all my thanks to Allah, who led me on my way to complete this work.

I would like to express my cordial thanks and deepest gratitude to my supervisor, **Prof. Dr. Abdulkhaliq A. Jaafar**, under whose supervision I had the honor of being, for his advice, help, and encouragement during the course of this study.

I would like to extend my thanks to **Prof. Dr. Abbas Oda Dawood**, Dean of the College of Engineering, and **Prof. Dr. Murtada Abass Abd Ali**, Head of the Civil Engineering Department.

I would like to express my deepest feeling of My family (Russull, Al hur and Rahiq), My brother and My Parents for their care, patience and great support during the research period.

Hayder Lateef Naji

Table of Contents

Abstract.....	i
Supervisor Certification.....	iii
Examining Committee's Report.....	iv
Dedication.....	v
Acknowledgements.....	vi
Table of Contents.....	vii
List of Tables	xii
List of Figures.....	xiv
List of Symbols.....	xix
List of Abbreviations	xx
CHAPTER One: INTRODUCTION	1
1.1 General.....	1
1.2 Definition of Column	2
1.2.1 Failure Mode of Columns	2
1.3 Techniques for Strengthening RC Columns.....	3
1.4 Ultra-High Performance Fiber Reinforced Concrete (HPFRC).....	9
1.4.1 Definition of HPFRC	9
1.4.2 HPFRC Materials.....	10
1.5 Honeycomb in concrete.....	12
1.6 Aim of Study	14
1.7 Study Objectives.....	14

1.8 Thesis Layout	15
CHAPTER Two: Literature Review	16
2.1 Introduction:	16
2.2 Studies on the Behavior of RC Column Strengthening with HPFRC under Different Loading Cases:	16
2.3 Studies on the behavior of RC Column Strengthening with FRP:.....	35
CHAPTER Three: Experimental Program.....	41
3.1 General.....	41
3.2 Overall description of RC column specimens.....	41
3.3 The Experimental Parameters	42
3.4 Material Properties	42
3.4.1 Cement	42
3.4.2 Fine Aggregate (Sand)	44
3.4.3 Quartz Sand.....	45
3.4.4 Coarse Aggregate (Gravel)	46
3.4.5 Silica Fume	47
3.4.6 Micro Steel Fiber	48
3.4.7 Superplasticizer.....	49
3.4.8 Mixing Water	51
3.4.9 Reinforcement Steel Bar	51
3.4.10 Foam	52
3.4.11 Carbon Fiber Reinforced Polymer (CFRP)	53
3.4.12 Epoxy Resin (Sikadure LB32).....	54

3.4.13 Epoxy Resin (Sikadur-330)	54
3.5 Fabrication of Column Specimens	55
3.5.1 Geometry of Column Specimens.....	55
3.5.2 Labeling of Column Specimens.....	57
3.5.3 Design of the formwork.....	61
3.5.4 Honeycomb Formation Method in Column Specimens	62
3.5.5 Mix Proportion and Placement of NSC	63
3.5.6 Demolding and Curing Process of the Specimens.....	64
3.5.7 Mix Proportion and Process of HPFRC.....	65
3.6 Properties of NSC and HPFRC	66
3.7 Strengthening of Column Specimens with HPFRC Jacketing and CFRP Wrapping.....	71
3.7.1 Strengthening with HPFRC Jacketing	71
3.7.2 Strengthening with CFRP Wrapping	73
3.8 Painting the specimens after jacketing with HPFRC	74
3.9 Equipment and Instruments Used for Testing.....	74
3.9.1 Data logger series.....	74
3.9.2 Deflection Measurement (LVDT)	75
3.9.3 Strain Gauge.....	76
3.9.4 Loading Head.....	78
3.10 Column Specimens Testing Procedure	78
CHAPTER Four: Result and Discussion	79
4.1 General.....	79

4.2 Experimental Results.....	80
4.2.1 Mode of Failure and Load-Displacement Relation	81
4.3 Discussion of Experimental Results.....	94
4.3.1 Load-Displacement Relationships	94
4.3.2 Axial Load Capacity	94
4.3.3 Ductility Index	97
4.3.4 Stiffness.....	101
4.3.5 Toughness	105
4.3.6 Effect of Side Numbers of Strengthening and Jacket Thickness on Load Carrying Capacity of RC Columns	108
4.3.7 Effect of CFRP on Load Carrying Capacity of RC Columns	110
Chapter Five: Conclusions & Recommendations	109
5.1 Summary.....	109
5.2 Conclusion.....	109
5.3 Recommendation.....	111
Appendices	112
Appendix A.....	112
Material Properties	112
A.1. Data Sheet of Quartz Sand	112
A.2. Data Sheet of Silica Fume	123
A.3. Data Sheet of Superplasticizer.....	125
A.4. Data Sheet of CFRP.....	127
A.5. Data Sheet of Sikadur®-32 LP	131

A.6. Data Sheet of Sikadur®-330.....	135
References.....	104

List of Tables

Table 2.1 Test Matrix.	20
Table 2.2 Details of Column Specimens.	24
Table 2.3 Column Specimen's Detail.	32
Table 3.1 Experimental Parameters.....	42
Table 3.2 Chemical analysis of cement.....	43
Table 3.3 Physical properties of cement.....	44
Table 3.4 Classification of fine aggregate.....	45
Table 3.5 Physical and chemical properties of fine aggregate.	45
Table 3.6 Classification of Coarse Aggregate.....	47
Table 3.7 Chemical and Physical Properties of Silica Fume.	48
Table 3.8 Micro Steel Fiber Properties.....	49
Table 3.9 Visco Crete -180GS Technical Data.	50
Table 3.10 Steel Reinforcement Testing Results	52
Table 3.11 Technical Properties of Synthetic Cork.	52
Table 3.12 CFRP Properties.	53
Table 3.13 Details of Sikadur ® - 330 Resins Properties.	55
Table 3.14 Details of the column specimens.....	59
Table 3.15 Mix Proportion (Kg/m ³).	63
Table 3.16 Mix Proportions of HPFRC (Kg/m ³).....	65
Table 3.17 Mechanical Properties of Test Results.	69
Table 4.1 The experimental results of specimens.	80

Table 4.2 Ductility index of column specimens.....	98
Table 4.3 Stiffness of column specimens.....	102

List of Figures

Figure 1.1 Mode Failure of Columns. [6].....	3
Figure 1.2 Details of Steel Jacketing Technique.[8]	4
Figure 1.3 Details of Reinforced Concrete Jacketing Technique.[9]	5
Figure 1.4 Details of Partially Ferro-cement Jacketing Technique.[10]	6
Figure 1.5 Details of CFRP Jackets Technique.[12]	7
Figure 1.6 Details of HPFRC Jacketing technique.[13]	8
Figure 1.7 Honeycomb in Columns.....	13
Figure 1.8 Thesis Layout.	15
Figure 2.1 Specimen Details.[32]	17
Figure 2.2 Details of The Original and Strengthened.[33].....	18
Figure 2.3 Details of Specimens.[34]	19
Figure 2.4 Cross-sections of The Specimens:	22
Figure 2.5 Geometry and Reinforcement Details of Columns.[38]	23
Figure 2.6 Details of Tested Columns.[40]	25
Figure 2.7 Details of Specimens.[41]	26
Figure 2.8 Geometry and Rebar Arrangement (unit: mm).[44]	28
Figure 2.9 Strengthening Schemes for Test Specimens.[46]	30
Figure 2.10 Schematic for Structural Work.[48].....	31
Figure 2.11 Geometry of Column Specimens.[50]	34
Figure 2.12 Details of Specimens.[51]	35
Figure 2.13 Geometry of Column Specimens.	38

Figure 3.1 Cement.[56].....	43
Figure 3.2 Sand Utilized.....	44
Figure 3.3 Quartz Sand.....	46
Figure 3.4 Coarse Aggregate.....	46
Figure 3.5 Silica Fume.....	48
Figure 3.6 Golden-colored steel fiber.....	49
Figure 3.7 Visco Crete -180GS.	50
Figure 3.8 Main Rebar Tension Test.....	51
Figure 3.9 Synthetic cork.[63].....	52
Figure 3.10 CFRP Sheet.....	53
Figure 3.11 Sikadure LB32 Bonding Material.....	54
Figure 3.12 Mixing Two Components of Epoxy Resin.	55
Figure 3.13 The Geometry and Reinforcement Details of The Column in (cm).	56
Figure 3.14 The Reinforcement Details of Specimens.....	57
Figure 3.15 Symbol Detail's Designation.	58
Figure 3.16 Schematic Plan of Column specimen	60
Figure 3.17 Integrated Formwork Plan (all units in millimeters).	61
Figure 3.18 The Constructed Formwork.....	61
Figure 3.19 Honeycomb Zone Formation of Specimens.	62
Figure 3.20 Concrete Casting into Sample molds.....	64
Figure 3.21 Pouring and Compacting Process of Concrete.	64
Figure 3.22 Demolding and Curing Process of Specimens.....	65

Figure 3.23 HPFRC Mixing Time Process.....	66
Figure 3.24 The Compressive Strength Test.	70
Figure 3.25 Splitting Tensile Strength.....	70
Figure 3.26 The Modulus of Rupture Test.	70
Figure 3.27 HPFRC Strengthening Process.	71
Figure 3.28 Curing of HPFRC Jacketing Specimens.	72
Figure 3.29 CFRP Wrapping Process.....	73
Figure 3.30 Painted Column Specimens.	74
Figure 3.31 Data Logger.....	75
Figure 3.32 Instrument for Deflection Measurement.	75
Figure 3.33 Installation of LDVT.....	76
Figure 3.34 Strain Gauge.....	76
Figure 3.35 Strain Gauge.....	77
Figure 3.36 Steps of Installation Strain Gauge.....	77
Figure 3.37 Steps of installation of Strain gage	77
Figure 3.38 Constructed Loading Head.....	78
Figure 3.39 Setup of Typical Tested Specimens	79
Figure 4.1 Mode Failure and Cracks Pattern for Group a References columns.	82
Figure 4.2 Load-Displacement Curve for Group a References columns.	83
Figure 4.3 Load-Displacement Curve for Group b 0% Defect Ratio.....	84
Figure 4.4 Mode Failure and Cracks Pattern for Group b 0% Defect Ratio.	85

Figure 4.5 Mode Failure and Cracks Pattern for Group c 35% Defect Ratio Foam.....	86
Figure 4.6 Load-Displacement Curve for Group c 35% Defect Ratio.....	86
Figure 4.7 Mode Failure and Cracks Pattern for Group d 70% Defect Ratio Foam.....	88
Figure 4.8 Load-Displacement Curve for Group d 70% Defect Ratio.....	88
Figure 4.9 Mode Failure and Cracks Pattern for Group e 70% Defect Ratio Foam.....	89
Figure 4.10 Load-Displacement Curve for Group e 70% Defect Ratio.....	90
Figure 4.11 Load-Displacement Curve for Group f 70% Defect Ratio.	91
Figure 4.12 Mode Failure and Cracks Pattern for Group f 70% Defect Ratio WSC.	92
Figure 4.13 Mode Failure and Cracks Pattern for Group g 70% Defect Ratio.....	93
Figure 4.14 Load-Displacement Curve for Group g 70% Defect Ratio.....	93
Figure 4.15 Gaining in Strength for group e.	96
Figure 4.16 Gaining in Strength for group d.	96
Figure 4.17 Gaining in Strength for group b.	96
Figure 4.18 Gaining in Strength for group c.	96
Figure 4.19 Gaining in Strength for group f.....	96
Figure 4.20 Gaining in Strength for group g.	96
Figure 4.21 Determination Procedures of Column Ductility Displacement.....	97
Figure 4.22 Gaining in Ductility for Group b.	99
Figure 4.23 Gaining in Ductility for Group c.....	99
Figure 4.24 Gaining in Ductility for Group d.	99

Figure 4.25 Gaining in Ductility for Group e.....	100
Figure 4.26 Gaining in Ductility for Group g.	100
Figure 4.27 Gaining in Ductility for Group f.	100
Figure 4.28 Gaining in stiffness for group b.	103
Figure 4.29 Gaining in Stiffness for Group c.....	103
Figure 4.30 Gaining in Stiffness for Group d.....	103
Figure 4.31 Gaining in Stiffness for Group e.	104
Figure 4.32 Gaining in Stiffness for Group f.	104
Figure 4.33 Gaining in Stiffness for Group g.....	104
Figure 4.34 Toughness Factor for Group b.	106
Figure 4.35 Toughness Factor for Group c.	107
Figure 4.36 Toughness Factor for Group d.	107
Figure 4.37 Toughness Factor for Group e.	107
Figure 4.38 Toughness Factor for Group f.....	108
Figure 4.39 Toughness Factor for Group g.	108
Figure 4.40 Effect of Strengthening face and Jacket Thickness on Load capacity.	109

List of Symbols

TF	Toughness Factor
f'_c	Cylinder concrete compressive strength in MPa
f_{cu}	Cube Compressive Strength in MPa
\emptyset	Diameter of Reinforcement mm
ϵ_c	Concrete Strain
E_c	Concrete modulus of elasticity, GPa
DI	Ductility Index
f_r	Modulus of Rupture in MPa
f_t	Tensile Strength in MPa
f_y	Yield Strength in MPa
Δ_y	Yield Deflection in mm
Δ_u	Ultimate Deflection in mm

List of Abbreviations

ACI	American Concrete Institute
ASTM	American Society of Testing and Material
EC	Euro Code
R.C	Reinforcement Concrete
Rb	Traditional Rebar
Rs	Rectangular section
CFRP	Carbon fiber reinforced polymer
UHPFRC	Ultra High-Performance Fiber Reinforced Concrete
HPFRC	High-Performance Fiber Reinforced Concrete
UHPC	Ultra High-Performance Concrete
RPC	Reactive Powder Concrete
UHPFRSCC	Ultra High-Performance Fiber Reinforced Self Compacting Concrete
DSP	Defined with Small Particles
MDF	Macro-Defect Free Pastes
HSC	High Strength Concrete
ECC	Engineering Concrete Cementitious

HSC	High Strength Concrete
NSC	Normal strength concrete
WSC	Weak strength concrete
IQS	Iraqi Standard
W/C	Water- cement ratio
V _f	Fiber Volume Fraction
FE	Finite Element

CHAPTER ONE: INTRODUCTION

1.1 General

Recently, there has been a growing focus on researching the strengthening of concrete structures through various approaches. Several research investigations have provided evidence that structural concrete elements, such as RC columns, may experience substantial enhancements in their ability to bear loads and flexibility when enhanced with a concrete jacket. Although many studies have been conducted, most of them have not taken into account the use of HPFRC as a jacketing material. Strengthening concrete members is an essential objective for civil engineers and much research has been committed to understanding the behavior of structures under various loading conditions and disasters. The reinforced concrete columns are important elements in the reinforced concrete structures, which provide bracing against the horizontal loads and support the vertical loads with or without moments. The damage to RC columns is perhaps caused by poor construction practices and quality control, overloading, corrosion, fire damage, foundation settlement, inadequate maintenance, and surface deterioration. Honeycombing is a frequent issue in concrete when there are voids or gaps in the structure. These voids can penetrate deep into the concrete. The restoration procedures must address the depth and extent of the damage, ensuring that it is eliminated or hidden, depending on its severity. The occurrence of concrete degradation, particularly honeycombing, is a significant issue that requires careful attention [1-3].

The terms restoration, repairing, and strengthening have been defined below to provide precise distinctions among them:

- 1- **Restoration:** The process of enhancing structures that are damaged to make them useful once again.
- 2- **Repairing:** The process of returning the structural performance of damaged structures to their original condition.
- 3- **Strengthening:** The process that involves enhancing the structural performance of compromised structures beyond their initial capacities. [4]

1.2 Definition of Column

A column is a critical component in reinforced concrete buildings, offering resistance to horizontal loads and supporting vertical loads with or without moments, responsible for transferring the load from the superstructure to the foundation in a secure manner.

1.2.1 Failure Mode of Columns

Columns may fail in one of the following mechanisms, as shown in Fig. (1.1):

- 1- **Crushing:** This is the most common failure mode for columns. It occurs when the column is loaded with a compressive force that exceeds its load-carrying capacity, causing it to buckle or crush.
- 2- **Buckling:** Buckling happens when a column is subjected to an axial compressive load, causing it to bend or deform laterally. This can lead to sudden and catastrophic failure.
- 3- **Combination of buckling and crushing:** Columns can also fail due to a combination of different loading conditions, such as axial compression, bending, and shear acting simultaneously, leading to complex failure modes.

- 4- Shear Failure: Shear failure can occur in short columns when they are subjected to lateral forces that exceed their shear capacity, causing them to fail along a diagonal plane.[5]

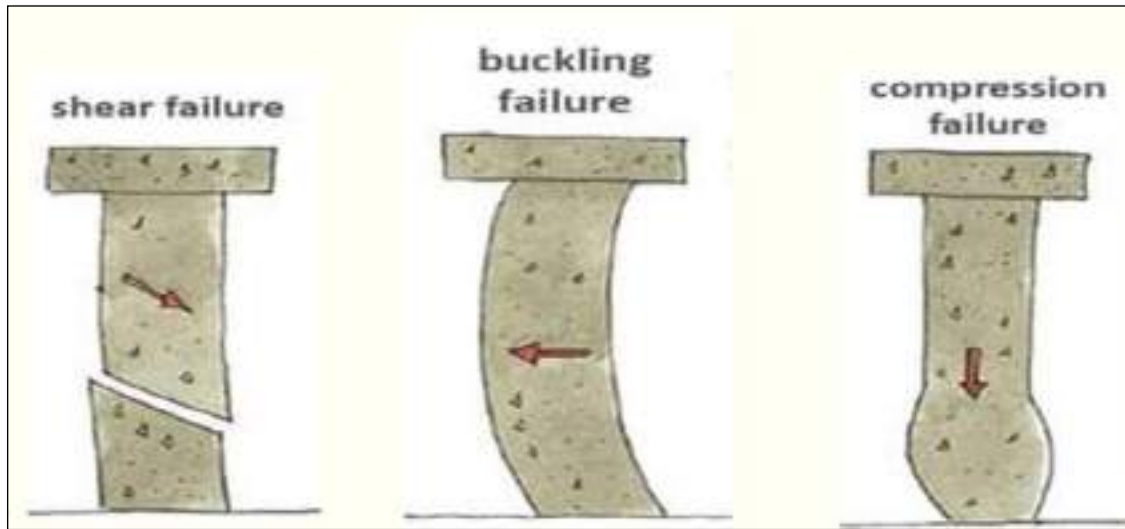


Figure 1.1 Mode Failure of Columns. [6]

1

1.3 Techniques for Strengthening RC Columns

The failure of reinforced concrete (RC) facilities has become more common during the last twenty years, in part due to increasing loads and durability challenges. Structural parts may need repair or strengthening due to both chemical and physical forces. Cracks resulting from dynamic loads, impact loads, inadequate maintenance, creep, non-standard design, deterioration of steel reinforcement, and inadequate quality control contribute to the degradation of reinforced concrete frameworks. Structure kinds and loading configurations influence methods of strengthening. For buildings primarily exposed to static loads, enhancing axial and flexural strength should be prioritized, while for those mostly subjected to dynamic loads, augmenting shear and flexural strength is more important. The following is

an outline of different strengthening and retrofitting approaches for reinforced concrete columns carried out in recent years:[7]

1- Steel Jackets Technique

Steel-jacketed concrete columns are the oldest way of strengthening them. Strengthening non-ductile columns with steel jackets is common. Increase column strength using steel jackets, plates, external ties, partial jackets, complete jackets, and varied steel forms. The basic structure includes longitudinal steel angles or channel sections at each column corner and horizontal steel sheets welded at suitable intervals. Filling the area between the steel jacket and the column with a specific mortar improves system performance. Add reinforcement to transmit stress between the mortar layer and the column. Fig. (1.2) illustrates a control RC column with angle, channel, and plate steel jackets. Steel jacketing strengthens undamaged, non-ductile columns. Partial steel jacketing with steel ties is suitable for columns with improper strap arrangement. Steel jacketing also reduces construction time, costs, and column dimensions. Steel jackets may significantly deteriorate in corrosive conditions and fire, resulting in an unsightly look, particularly with large steel dimensions. In instances of incomplete steel jacketing, the enhancement just increases shear strength [8].



Figure 1.2 Details of Steel Jacketing Technique.[8]

2- Reinforced Concrete Jacket Technique

A reinforced concrete jacket is extensively used to repair severely damaged columns. Around the damaged column, an additional reinforced concrete layer, including a reinforcing steel cage and an alternative concrete substance, is applied. Adhesive materials or anchoring bolts enhance the connection between the column and the additional layers; Fig. (1.3) illustrates the specifics of concrete jacketing types of jackets. Concrete jacketing improves the seismic performance of the column by increasing its axial load-bearing capacity, flexural strength, and ductility. It further increases the rigidity of the building practices. Concrete jackets increase column section dimensions, add extra weight, need expert labor and quality control, involve higher costs, and creation takes time [9].

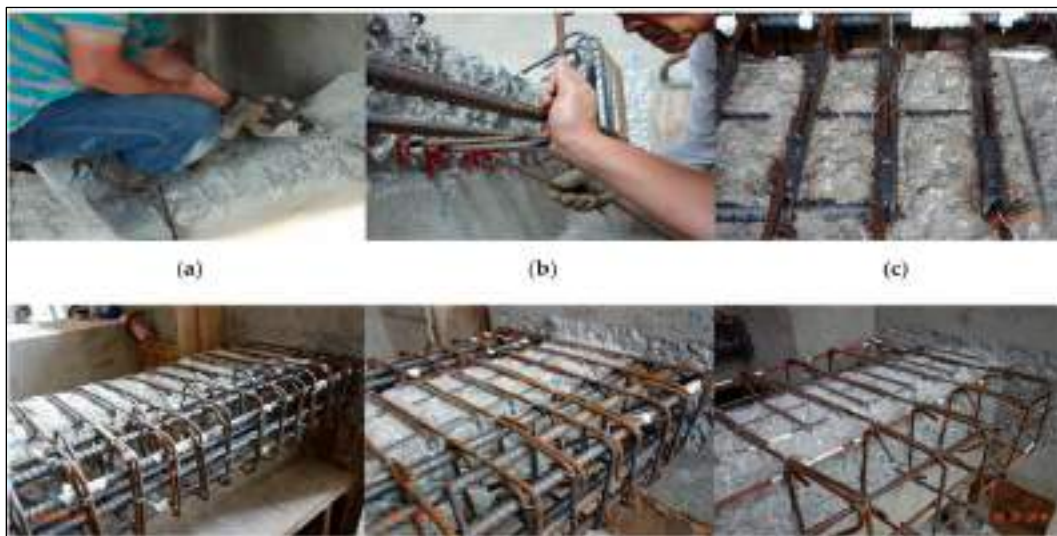


Figure 1.3 Details of Reinforced Concrete Jacketing Technique.[9]

3- Ferro Cement Jacket Technique

The process of Ferro-cement jackets is an efficient rehabilitation method for reinforced concrete columns. The ferro-cement jacketing system includes a thin reinforced mortar wall, constructed from cement-sand mortar, with one or several layers of wove or welded wire mesh as shown in Fig. (1.4). It offers a cost-

effective option for improving reinforced concrete columns in comparison to costlier methods such as steel jacketing and concrete jacketing. Ferro-cement jacketing is simple and requires few qualified people. Ferro-cement confinement enhances ultimate load capacity, impact resistance, seismic vibration resistance, fire and corrosion resistance, and maintenance cost. However, ferro-cement jacketing enlarges columns and adds weight [10].

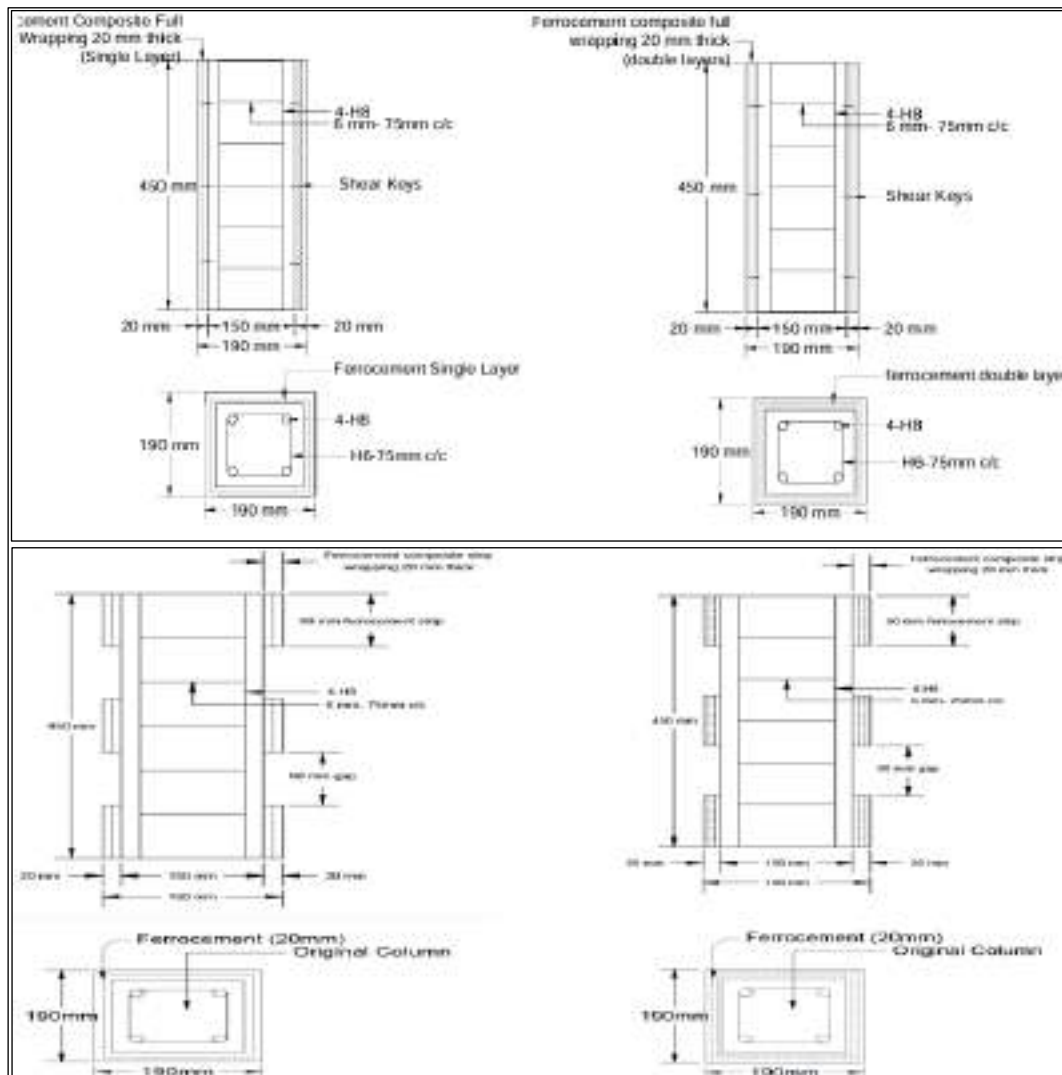


Figure 1.4 Details of Partially Ferro-cement Jacketing Technique.[10]

4- CFRP Jackets Technique

Since the 1960s, carbon fiber has been used for strengthening and restoring structural components, replacing conventional techniques that depend on increasing cross-sectional dimensions. Carbon Fiber-reinforced polymer (CFRP) is a lightweight composite composed of carbon fibers and a polymer matrix, as shown in Fig. (1.5). The installation of CFRP typically uses epoxy or polyurethane resins. Epoxy resin penetrates carbon fibers and adheres the composite wrap to the structural component. A significant use of CFRP sheets is the strengthening of concrete columns by jacketing with CFRP wrapping. CFRP wrapping is a lightweight substance that could be simply erected on-site without difficult issues. They also lack corrosion issues, unlike steel jacketing, and exhibit outstanding resistance to chemical attack. They defend against fire. Carbon fiber reinforced polymer jackets are expensive [11].



Figure 1.5 Details of CFRP Jackets Technique.[12]

5- HPFRC Jackets Technique

HPFRC is a fiber-reinforced cementitious material composed of cement, quartz powder, silica fume, and steel fibers, exhibiting significantly superior compressive, tensile, and flexural strength, as well as enhanced ductility compared to conventional concrete. In recent years, efforts have enhanced the properties of cementitious materials by the use of fibers, resulting in the emergence of Ultra-High Performance Fiber Reinforced Concrete (HPFRC). This kind of technique was used to improve the strength of reinforced concrete buildings. Many investigations have shown improvements in the mechanical characteristics of HPFRC and its efficiency in the strengthening process as shown in Fig. (1.6). Owing to the increased fluidity of HPFRC, the jacket thickness may be lowered to below 30-50 mm, so reducing the primary drawback of the conventional concrete jacketing technique. Additional benefits of HPFRC strengthening include exceptional durability, versatile adaptability in many situations, and compatibility with other materials like wire mesh, textile mesh, and CFRP to enhance performance [13].



Figure 1.6 Details of HPFRC Jacketing technique.[13]

1.4 Ultra-High Performance Fiber Reinforced Concrete (HPFRC)

1.4.1 Definition of HPFRC

HPFRC is a cementitious composite material containing steel fibers as reinforcement, substituting traditional reinforcement rebar [14]. HPFRC is an efficient material for strengthening because of its exceptional mechanical qualities. Moreover, HPFRC has exceptional durability, ductility, and workability; low permeability; and strong resistance to abrasion and fire. For these reasons, HPFRC has shown to be an efficient material for structural strengthening. The enhanced properties of HPFRC are achieved by minimizing the amount of water present in the concrete mixing (resulting in fewer air pores), incorporating high-strength ductile steel fibers, substituting coarse aggregates with well-graded fine aggregates, and integrating highly reactive pozzolanic materials. HPFRC exhibits superior adhesion to normal-strength concrete, thus resolving the debonding problem prevalent in alternative retrofitting methods that use fiber-reinforced polymers or externally attached steel plates. Consequently, HPFRC-based structural retrofitting offers many benefits when different elements are considered. Structural strengthening using HPFRC is an efficient method of improving the stiffness and load-bearing capability of reinforced concrete components while reducing a change in member dimensions. Consequently, the HPFRC approach has been used in a diverse range of concrete buildings globally [15]. The preliminary development of HPFRC started in the 1970s via the examination of high-strength cement pastes with reduced water/cement ratios. These pastes were enhanced with fibers, superplasticizers, and pozzolanic admixtures, facilitating the development of HPFRC [16].

HPFRC is a composite of high-performance concrete and fiber reinforcement. The constituents of HPFRC typically include cement, silica fume,

sand, superplasticizer, water, and high-strength steel fibers. These substances exhibit a compact microstructure [17-19].

1.4.2 HPFRC Materials

HPFRC is composed of cement, quartz sand, silica fume, water, superplasticizer, and micro steel fiber.

1.4.2.1 Cement

HPFRC is composed of A significantly higher amount of cement has been utilized ($\geq 700 \text{ kg/m}^3$), which is twice that of conventional concrete strength. Moreover, it has an average diameter of around $15 \mu\text{m}$ [20].

1.4.2.2 Quartz Sand

Fine sand typically ranges from 150 to 600 micrometers (μm) and is the biggest granular substance dimensionally. Fine sand constitutes the biggest particle in the matrix due to the absence of coarse aggregate in the mixture. It may originate from crushed sand that is screened, classified as manufactured sand, or from natural quarry sand. In the HPFRC, particle size has been limited to a maximum of $600 \mu\text{m}$ and a minimum of $150 \mu\text{m}$ [21].

1.4.2.3 Silica Fume

Silica fume is an excessively fine, spherical powder used as an additive to enhance concrete performance; it is a potent pozzolanic substance employed to enhance the qualities of concrete [22]. According to ASTM 1240, it is defined as a highly refined pozzolanic substance, mostly consisting of amorphous silica generated by electric arc furnaces as a by-product in the manufacture of elemental silicon or ferrosilicon alloys [23].

1.4.2.4 Superplasticizer

It is essential for processing the workability of HPFRC with low water content. Superplasticizers, or high-range water reducers, are admixtures that provide significant water reduction or enhanced flowability without delaying set time or increasing air entrainment [24]. There is no definitive way to determine the necessary dose of superplasticizer. It must be ascertained by a procedure of trial and error. Several tests were conducted to ascertain the necessary dose of superplasticizer.

1.4.2.5 Water

Water is the most essential and least costly component of concrete. A portion of the water used is for the hydration of cement, which has solidified to provide the binding matrix. The quality of hardened concrete is significantly affected by the water-to-cement ratio; increased water content weakens the cement paste [25].

1.4.2.6 Micro Steel Fibers

Steel fibers are the largest component of HPFRC, with a nominal diameter of 0.2 mm and a nominal length of 12.7 mm. The purpose of these fibers in HPFRC necessitates that they possess exceptional tensile strength to minimize cracks. Nevertheless, if the fiber volume fraction (V_f) surpasses 2%, attaining a sufficient degree of workability for placement and compaction becomes challenging [21].

1.4.3 Historical Background of HPFRC Development

In recent years, multiple efforts have enhanced the properties of cementitious materials through the use of fibers, resulting in the development of HPFRC. The initial development of HPFRC started in the 1970s via the examination of high-strength cement pastes that had lower water-to-cement ratios. These pastes were enhanced with fibers, superplasticizers, and pozzolanic admixtures, facilitating the

development of HPFRC. A cement pastes with a compressive strength of approximately 240 MPa was obtained after 180 days by providing special treatment to the ground clinker by using a low W/C of 0.2 [22]. Alternatively, it obtained a cement paste with near-zero porosity and a compressive strength of about 510 MPa by applying heat curing with a pressure of 50 MPa [23].

In the early 1980s, with the development of pozzolanic admixtures and high-range water-reducing agents such as superplasticizers, two different types of ultra-high-strength and low porous concretes were developed (densified with small particles (DSP) concrete and macro-defect free (MDF) pastes) [17-18]. Finally, in the mid-1990s, reactive powder concrete (RPC), which is the forerunner of the HPFRC that is currently available, was developed and exhibited compressive strengths ranging from 200 to 800 MPa and fracture energies up to 40 kJ/m² [19].

1.5 Honeycomb in concrete

Honeycombs in concrete refer to voids or gaps that appear within the concrete structure after it has hardened. These voids resemble a honeycomb pattern and are a result of improper compaction or other issues during the pouring and curing process, as shown in Fig. (1.7). Honeycombs are created by air gaps that get trapped around coarse aggregates during the concreting process. These may develop inside the concrete buildings and on the outside surface additionally [27]. Surface honeycombs influence aesthetics and are readily recoverable, however, interior honeycombs could decrease load-carrying capability and impact the permeability of the components. Detecting honeycombs remains challenging due to their diverse sizes, shapes, and placements [28].



Figure 1.7 Honeycomb in Columns.

In reinforced concrete structures, damage may result from cracking, surface degradation, deposits, deformation, and construction errors or characteristics. Substantial efforts have been made to identify the locations of flaws in reinforced concrete buildings using one or several modal features [29]. Honeycombing is one of the most common defects in concrete. It is classified as a construction defect. While many popular in-situ testing methods exist for identifying honeycombs in concrete, including hammer testing, shaker testing, and ultrasonic pulse velocity testing, research on honeycombing damage remains limited [30].

Honeycomb is a significant issue in concrete that requires careful attention. Otherwise, the structure or component may compromise its structural strength. The causes for honeycombing in concrete are as follows [24]:

1. Inappropriate workability of concrete.
2. Use of stiff concrete mix or the concrete is already set before placing.

3. Improper vibration of concrete in formwork.
4. Over-reinforcement.
5. Use of larger size aggregates in excessive amounts.
6. Formwork is not rigid and watertight.
7. Concrete is poured from more than the allowable height.
8. Congestion of steel is preventing the concrete from flowing over all corners.
9. Lack of quality control by workers during the casting stage.

1.6 Aim of Study

Experimental research is used in this work to investigate the performance of rehabilitated honeycombed RC columns and the carrying capacity of these samples. The honeycomb was damaged with different locations and volumes. Thirty RC column specimens have been considered in the experimental tests. The behavior of RC columns was studied in the experimental tests and subjected to different axial compressive loads up to failure. The behavior of these RC columns will be measured by presenting and discussing the load-displacement for lateral and axial displacement along with modes of failure, load of first crack, and load of failure patterns.

1.7 Study Objectives

The main purpose of this work is to scientifically investigate the structural response of reinforced concrete (RC) columns damaged with honeycomb and strengthened with high performance fiber reinforced concrete (HPFRC) under eccentric loadings.

1.8 Thesis Layout

The research study included five chapters, as shown in Fig. (1.8).

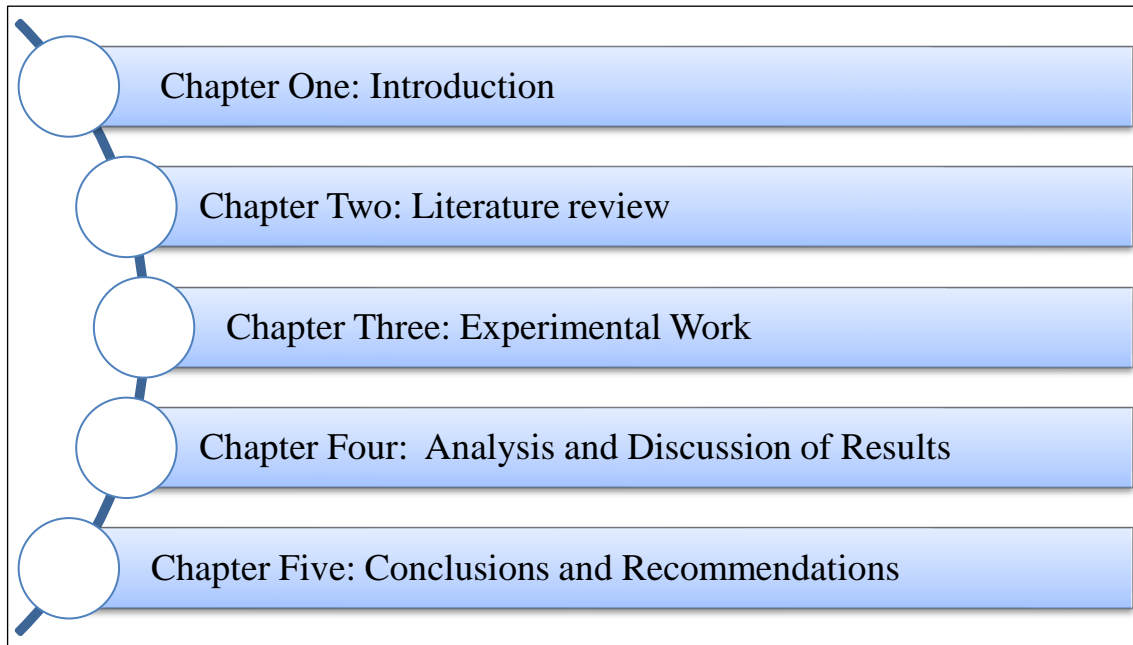


Figure 1.8 Thesis Layout.

CHAPTER TWO: LITERATURE REVIEW

2.1 Introduction:

Due to the columns are the most important structural members of the buildings. Because of the responsibility for transferring the loads to the foundations. Thus, any failure in a column with a critical location causes a failure in that location and all the adjacent structural parts and may cause a complete collapse of the structure. Strengthening and rehabilitation of existing structures are becoming the main parts of the construction activities. This chapter focused on presenting the previous studies that dealt with the strengthening of RC columns using different techniques that will be covered. Then, the previous studies concerned the strengthened RC column using HPFRC and CFRP under concentric and eccentric loading.

2.2 Studies on the Behavior of RC Column Strengthening with HPFRC under Different Loading Cases:

In 2015, MARQUES et al. [32] studied the findings of eight rectangular reinforced concrete columns exposed to combined compression and bending. The purpose of the study was to assess the effectiveness of employing sleeve wedge bolts at the interface between new and old concrete to prevent detachment. The strengthening approach involves applying an outer layer of self-compacting concrete to one side of the column. To enhance the bond between the pre-existing concrete and the newly poured concrete, the concrete surface was roughened, and the outermost covering of aggregate was exposed through the process of hydro jetting. Wedge bolts were inserted into holes in the concrete surface to enhance the binding between the two concrete surfaces, as illustrated in Fig. (2.1). The

conclusions were that the use of sleeve wedge bolts can improve the bond between old and new concrete surfaces in strengthened reinforced concrete columns, and increasing their strength capacity. The number and positioning of bolts can impact the durability of reinforced columns. The column with the fewest number of bolts exhibited the greatest ultimate load. Positioning bolts internally proved to be more efficient than externally. Bolts produced good behavior of cases at all, and shear failure did not occur.

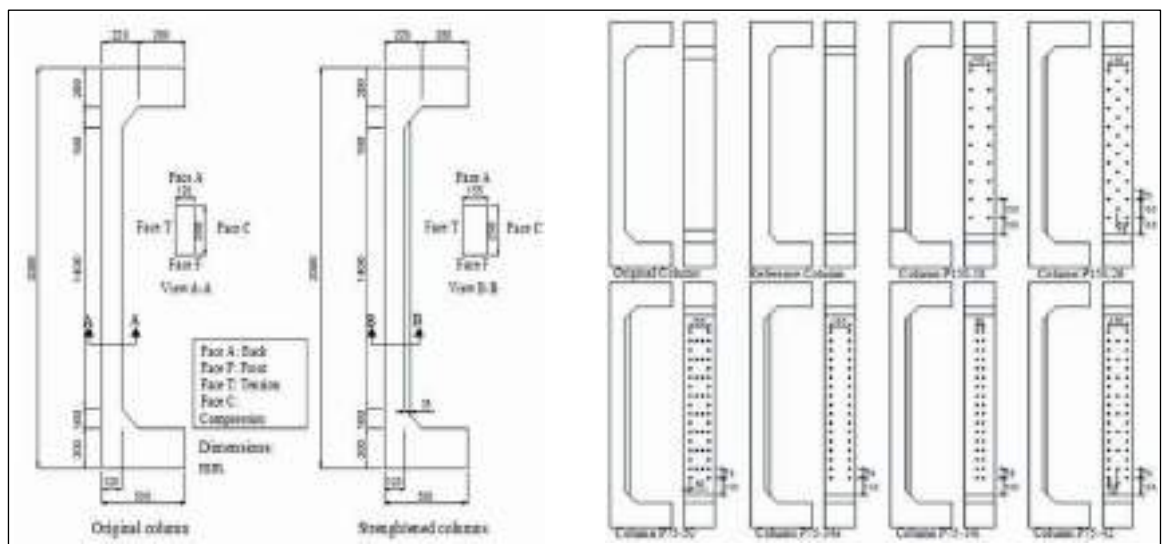


Figure 2.1 Specimen Details.[32]

In 2016, Cassese et al. [33] studied the investigation of the use of High-Performance Fiber-Reinforced Concrete (HPFRC) jacketing to strengthen existing RC columns and presented a method for calculating the capacity envelopes for axial load and bending moment using analytical calculations. To enhance the average dimensions of the current column section, the existing concrete cover can be replaced with an external jacketing made of HPFRC. Six small square reinforced concrete RC columns were fabricated that use a low-performance concrete mixture to compensate for the inadequate mechanical characteristics of the previous RC elements. Subsequently, three of them had strengthened via the

utilization of HPFRC jacketing. The columns were exposed to a combination of bending and axial load, illustrated in Fig. (2.2). The results of the experimental study showed that the HPFRC jacketing technique was an effective method for improving the attitude of RC columns with a combination of bending and axial loads. Also, the HPFRC jacket effectively postponed the initiation of structural collapse in unstrengthened columns. Also, the study proposed a method for obtaining the capacity for axial force and bending moment for RC columns strengthened using a simplified analytical technique. The suggested analytical technique serves as the basis for the retrofitting design of existing reinforced concrete RC columns utilizing high-performance fiber-reinforced concrete (HPFRC) jacketing.

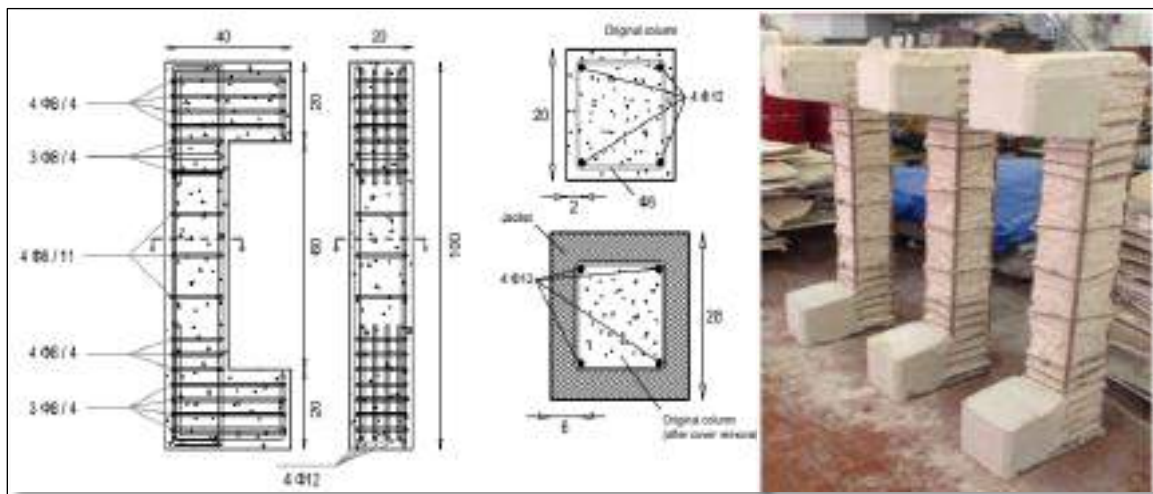


Figure 2.2 Details of The Original and Strengthened.[33]

In 2016, Koo et al. [34] developed an appropriate retrofit method and assessed the columns strengthened with HPFRC jackets. The experimental program involved four identical RC column specimens, with one left unstrengthened and the others retrofitted with HPFRC jackets of varying thickness and stirrup configurations as shown in Fig. (2.3). The specimens were subjected to double curvature cyclic load tests to simulate seismic loads. Their testing results showed that the greatest weight

that may be supported by the columns increases by applying the HPFRC jacketing method, with the addition of transverse reinforcements further improving the shear strength and ductility.





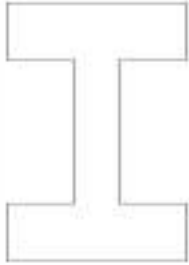

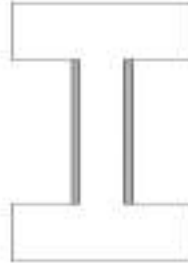
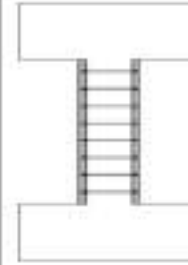
	R0	R3	R5	R5S
Retrofit method	unstrengthened	30mm jacket (10% thickness of column)	50mm jacket (16.7% thickness of column)	50mm jacket + stirrups (D10@150)
Section				
Elevation				

Figure 2.3 Details of Specimens.[34]

Their findings also indicated that the HPFRC jacketing technique was an advantageous choice for retrofitting RC columns, as it provides an important improvement in strength without a substantial increase in column size. This approach was possible to change the mode failure from shear to flexural shear failure, hence enhancing the ductile behavior of column specimens. The study notes that the HPFRC jacketing method may have limitations in terms of durability, such as fire or corrosion resistance, which should be considered in practical applications.

In 2018, Hadi et al. [35] investigated the behavior of sixteen RC specimens under concentric axial loading, eccentric axial loading, and four-point bending and proposed a new jacketing technique to retrofit existing deficient circular RC columns. The experiment of this investigation involved the preparation and testing

of 16 reinforced concrete (RC) column specimens. The specimens were categorized into four groups, each one consisting of 4 column specimens, according to the implemented strengthening procedure. The specimens were tested under different loading conditions, including concentric axial load, eccentric axial loads, and four-point bending, as shown in Table (2.1).

Table 2.1 Test Matrix.

Specimen	Dimensions (mm)	Longitudinal reinforcement	Transverse reinforcement	Jacket type	Loading condition
C-0	Ø150 x 800	6 N10	R6@50 mm	None	Concentric
C-15					15 mm eccentric
C-25					25 mm eccentric
C-B					Four-point bending
CF-0	Ø150 x 800			Two layers of CFRP	Concentric
CF-15					15 mm eccentric
CF-25					25 mm eccentric
CF-B					Four-point bending
CJ-0	Ø200 x 800			RPC	Concentric
CJ-15					15 mm eccentric
CJ-25					25 mm eccentric
CJ-B	Ø200 x 800				Four-point bending
CJF-0				RPC + One layer of CFRP	Concentric
CJF-15					15 mm eccentric
CJF-25					25 mm eccentric
CJF-B					Four-point bending

As can be seen from Table (2.1), the researchers tried to employ different materials to strengthen the RC column. The response of the specimens under different conditions such as yield load, ultimate load, and energy absorption was

recorded and presented. The study proved that the combination of RPC jacketing and CFRP wrapping was an effective strengthening method for RC columns. It enhanced and improved the axial load capacity, ductility, and energy absorption of the specimens. Moreover, strengthening of circular RC columns using RPC and RPC combined with CFRP was more efficient than using CFRP alone to achieve a greater yield strength.

In 2019, Al-Khazragi [36] conducted an experimental investigation to evaluate the performance of RC columns strengthened with HPFRC and CFRP. The variables of the study were the number of RC sides, which were covered by strengthened materials. These were two or four sides. The thickness of the strengthened material was also considered. To achieve the goals of the study, 13 specimens of square cross-sections of normal concrete with the same longitudinal and transverse reinforcement were cast and tested. The conclusion revealed that strengthening structures using HPFRC and CFRP led to improvement in the RC columns performance under the concentric and eccentric loads. The combination of CFRP and HPFRC jacketing provided better strength and ductility than using a single material. The dimensions of CFRP strips and the amount of HPFRC jacketing applied to the faces of reinforced concrete columns were important variables that influenced their structural performance.

In 2019, Algburi et al. [37] introduced a novel method to improve or increase the strength of RC columns. The method involved circularizing the columns using reactive powder concrete (RPC) and then wrapping with Fiber Reinforced Polymer (FRP). The effectiveness of this technique was evaluated by conducting tests on 16 specimens. These specimens were separated into four groups, each representing a different strengthening methodology, as illustrated in Fig. (2.4). The specimens conducted testing under various loading instances, including concentric axial load,

eccentric axial loads, and four-point bending. The experimental findings suggested that the combination of circularization with RPC and wrapping with CFRP is more efficient in enhancing the strength of square RC columns, as compared to circularization with RPC alone. This combination results in enhanced both strength and energy absorption. Additionally, it was demonstrated that the RPC may be utilized effectively as both a shape modifier and a strengthening jacket for square reinforced concrete (RC) columns.

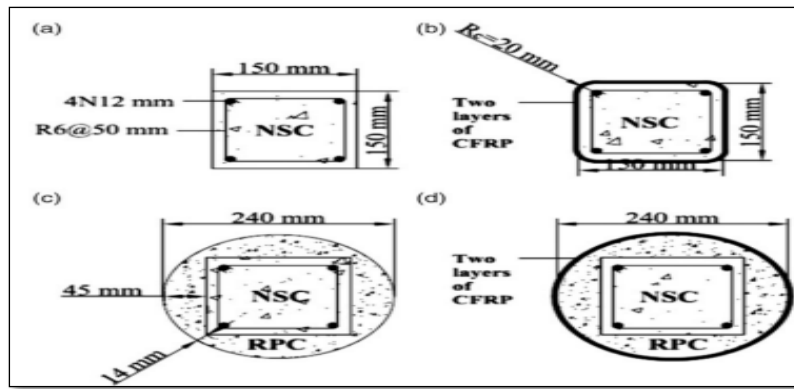


Figure 2.4 Cross-sections of The Specimens:
(a) Group S, (b) Group SF, (c) Group SJ, and (d) Group SJF.[37]

In 2019, Tayeh et al. [38] introduced experimental research aimed at assessing the efficacy of mending deteriorated concrete columns through the application of a thin-layer concrete jacket. The experimental program involved creating nine reinforced concrete column specimens, each measuring 30 cm in length. The specimens were partitioned into three groups based on their cross-sectional dimensions: three specimens measured (10×10) cm, three specimens measured (15 × 15) cm, and three specimens measured (17×17) cm. There was a total of thirty-six column specimen cores that were cast. These cores had the same cross sections, measuring (10× 10) cm, and a total height of 30 cm. Those cores sustained damage due to being loaded with approximately 90% of their maximum axial loading

capabilities. Subsequently, the columns underwent restoration and reinforcement by employing two jacketing materials, measuring 2.5 and 3.5 cm in thickness, on each of the four sides. Group 1 included eighteen-column cores encased in regular strength concrete, while group 2 comprised eighteen-column cores encased in ultrahigh-performance fiber-reinforced self-compacting concrete with steel reinforcement, as depicted in Fig. (2.5). The study concluded that thin concrete jacketing with normal-strength concrete and ultrahigh-performance fiber-reinforced self-compacting concrete can be a highly efficient method for repairing and strengthening damaged concrete columns. Moreover, the use of different jacketing types and surface preparation methods can significantly improve the compressive strength of RC column specimens. Therefore, using UHPFRSCC jacketing is an effective method for the rehabilitation and repair of deteriorated reinforced concrete columns, with the use of shear studs for bonding column cores and jackets being the most effective method among the three surface roughening methods tested (mechanical wire brushing, mechanical scarification, and shear studs).



Figure 2.5 Geometry and Reinforcement Details of Columns.[38]

In 2019, Heiza et al. [39] investigated the effect of corrosion on RC columns and the effectiveness of using HPFRC and NSC jackets as a repairing technique. An experimental test program was prepared to test 12 reinforced concrete columns having sections of (120 x 120) mm and lengths of 1000, 1500, and 2000 mm. The details of the tested specimens are shown in Table (2.2). The columns were tested as hinged-hinged under concentrated load at both ends up to failure. The behavior of the tested columns was estimated in terms of ultimate load, vertical displacement, horizontal displacement, strain in concrete, and strain in the main steel rebar.

Table 2.2 Details of Column Specimens.

Group	Code	Cross section mm ²	Height mm	Discretion
1	UC-100	120 x 120	1000	uncorroded
	UC-150		1500	
	UC-200		2000	
2	C-100	120 x 120	1000	Corroded
	C-150		1500	
	C-200		2000	
3	RH-100	160 x 160	1000	Repaired by HPFRC
	RH-150		1500	
	RH-200		2000	
4	RN-100	160 x 160	1000	Repaired by NSC
	RN-150		1500	
	RN-200		2000	

The results showed that the column enhanced by HPFRC produced the best structural results, with a raised load capacity for corroded column specimens.

Moreover, High-performance jacketing enhances column bearing capacity in corroded rebar, doubling capacity load, suitable for existing RC structures with low concrete strength, low reinforcement ratio, and corrosion.

In 2020, Mashshay et al. [40] employed innovative engineering concrete cementitious ECC materials for strengthening RC columns under eccentric loading conditions. For ECC material two types of fibers were selected. These were steel and polypropylene fibers. Eight RC columns of square cross-section were cast and tested as illustrated in Fig. (2.6). The columns were subjected to eccentric loading, with two eccentricities ($h/6$ and $5h/12$), and the load-deformation behavior was recorded. The findings demonstrated that the specimens with ECC displayed superior load-carrying capacity in comparison to both self-compacting concrete and regular ECC specimens. The load-deformation behavior of the hybrid ECC columns was not significantly different when the proportion of steel fibers was raised from 0.5% to 1%. The eccentricity of the loads had a significant effect on the global behavior of the tested columns.

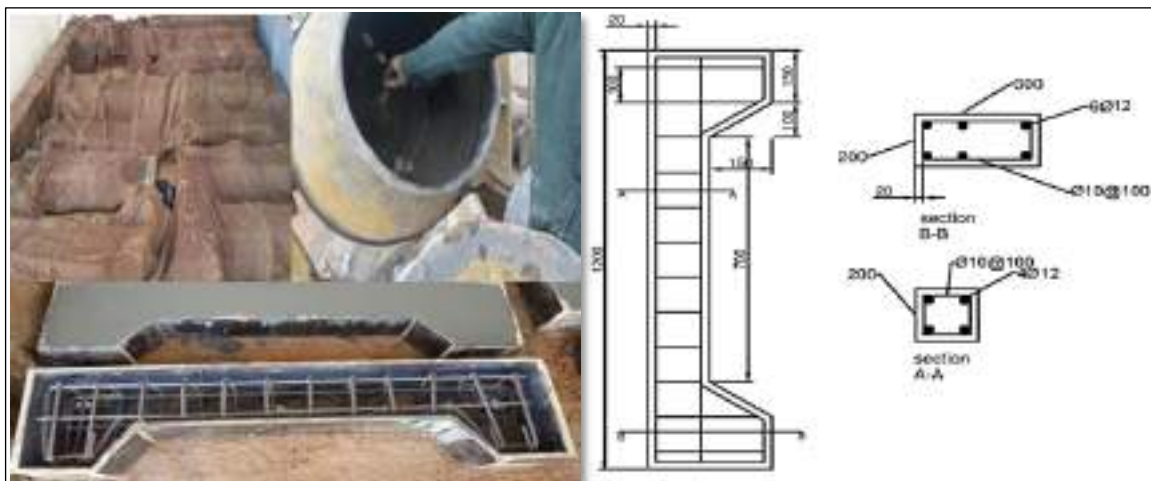


Figure 2.6 Details of Tested Columns.[40]

In 2020, Sakr et al. [41] developed a precise numerical model of a reinforced concrete column strengthened with HPFRC under eccentric loading. The

cohesiveness surface was considered and the bond between the jacket and core concrete was conjoined. The ABAQUS program was utilized for simulation purposes of both the reference RC columns and the RC columns that have been reinforced with HPFRC jackets. The other factors that also considered were the concrete core, concrete jacket, dowels, and reinforcement of steel in the jacketing layers and core. The specific characteristics of the specimens are presented in Fig. (2.7)

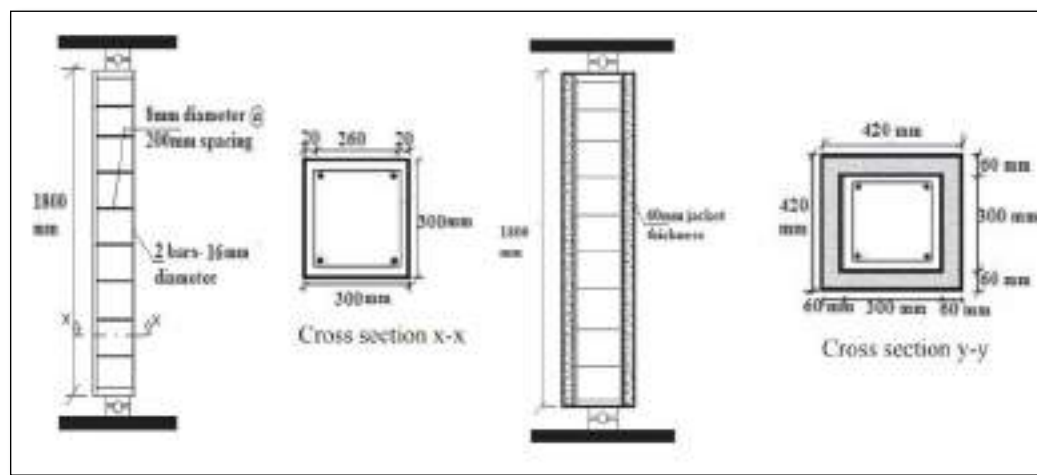


Figure 2.7 Details of Specimens.[41]

The study conclusions were that the proposed finite element (FE) model accurately predicts ultimate load capacities and failure causes for reinforced concrete columns with RC jackets. Additionally, the cohesive surface appropriately captures core-jacket interface connection behavior. The FE results also match experimental test results well. The maximum load capacity of the jacketed specimens increases with the increase of jacket thickness. Moreover, installing dowels enhances the load capacity and bond between core concrete and HPFRC jackets.

In 2020, Dadvar et al. [42] investigated the strengthening technique of HPFRC jacketing for confining circular RC columns and proposed a model for the stress-

strain relation of the column specimens confined with the HPFRC jacket. For this purpose, fourteen circular base column specimens were cast, and their contact surfaces were prepared through longitudinal or horizontal grooving, sandblasting, and abrasion techniques. Ten specimens were strengthened with HPFRC jackets 15 mm in thickness and containing either steel fibers or synthetic macro-fibers, while three more were strengthened with full or intermittent glass fiber-reinforced polymer (GFRP) hoop wraps. The study concluded that HPFRC jacketing can increase the load-carrying capacity and energy absorption of RC columns, and a model was proposed to predict the stress-strain relation of concrete columns jacketed by HPFRC, and HPFRC jackets with steel fibers and longitudinal grooving surface preparation technique are effective in improving the compressive behavior of NSC columns. Furthermore, suggested that the surface preparation technique and the type of fibers used in the HPFRC jacket can significantly affect the load-carrying capacity and ductility of the columns. Longitudinal grooving as a novel interface treatment produced significant enhancements in the load-carrying capacity and energy absorption of the jacketed specimens. Specimens strengthened with HPFRC jackets containing steel fibers recorded higher load-carrying capacity and energy absorption compared to those containing synthetic fibers.

In 2021, Al-Osta et al. [43] presented an analytical model to forecast the structural integrity of reinforced concrete columns that were square in shape and have been reinforced using UHPC under axial and eccentric load. The FE models were validated with the result of the experimental study. The exploration involved cast-on 15 reinforced concrete columns with a cross-section of 125×125 mm and a height of 500 mm. The columns were categorized into three groups based on

their confinement with UHPC. A 3D nonlinear numerical model was created using ABAQUS software and verified using experimental results.

The study conclusions revealed that UHPC jacketing was an effective way to improve the strength and ductility of RC columns. The finite element model developed in this research study can accurately predict the performance of UHPC jacketed RC columns. The analytical models accurately forecasted the point at which RC columns, reinforced with UHPC, would break under stress.

In 2021, Chen et al. [44] investigated a numerical and experimental study for following the performance of eccentric RC columns jacketed by HPFRC. The parameters considered in the study were the reinforcement ratio of HPFRC and the thickness of the jacketed material. To achieve the purpose of the study, nine specimens were tested. Dimensions and details of the specimens were illustrated in Fig. (2.8).

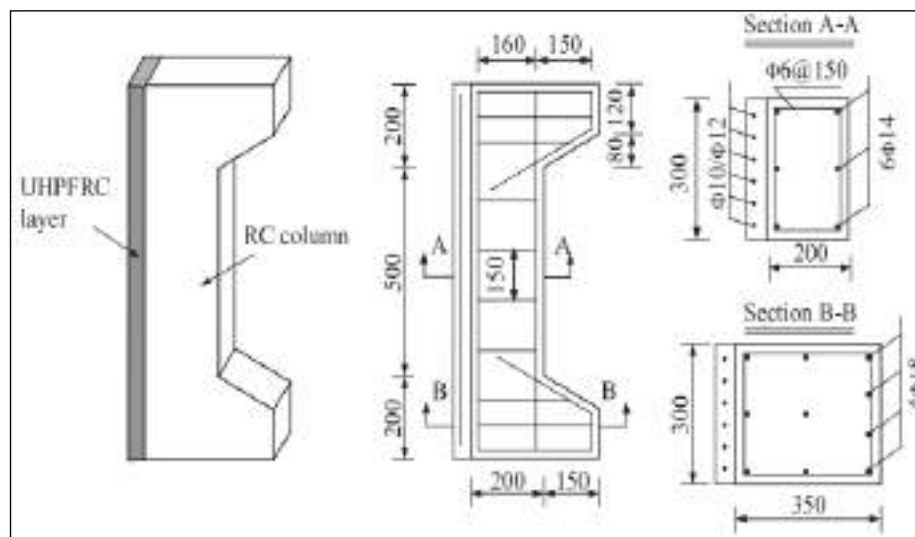


Figure 2.8 Geometry and Rebar Arrangement (unit: mm).[44]

The ABAQUS program was used to predict the results of the numerical phase of the study. The results illustrated that HPFRC layer has good prospects for

strengthening RC structures. The HPFRC layer can improve the load-carrying capacity and ductility of RC columns under eccentric compression. HPFRC layer can also control on the development of cracks and improve the bending resistance of the column. The behavior of the columns was influenced by the HPFRC layer thickness, load eccentricity, and bond slip at the interface.

In 2021, Cassese et al. [45] introduced an investigation of RC columns retrofitted with HPFRC jacketing. Their experimental program involved conducting tests on four scaled-down specimens. One specimen was an RC non-strengthened column, while the other three columns were strengthened by using external HPFRC jacketing. The testing procedure involved applying a combination of axial and bending load conditions. The results indicate that the strengthened column U1 reached its maximal load at a deformation value of 0.17%, which was significantly lower than that of the unstrengthened column. The damage condition was defined by the emergence of pseudo-vertical cracks on the outer surface of the specimen. The measured maximum values of the axial load and bending moment were lower than the expected values due to the adverse rise in transverse stress on the HPFRC jacket.

In 2020, Elsayed et al. [46] examined the structural response of RC columns reinforced with HPFRC when subjected to eccentric loads. The considered various parameters were the eccentric load ratio, HPFRC thickness, steel fiber ratio, and strengthening schemes. Two different schemes were laminates on two sides or full around all sides as demonstrated in Fig. (2.9). The experimental study involved cast twelve-column specimens subjected to compressive load. The theoretical framework established by **Sakr et al. [47]** was used to evaluate and determine the axial load and moment capacities of the tested columns. The study concluded that HPFRC was a highly effective method for enhancing the performance of RC

columns when subjected to eccentric loading. The application of HPFRC jackets and laminates was the most efficient approach for strengthening reinforced concrete columns under eccentric loading. The thickness of the HPFRC jacket and the volume of steel fibers had a significant impact on the strength and stiffness of the enhanced specimens.

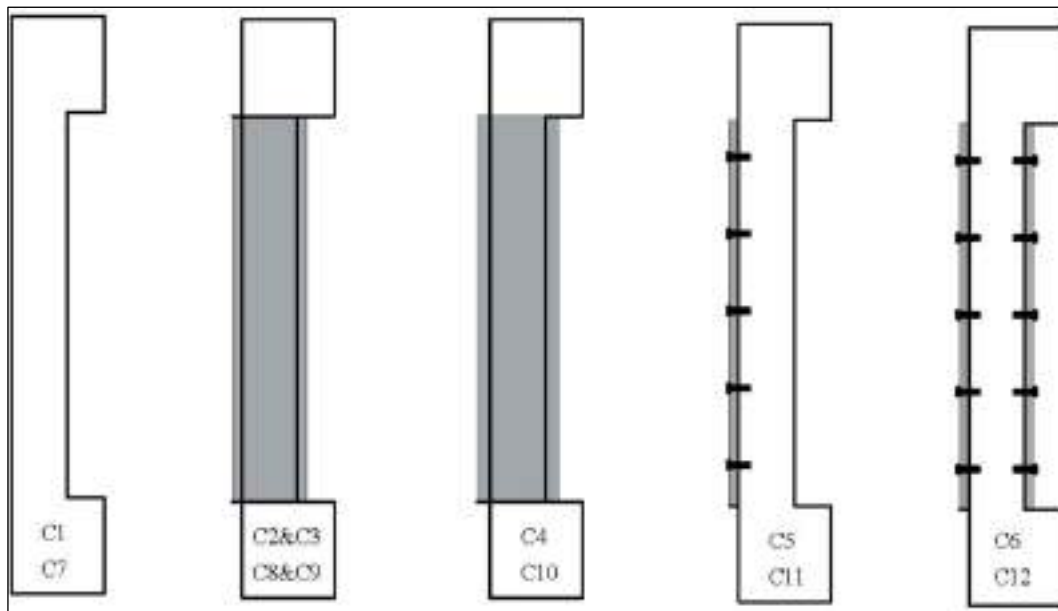


Figure 2.9 Strengthening Schemes for Test Specimens.[46]

In 2022, Suleman. [48] one of the factors that affect the performance of the strengthened column with UHPC is the interfacial bond between the two materials (concrete core and strengthened jacket). Therefore, this study focused on exploring the effect of that factor on the strengthened column. For this purpose, sandblasting and epoxy binder were used to enhance the bond between the core concrete and jacketed material. This study proved that when the column was roughened by sandblasting and using an epoxy binder showed no debonding between the substrate and strengthened jacket. Moreover, the study extended to repair the corroded RC column using UHPC, considering the surface preparation in account. The study involved fourteen square and circular column samples with a square

cross-section of 150 x 150 mm and a total length of 950 mm as shown in Fig. (2.10). The thicknesses of the jacket and column shapes were subjected to varying degrees of deterioration (10 and 20 mass loss %). The outcomes showed that increasing the thickness of the UHPC jacket resulted in an enhanced carrying load by about 0.49 at 0.10 mass loss and 0.84 at 0.20 mass loss for square strengthened concrete columns, while the load carrying capacity changed by about 0.97 at 0.10 mass loss and 0.28 at 0.20 for circular columns. The axial deformation decreased for square columns but increased for circular columns. In addition, the ductility of corroded concrete columns strengthened with UHPC jacket significantly enhanced by (0.06, 0.47) for 0.10 mass loss and (0.82, 0.83) for 0.20 mass loss for square columns and (0.63, 0.68) and (0.21, 0.49) for circular columns with mass loss 0.10 and 0.20 respectively.

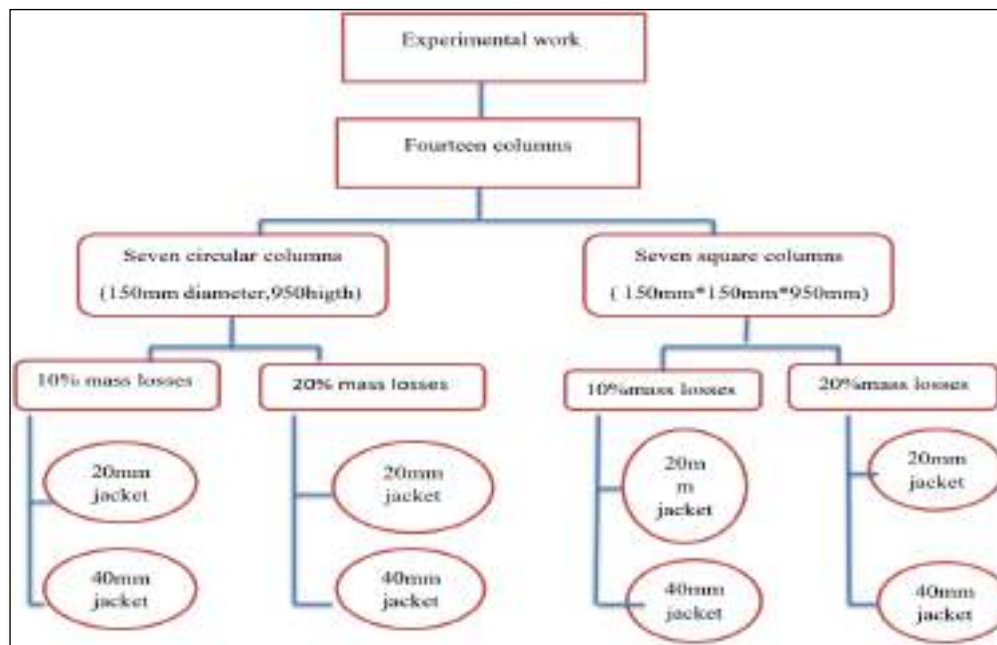


Figure 2.10 Schematic for Structural Work.[48]

In 2023, Susilorini et al. [49] examined the advanced performance of columns with UHPC and HPFRC jacketing, focusing on the strength and ductility of these

columns, including load capacity, stress-strain behavior, and crack patterns in failure modes. This study employs experimental and analytical approaches. The experiment conducted cast 12 short normal strength concrete columns with dimensions of 200 mm x 200 mm, a height of 750 mm, and a concrete cover thickness of 25 mm. The NSC columns used 4Ø12 mm deformed steel bars as longitudinal reinforcements, and Ø8 mm bars as ties with a spacing of 100 mm (external lap section) and 50 mm (internal lap section) strengthened by UHPC and HPFRC, including 0%, 1%, and 2% fiber, which were tested under axial load and different eccentricities: $e = 0, 35$, and 70 mm, as shown in Table (2.3).

Table 2.3 Column Specimen's Detail.

No.	Specimen Code	Description	Fiber Percentage	Loading Type
1	C-0	CONTROL 1	0%	concentric
2	CF0-0	NSC + UHPC 0%	0%	concentric
3	CF1-0	NSC + HPFRC 1%	1%	concentric
4	CF2-0	NSC + HPFRC 2%	2%	concentric
5	C-35	CONTROL 2	0%	eccentric
6	CF0-35	NSC + UHPC 0%	0%	eccentric
7	CF1-35	NSC + HPFRC 1%	1%	eccentric
8	CF2-35	NSC + HPFRC 2%	2%	eccentric
9	C-70	CONTROL 3	0%	eccentric
10	CF0-70	NSC + UHPC 0%	0%	eccentric
11	CF1-70	NSC + HPFRC 1%	1%	eccentric
12	CF2-70	NSC + HPFRC 2%	2%	eccentric

Sandblasting was used to provide a monolithic surface contact between the substrate and the UHPC and HPFRC confinements. The findings indicated that NSC columns strengthened by UHPC and HPFRC were able to resist a greater maximum load and stress, as well as serve increased vertical deformation and strain compared to the control specimens. Moreover, it showed that including a 2% fiber volume into the HPFRC reduces crack propagation in the failure mode and

delays confinement spalling of the column. Finally, the study confirms that UHPC and HPFRC confinements can enhance the strength and ductility of the column.

In 2023, Shehab et al. [50] analyzed the axial performance of square-reinforced concrete columns that were reinforced with HPFRC jackets. The study specifically investigated the impact of interface treatment methods, jacket thickness, and the number of strengthened sides on the behavior of the columns. The research project involved the production of nineteen specimens, each with a specific height of 1000 mm and a cross-section of 150 × 150 mm as shown in Fig. (2.11). The study used HPFRC jackets with different grooving patterns (VG, HG, and NG) and varying jacket thicknesses (20 mm and 40 mm) to strengthen columns. All reinforced specimens failed in a brittle manner throughout the study. The "HPFRC" reinforced concrete column specimens with vertical grooves exhibited a greater ultimate load capacity in comparison to the columns with horizontal grooves and columns with no grooving. Moreover, the outcomes showed that the average load increases by 44.4%, 119.4%, and 236.4% for VG with a 2 cm jacket thickness and by 103.2%, 264.3%, and 421.8% for VG with a 4 cm jacket thickness. Finally, the study concluded that HPFRC jackets can be used to strengthen RC columns, and the interface treatment method, jacket thickness, and number of strengthened sides affect the columns' behavior. The load-carrying capacity of column specimens, when strengthened with a HPFRC jacket, is significantly influenced by the jacketing thickness. This holds regardless of the treatment procedures used at the interface or the number of sides of the column that are strengthened. The vertical grooving (VG) method has consistently demonstrated superior outcomes in comparison to alternative interface treatment

procedures, regardless of specimen jacketing thickness or stronger sides.

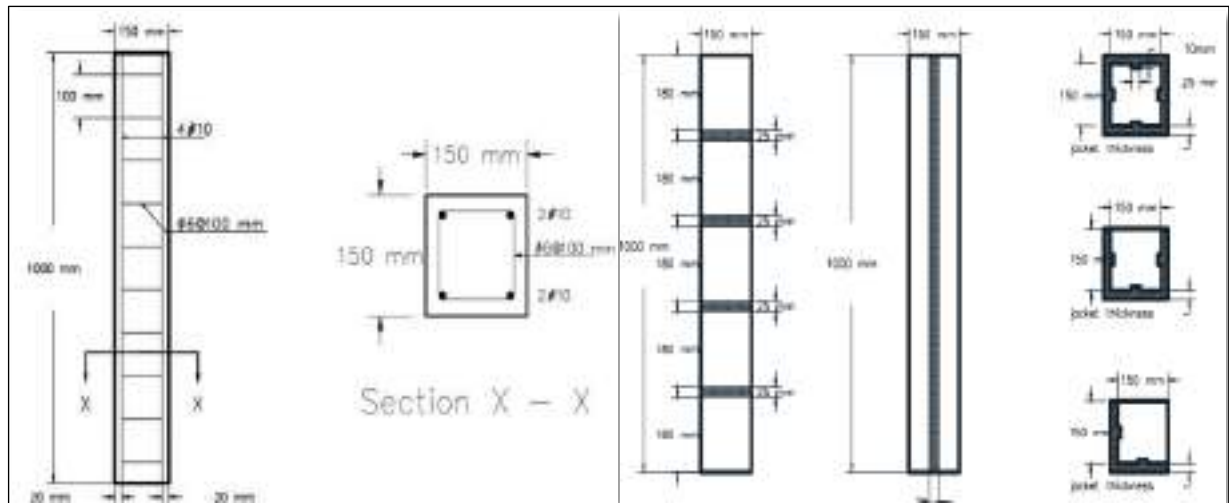


Figure 2.11 Geometry of Column Specimens.[50]

In 2023, Al Zeyadi. [51] investigated the behavior and load-carrying capacity of rehabilitated reinforced concrete (RC) columns with honeycomb damage in different locations and volumes. Twenty RC columns were considered with details in Fig. (2.12), with ten for the square section and ten for the circular section. The honeycombed zone in the base and middle of the specimens was considered as a percentage of the total column size, with a range of 3% to 26% and 4% to 57% for the square and circle sections, respectively. The honeycombed columns were repaired with epoxy or cement-based materials before the test. The test results showed that the strength and load capacity of the treated column exceeded that of the control column, with different percentages based on the cross-section of the column, and the size and location of the honeycomb defect. The increase in ultimate load ranged from 3% to 16% for the square section and from 3% to 17% for the circular section. The percentage of increase was higher as the size of the honeycomb increased. For the square section RC column, the control column failed, while the specimens with cover defects had an increase in ultimate load (10%, 16%, 3, and 7.7%), respectively. For the core defect specimens, the ultimate

load increased by 24%, 17%, and 18%. The cover-core defect specimens failed with an increase in ultimate load (6% and 7%).



Figure 2.12 Details of Specimens.[51]

2.3 Studies on the behavior of RC Column Strengthening with FRP:

In 2024, Li et al. [52] investigated the effects of concrete canvas (CC) and carbon fiber-reinforced plastic (CFRP) reinforcement on the mechanical characteristics of corroded reinforced concrete columns. Forty-two columns were engineered, and axial compression tests were performed. The influence of initial corrosion rate, secondary corrosion duration, quantity of CC layers, and quantity of CFRP layers on failure morphology, load-bearing capacity, and ductility was examined. The findings indicated that specimens confined with single-layer CC exhibited improvements, and ductility qualities were increased. CC-CFRP composite-constrained specimens exhibited substantial enhancements, demonstrating improved plastic deformation capacity and distinctive ductile damage traits. The corrosion inhibition of CC for specimens exhibiting a theoretical corrosion rate

under 20% showed an upward trend, ranging from 23.0% to 31.2%. CC and CFRP collaboratively restrict concrete, resulting in substantial alterations in joint restraint specimens and little total peak strain under the influence of joint steel bars. A precise peak stress-strain model for corroded reinforced concrete columns was developed, providing a theoretical foundation for further study. The research indicated that unconfined reinforced concrete columns exhibited brittle failure, enhanced load-bearing capability with single-layer concrete, and ductile failure. The damage process was slower and more ductile when integrated with concrete reinforcing panels. As the layers of CFRP rose, the noise of damage intensified, and the concrete was fractured. The research analyzed the damage characteristics of unconfined reinforced concrete columns, indicating brittle failure without apparent indicators. Single-layer concrete columns demonstrated enhanced bearing ability but with a little improvement in capacity. The specimens exhibited ductile damage throughout testing. The damage process of CFRP-constrained reinforced concrete columns was slower and more ductile when damaged. With the rise in CFRP layers, the damage process exhibited a deceleration, amplified noise, and resulted in the crushing of the concrete in the core region. This study introduces a primary model for axial compression of corroded reinforced concrete columns that are simultaneously constrained by CFRPs, demonstrating great accuracy and effectively characterizing the mechanical features of these columns. The stress-strain curves of these columns exhibit an initial increase, followed by a little decline, and then another increase, underscoring the need for a deeper comprehension of their axial compression characteristics.

In 2023, Blikharskyy et al. [53] analyzed the performance of columns reinforced with CFRP laminates subjected to eccentrically applied axial loads. The study examines the impact of pre-loading on the observed behavior of the columns. The

specimens are first subjected to eccentrically applied axial forces at varying capacity levels. Upon reinforcement, they are progressively loaded to failure, with stresses and deflections documented. The characteristics of strength, deformability, and ductility of the columns are assessed and analyzed. A comparative study is performed to assess the efficacy of the strengthening. The research indicates that increased starting loading levels diminish the strengthening effect from 31.8% to 15%, resulting in a reduction of the final displacement at the maximum load. The augmentation of stiffness and reduction of deflections resulting from CFRP strengthening is seen, but the existence of initial loading somewhat diminishes the ductility of CFRP-strengthened columns. The specific characteristics of CFRP efficacy must be taken into account in engineering applications.

In 2021, Wang et al. [54] presented an experimental study on eccentrically loaded rectangular reinforced concrete columns with various CFRP strengthening methods and preloading levels showing that load-bearing capacity and ultimate deformations may be markedly improved after CFRP reinforcement as shown in Fig. (2.13). The comprehensive wrapping method was more efficacious for columns with minor eccentricity while augmenting longitudinal CFRP layers on the tensile side enhanced strength for columns with considerable eccentricity. A novel stress-strain model including preload effects was introduced, demonstrating superior performance relative to actual observations and theoretical calculations. CFRP-reinforced concrete columns exhibit substantial enhancements in load-bearing capacity and ductility under eccentric compression, with maximum increases of 47.3% and 80.2%, respectively. The complete CFRP wrapping method is more efficacious for specimens with less eccentricity. Preloading before CFRP strengthening adversely affects load capacity and ductility, resulting in a nonlinear

reduction in peak axial load under eccentric compression, while the deterioration of lateral deformation capacity exacerbates with increased eccentricity.

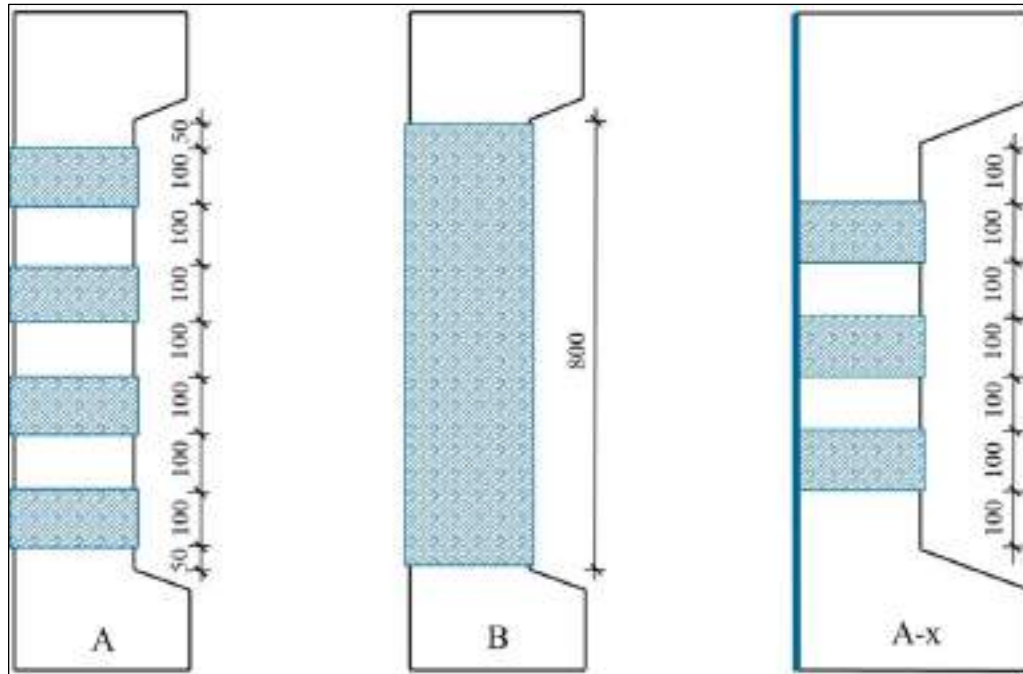


Figure 2.13 Geometry of Column Specimens.

In 2021, Sahi. [55] investigated the behavior of slender hollow reinforced concrete columns when applied to their axial and eccentricity loaded. The research involved testing fifteen hollow slender RC columns with dimensions of (140 x 80 x 2000) mm and a slenderness ratio of (80.54). The columns were divided into nine groups to study important parameters such as strengthening by lateral reinforcement (ties), strengthening by CFRP, the presence of eccentricity, and the shape of the longitudinal hole. The results showed that strengthening by CFRP alone or combined with lateral reinforcement (ties) resulted in better performance in terms of ultimate load, ultimate moment, maximum lateral displacement, ductility, energy absorption, and failure mode. The use of lateral reinforcement (ties) at different lengths at both ends of columns increased ultimate load by (2.7, 8.3, and 61.1%) when the distance of strengthening by ties changed from (140, 333 to 500)

mm, respectively. The eccentricity of load was another important factor in the load-carrying capacity of columns, especially slender columns. Two eccentricity values ($e = 20$ mm and $e = 40$ mm) caused a decrease in the ultimate load for hollow slender columns. For eccentricities of 20 mm and 40 mm, columns with a rectangular opening resulted in a decrease in load-carrying capacity of about (10.26% and 17.95%) when compared with slender columns subjected to axial load. Reinforced concrete columns with circular holes, either with or without CFRP sheet, had better performance in terms of ultimate load, ultimate moment, maximum lateral displacement, ductility, and energy absorption compared to those with rectangular holes. The increase in ultimate load was 14.29% in a column with a circular hole compared to a column with a rectangular hole.

2.5 Summary

According to the literature reviews (previous studies), very little work has been performed on the structural behavior of RC columns strengthened with HPFRC under eccentric loading, especially the columns that were damaged with honeycomb for many reasons, such as surface deterioration, surface deposits, deformation, cracks, and structural faults due to lack of quality control at the construction stage. This research covers the gap in the published literature as identified above, and investigates the variables that have not been studied previously. The purpose of this study is to experimentally investigate the structural behavior of RC columns strengthened by HPFRC under eccentric loadings with the presence of honeycomb as a defect. For this purpose, thirty RC square columns were cast and tested. Several variables were taken into consideration, such as load eccentricity ratio, the thickness of the HPFRC layer, honeycomb defect ratio, and the strengthening schemes. The detailed experimental work will be explained in the next chapter accordingly.

CHAPTER THREE: EXPERIMENTAL PROGRAM

3.1 General

A study was conducted at the Laboratory of Civil Engineering at the College of Engineering at the University of Misan to examine the behavior of square-reinforced concrete columns strengthened with high-performance fiber-reinforced concrete (HPFRC) under eccentric load. Furthermore, it is necessary to precisely determine and describe the shape and dimensions of the test specimens, the arrangement of steel components, the equipment used for measurement, and the proportions of the normal strength concrete (NSC) and the high-performance fiber reinforced concrete (HPFRC) used in the current research study. The properties of used materials were investigated in this chapter as well as the mechanical interface bonding, casting, and curing procedures of the fabricated column specimens.

3.2 Overall description of RC column specimens

Thirty square short (NSC) column samples were conducted in this research study. Several samples were strengthened with high-performance fiber reinforced concrete (HPFRC) and Carbon Fiber Reinforced Polymer (CFRP). The influence of jacket thickness, strengthening zone, the honeycomb defect ratio of the specimens, and the load eccentricity magnitude were the main concerns in this study. One specimen was tested with a concentric load, and twenty-nine columns were investigated under eccentric load. The details of the experimental program are described in the following section.

3.3 The Experimental Parameters

In this research study, the practical variables investigated are shown in Table (3.1).

Table 3.1 Experimental Parameters.

No.	Column Variables	Details
1	Load eccentricity (e)	e = 0, 50, 100 mm respectively.
2	Jacket thickness	15 mm and 30 mm.
3	Strengthening Face with (HPFRC and CFRP)	Fully and Partially Sides.
4	The honeycomb ratio (%)	(35% or 70%) of the specimen cross-section area under constant length ($L_e/4$).
5	Representing the honeycomb zone	Weak-strength concrete and foam block.

3.4 Material Properties

Commercially obtainable and clear descriptions of materials were used in this research study, as presented in the following subsection.

3.4.1 Cement

The investigation utilized Ordinary Portland Cement (OPC) of Type I. Which is commonly available in the local markets, as shown in Fig. (3.1). The required quantity was brought to the laboratory and well stored in a dry place and isolated from the ground. The chemical analysis and the physical properties are shown in Tables (3.3 and 3.4) respectively. The results of the chemical and physical properties conform with Iraqi Specification Standards (IQS 5/2019) [56]. The four main compounds in Portland Cement, C₃S, C₂S, C₃A, and C₄AF, were calculated for cement specimens using Bogue's Equation.



Figure 3.1 Cement.[56]

Table 3.2 Chemical analysis of cement.

Compound Composition	Oxide	Test Result	Limit according to I.Q.S. 5/2019 [56]	Conformed to I.Q. S
Lime Oxide	CaO %	62.43	-----	
Silica Dioxide	SiO ₂ %	19.44	-----	
Alumina Oxide	Al ₂ O ₃ %	4.98	-----	
Iron Oxide	Fe ₂ O ₃ %	3.4	-----	
Magnesia Oxide Contino	MgO %	2.57	≤ 5%	Satisfied
Sulfate Trioxide	SO ₃ %	2.41	≤2.5% if C ₃ A < 5% ≤2.8% if C ₃ A > 5%	Satisfied
Free Lime	F.L. %	1.18		
Loss on Ignition	L.O.I. %	4	≤ 4%	Satisfied
Insoluble Residue	I.R.%	1.25	≤ 1.5%	Satisfied
Lime Saturation Factor	L.S.F	0.95	0.66-1.02	Satisfied
	M.S	2.32	-----	
	M.A	1.46	-----	
	Total	99.22		
The main compounds percentage by weight of cement (Bogue's Equation)				
Compound Composition	Oxide	Test Result		
Tricalcium Silicate	C ₃ S	50.12		
Dicalcium Silicate	C ₂ S	21.26		
Tricalcium Aluminate	C ₃ A	9.29		
Tetra calcium Aluminon Ferrite	C ₄ AF	9.98		

Table 3.3 Physical properties of cement.

Physical properties		Test Result	Limit according to I.Q.S. 5/2019 [56]	Conformed to I.Q. S
Setting time (minute)	Initial	122	≥ 45	Satisfied
	Final	240	≤ 600	Satisfied
Fineness (Blaine), m^2/kg		314	≥ 230	Satisfied
Compressive Strength of mortar (MPa)	3 days	20	≥ 15	Satisfied
	7 days	33.3	≥ 23	

3.4.2 Fine Aggregate (Sand)

Natural silica sand from the Zubair area in Basra was used as fine aggregate, as shown in Fig. (3.2). The findings obtained demonstrated that the sand grading and sulfate concentration met the specified limitations of Iraqi Specification Standards (IQS 45/2019) [57] as shown in Table (3.4). Moreover, the classification of small particles is in the second category of fine aggregate. The physical and chemical properties are shown in Table (3.5).



Figure 3.2 Sand Utilized.

Table 3.4 Classification of fine aggregate.

Size of Sieve (mm)	Passing (%)	
	Fine aggregate	Limitations for Zone No. (IQS 45/2019) [57]
10	100	100
4.75	97	90-100
2.36	81	75-100
1.18	70	55-90
0.6	54	35-59
0.3	21	8-30
0.15	7	0-10

Table 3.5 Physical and chemical properties of fine aggregate.

Physical properties		
Properties	Test Result	Iraqi Specification No.45/2019[57]
Specific Gravity	2.65	
Absorption	0.94%	
Fine Material Passing from Sieve (75 μ m)	4.20%	Max \leq 5.0%
Fineness Modulus	2.6	
Chemical Properties		
Sulfate Content		Max \leq 0.5%

3.4.3 Quartz Sand

The use of quartz sand in high-performance reinforced concrete enhances particle packing, increases strength, reduces permeability, provides thermal stability, and improves workability. These properties contribute to the superior performance and durability of HPFRC. The grading of the used quartz sand (0.08-0.25 mm) met the specified limitations of Iraqi Specification Standards (IQS

45/2019) [57], produced by Sika Company of 25 kg bags. The sand is illustrated in Fig. (3.3), Appendix A.



Figure 3.3 Quartz Sand.

3.4.4 Coarse Aggregate (Gravel)

The gravel used was obtained from the Al-Tayeb region in Iraq with a maximum size of 10 mm. The gravel was sieved at a sieve size of 14 mm. The gravel was washed and cleaned with water; later, it was speared out and left in the air to dry before use as illustrated in Fig. (3.4) and Table (3.5). The gravel is in accordance with the Iraqi Specification Standard (IQS 45/2019) [57].



Figure 3.4 Coarse Aggregate.

Table 3.6 Classification of Coarse Aggregate.

Size of Sieve (mm)	Passing (%)	
	Fine aggregate	Limitations for Zone No. (IQS 45/2019) [57]
12.5	100	100
9.5	96	85-100
4.75	17	10-30
2.36	1	0-10

3.4.5 Silica Fume

Silica fume is a byproduct resulting from the reduction of high-purity quartz with coal or coke and wood chips in an electric arc furnace during the production of silicon metal or ferrosilicon alloys. The silica fume, which condenses from the gases escaping from the furnaces, has a very high content of amorphous silicon dioxide and consists of very fine spherical particles. Silica fume plays an important role in the production of essential materials for (HPFRC). It is available in local markets in bags of 20 kg, as shown in Fig. (3.5), with spherical particles less than 1 μm in diameter which made it approximately 100 times smaller than the cement particles. Furthermore, the silica used in this study conformed to (ASTM C 1240-04, 2019) [58]. The chemical and physical properties of silica fume are illustrated in Table (3.6). Appendix A.



Figure 3.5 Silica Fume.

Table 3.7 Chemical and Physical Properties of Silica Fume.

Chemical Properties		
Oxides composition	Oxides content %	ASTM C1240-15 %limit [58]
SiO ₂	92.5	Min. 85
Al ₂ O ₃	0.75	< 1
Fe ₂ O ₃	0.49	< 2.5
CaO	0.87	< 1
So ₃	0.88	< 1
L.O.I	5.3	Max.6
CI	0.1	< 0.2
K ₂ O+Na ₂ O	1.76	< 3
Physical Properties		
Property	Test result	ASTM C1240-15
Strength activity index	108	≥ 105%
Moisture content	0	≤ 2%
Specific surface area m ² /gm	16.5	> 15

3.4.6 Micro Steel Fiber

Ordinary concrete lacks the ability to withstand flexure in structural members due to its weak tensile characteristics. Hence, Steel fibers are utilized in (HPFRC) to enhance their ductility and reduce the spread of cracks, delaying their

appearance. The type of micro steel fibers used in this study were straight low-carbon steel wire and copper coated with a length (L) of 13 mm and a diameter (D) is 0.2 mm, clean of rust or oil with an aspect ratio ($L/D = 65$) as shown in Fig. (3.6). It is available in form of sacks weighing (20-25 Kg). The characteristics of steel fibers are outlined in Table (3.12). The specifications of used steel fibers referred to in ASTM-A820-04 [59],



Figure 3.6 Golden-colored steel fiber.

Table 3.8 Micro Steel Fiber Properties.

Type	Density (kg/m ³)	Length (mm)	Diameter (mm)	Tensile strength (MPa)	Modulus of elasticity (GPa)
Straight WSF0213	7800	13	0.2	2600	210

3.4.7 Superplasticizer

The superplasticizer is a type of high-range water reducer that plays an important role in the case of a low water-to-cement ratio to improve the workability, flowability, and self-compatibility of mixing concrete. The superplasticizer can enhance shrinkage, creep behavior, and water impermeability.

ViscoCrete-180GS superplasticizer was used in this research, it is produced by Sika Company, as shown in Fig. (3.8). The properties and specifications of ViscoCrete -180GS are shown in Table (3.7) [60].



Figure 3.7 Visco Crete -180GS.

Table 3.9 Visco Crete -180GS Technical Data.

Type	Property
Composition	Aqueous solution of modified polycarboxylates
Appearance	Light brownish
Specific gravity	$1.070 \pm (0.02)$ g/cm ³
pH-Value	4-6
Toxicity	Non-Toxic

3.4.8 Mixing Water

Clean and free from impurities drinking water was used for mixing and curing purposes [61]. Take into consideration the idea of using water for mixing concrete, which states that, what you can drink, you can make concrete with.

3.4.9 Reinforcement Steel Bar

The columns were reinforced with two types of deformed steel bar types. A Steel bar with a tensile strength of 585MPa for a diameter of 10 mm was utilized as longitudinal steel reinforcement, while steel stirrups with a tensile strength of 523MPa for a diameter of 8 mm were used.

Tests were conducted for each bar size, with three steel specimens made for a bar diameter of 10 mm and a length of 300 mm, and another three steel specimens prepared for a bar diameter of 8 mm and a length of 250 mm. The steel samples were acquired from bars selected at random. The testing results of the primary longitudinal steel reinforcement and the transverse steel stirrups are shown in Table (3.7), which have been verified to be accurate with the ASTM A615 Specification [62].



Figure 3.8 Main Rebar Tension Test.

Table 3.10 Steel Reinforcement Testing Results

Bar Type	Nominal diameter (mm)	Measured diameter (mm)	Yield stress (MPa)	Ultimate strength (MPa)
Deformed	10	9.85	585	725
	8	8	523	694

3.4.10 Foam

Synthetic cork is lightweight, relatively cheap, and can be formed into almost any shape. Synthetic cork density refers to how compact a foam's cells are relative to its volume; the properties of the foam are shown in Table (3.7) [63]. In this study, the purpose of the used foam was to represent the defect zone in the cover and core of specimens as a ratio of the cross-section. Flat sheet synthetic cork with 30 mm thickness as shown in Fig. (3.9).

Table 3.11 Technical Properties of Synthetic Cork.

Density	200 kg/m ³
Color	white
Grain size	2-5 mm
Specific weight	0.16 N/cm ³



Figure 3.9 Synthetic cork.[63]

3.4.11 Carbon Fiber Reinforced Polymer (CFRP)

The Sika Wrap®-301 C is a unidirectional woven carbon fiber fabric used for strengthening the column specimens in the transverse direction. Fig. (3.10) shows the CFRP sheets used in this work. All information related to this CFRP is shown in Table (3.14). Appendix A shows the properties of the CFRP sheets taken from the manufacturer's specifications.

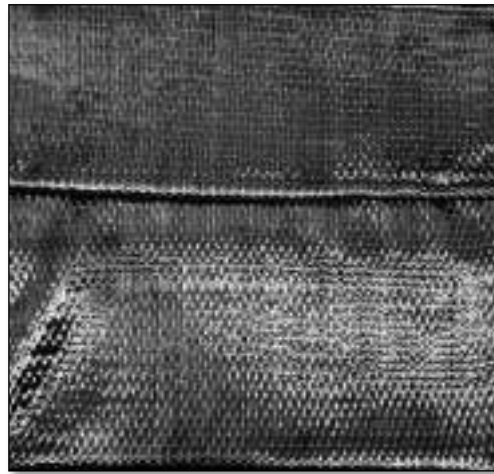


Figure 3.10 CFRP Sheet.

Table 3.12 CFRP Properties.

Property	Grade
Dry Fiber Density	1.82 g/cm ³
Dry Fiber Thickness	0.167 mm (based on fiber content)
Area Density	304 g/m ² ±10 g/m ² (carbon fibers only)
Dry Fiber Tensile Strength	4 000 N/mm ²
Dry Fiber Modulus of Elasticity in Tension	230 000 N/mm ²
Dry Fiber Elongation at Break	1.70%
Laminate Nominal Thickness	0.167 mm

3.4.12 Epoxy Resin (Sikadure LB32)

An adhesive material has been used between the normal concrete of the RC columns and the HPFRC jackets used for strengthening purposes. This material is composed of two components: a white and a grey portion. The final binding material was obtained by mixing these two components in a ratio of 1:2. The mixing process lasted for a duration of two to three minutes, resulting in the formation of a uniform mixture with a light grey color, as shown in Fig. (3.11). This was according to (ASTMC882/C882M-05, 2005) [64]. Appendix A.



Figure 3.11 Sikadure LB32 Bonding Material.

3.4.13 Epoxy Resin (Sikadur-330)

Impregnating resin of type Sikadur-330, which is composed of two parts (Resin part A + Hardener part B) has been used in this study for the bonding of CFRP sheet as shown in Fig. (3.12). Table 3.9 shows the properties of the bonding epoxy taken from the manufacturer's specification Appendix A.



Figure 3.12 Mixing Two Components of Epoxy Resin.

Table 3.13 Details of Sikadur ® - 330 Resins Properties.

Property	Grade
Density	1.30 ± 0.1 kg/l (component A+B mixed) (at +23 °C)
Viscosity @+35 °C	~5 000 mPas
Modulus of elasticity in flexure	~ 3 800 N/mm ² (7 days at +23 °C)
Tensile strength	~ 30 N/mm ² (7 days at +23 °C)
Modulus of elasticity in tension	~ 4 500 N/mm ² (7 days at +23 °C)
Tensile strain at break	0.9 % (7 days at +23 °C)
Tensile adhesion strength	Concrete fracture (> 4 N/mm ²) on sandblasted substrate

3.5 Fabrication of Column Specimens

3.5.1 Geometry of Column Specimens

Thirty short normal reinforced concrete column specimens were cast and tested from one batch. The strengthened columns had a square cross-section (120×120) mm, with a clear height of 750 mm and a concrete cover of 15 mm for all column sides. The total height of the columns was 950 mm. Each column had two corbel heads to accommodate eccentric loads during the test. Seven of these were proposed as control specimens. Moreover, the dimensions were chosen to be adaptable to the condition and capacity of the available testing machine. According

to ACI Code 318-19 Clause 6.2.5, for an unbraced column, a short column is defined as a column with a maximum slenderness ratio of 22. Meanwhile, the designed columns in this study had a slenderness ratio of 20.8, which can be classified as short columns. All columns were designed inadequately as their internal steel reinforcement ratio was about the lowest ratio of specified by the standard. The design produced 1% of the gross cross-sectional area of the column for longitudinal steel reinforcement. The purpose of this design was to simulate the condition of a column like an old column that has deteriorated and needs to be strengthened. Therefore, the columns have four 10 mm in diameter deformed bars as longitudinal reinforcement and 8 mm in diameter deformed bars as well as tie spacing at 100 mm. Column specimen geometry and reinforcement are presented in Figs. (3.13 and 3.14).

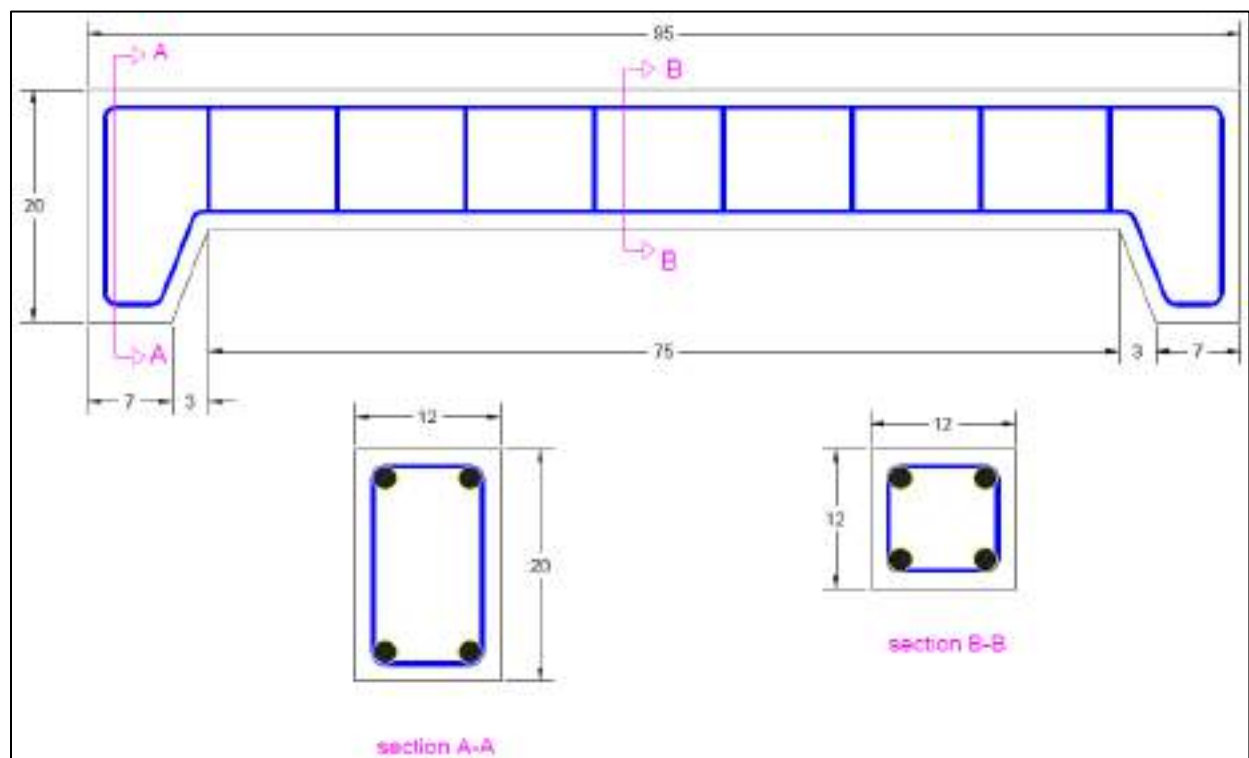


Figure 3.13 The Geometry and Reinforcement Details of The Column in (cm).



Figure 3.14 The Reinforcement Details of Specimens.

3.5.2 Labeling of Column Specimens

Column specimens were divided into seven groups that were Group (a) as reference columns, Groupe (b) with (0% defect ratio strengthening with HPFRC under eccentric load), Group (c) (35% foam defect ratio strengthening with HPFRC under eccentric load), Groupe (d)(70% foam defect ratio strengthening with HPFRC under concentric and eccentric load), Group (e) (70% foam defect ratio strengthening with HPFRC under concentric and eccentric load), Groupe (f) (70% Weak strength concrete defect ratio strengthening with HPFRC under eccentric load). For the seventh group (g), three columns were warped with CFRP under an eccentric load. The specimens were labeled as shown in the first column of Table (3.5). The label used for the specimens is composed of a combination of letters and numbers. In addition, the symbol notation is illustrated in Fig. (3.15).

For instance, to clarify the specimen designation, which is illustrated in Fig. (3.16), (CU4-15-100) means “Column specimen strengthening with HPFRC jacketing, 4 sides of jacketing, 15 mm of jacket thickness, and under 100 mm eccentric load.

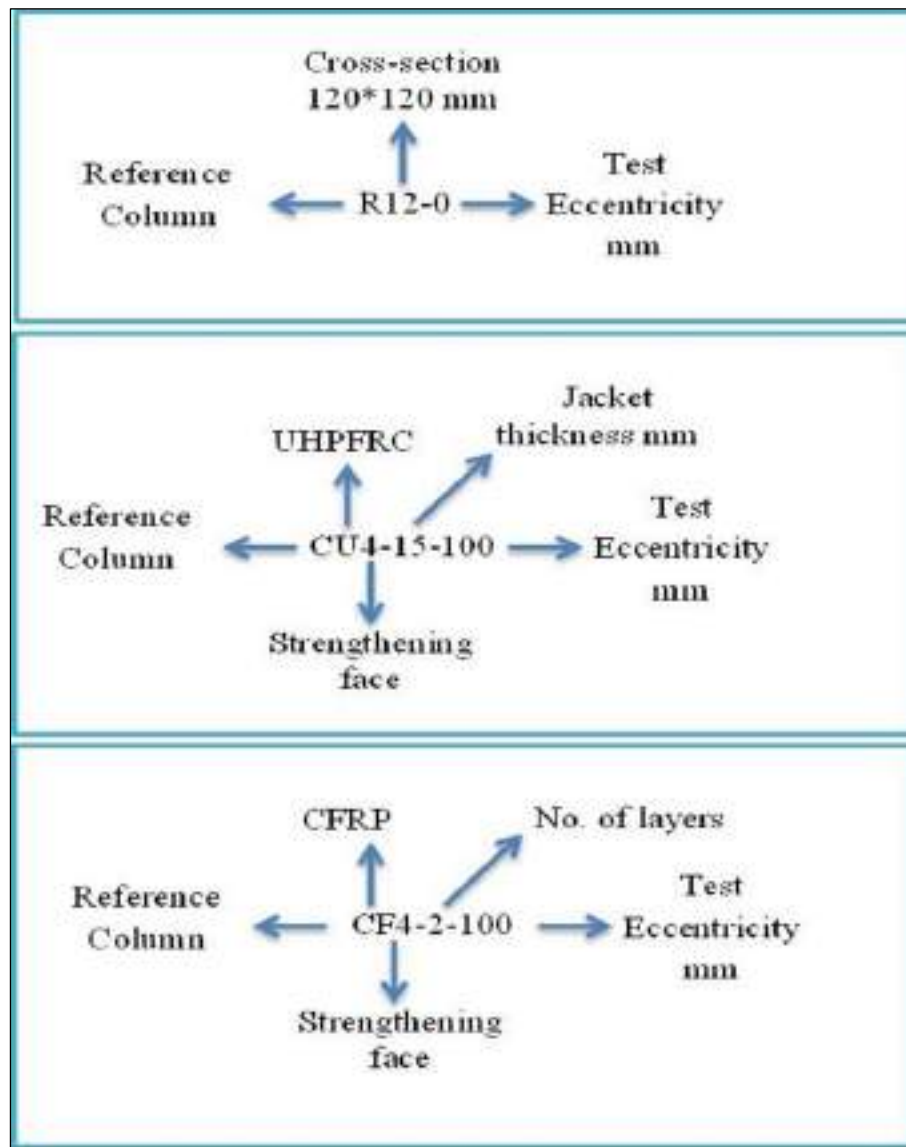


Figure 3.15 Symbol Detail's Designation.

Table 3.14 Details of the column specimens.

Group	Test Specimen	Strengthening Face	HPFRC Jacket Thickness mm	Test Eccentricity mm	Defect Ratio %	Number of CFRP Layers
a	R12-0	-	-	0	-	-
	R12-50	-	-	50	-	-
	R12-100	-	-	100	-	-
	R15-50	-	-	50	-	-
	R15-100	-	-	100	-	-
	R18-50	-	-	50	-	-
	R18-100	-	-	100	-	-
b	CU4-15-100	Fully	15	100	-	-
	CU2-15-100	Partially	15	100	-	-
	CU4-30-100	Fully	30	100	-	-
	CU2-30-100	Partially	30	100	-	-
c	CU4-15-100	Fully	15	100	35	-
	CU2-15-100	Partially	15	100	35	-
	CU4-30-100	Fully	30	100	35	-
	CU2-30-100	Partially	30	100	35	-
d	CU4-15-100	Fully	15	100	70	-
	CU2-15-100	Partially	15	100	70	-
	CU4-15-50	Fully	15	50	70	-
	CU2-15-50	Partially	15	50	70	-
e	CU4-30-100	Fully	30	100	70	-
	CU2-30-100	Partially	30	100	70	-
	CU4-30-50	Fully	30	50	70	-
	CU2-30-50	Partially	30	50	70	-
f	CU4-15-100	Fully	15	100	70	-
	CU2-15-100	Partially	15	100	70	-
	CU4-30-100	Fully	30	100	70	-
	CU2-30-100	Partially	30	100	70	-
g	CF4-1-100	Fully	-	100	70	1
	CF4-1-50	Fully	-	50	70	1
	CF4-1-100	Fully	-	100	70	1

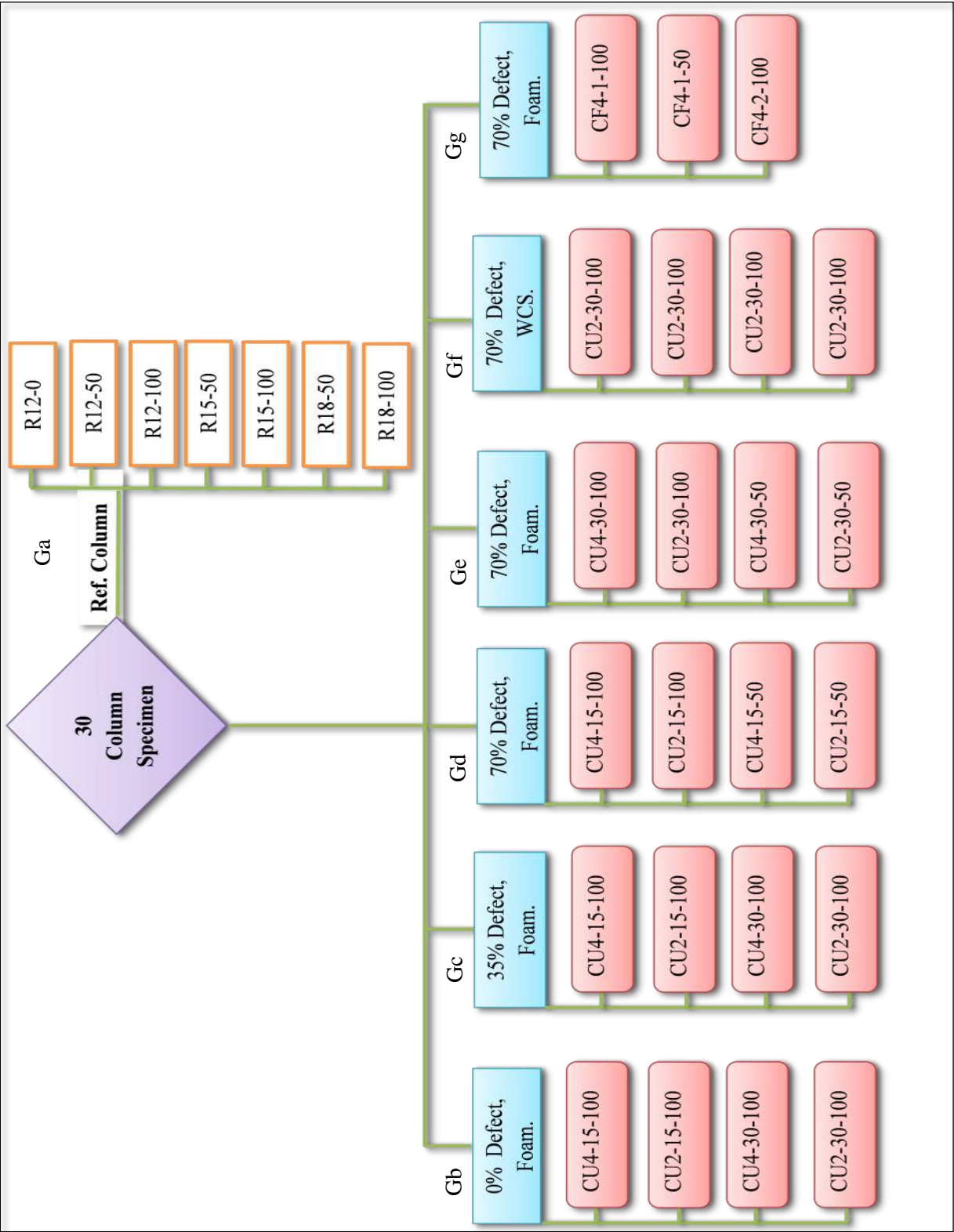


Figure 3.16 Schematic Plan of Column specimen

3.5.3 Design of the formwork

All specimens were cast horizontally, as in the normal practice for reinforced concrete columns. An integrated steel formwork, as shown in Figs. (3.17 and 3.18) was built to cast all column specimens. By using the integrated formwork instead of using some single formwork (one formwork for one specimen), some advantages were obtained. It produced a small size of formwork. Small formwork needs less material, and the specimen-casting process becomes faster. All steel formworks were fastened and opened with bolts. Before placing the steel reinforcing cages into the steel formworks, the inner surface of the formwork was cleaned to avoid bonding between the steel surface and the concrete; therefore, the specimens can be removed easily from the formworks after the concrete is cured.

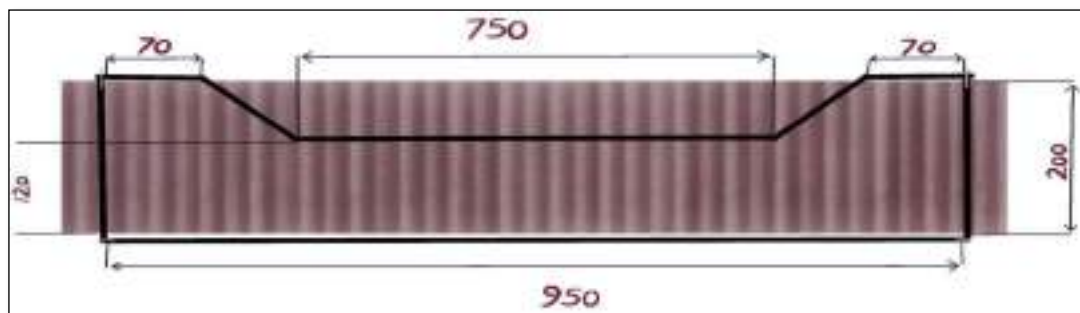


Figure 3.17 Integrated Formwork Plan (all units in millimeters).



Figure 3.18 The Constructed Formwork.

3.5.4 Honeycomb Formation Method in Column Specimens

In this research study, the honeycomb was configured in a column specimen as a ratio of the cross-section. Two ratios were chosen (35% and 70%) of specimen gross area at constant length ($L_e/4$). To configure the honeycomb, two ways were used to make defects or failures in cover and core defects at the specific zones of the specimens:

- 1- Use weak-strength concrete (8Mpa).
- 2- Use synthetic slices 30 mm thick, divided by a sharp tool according to the required dimensions.

The configuration of the honeycomb specimen is shown in Fig. (3.19).

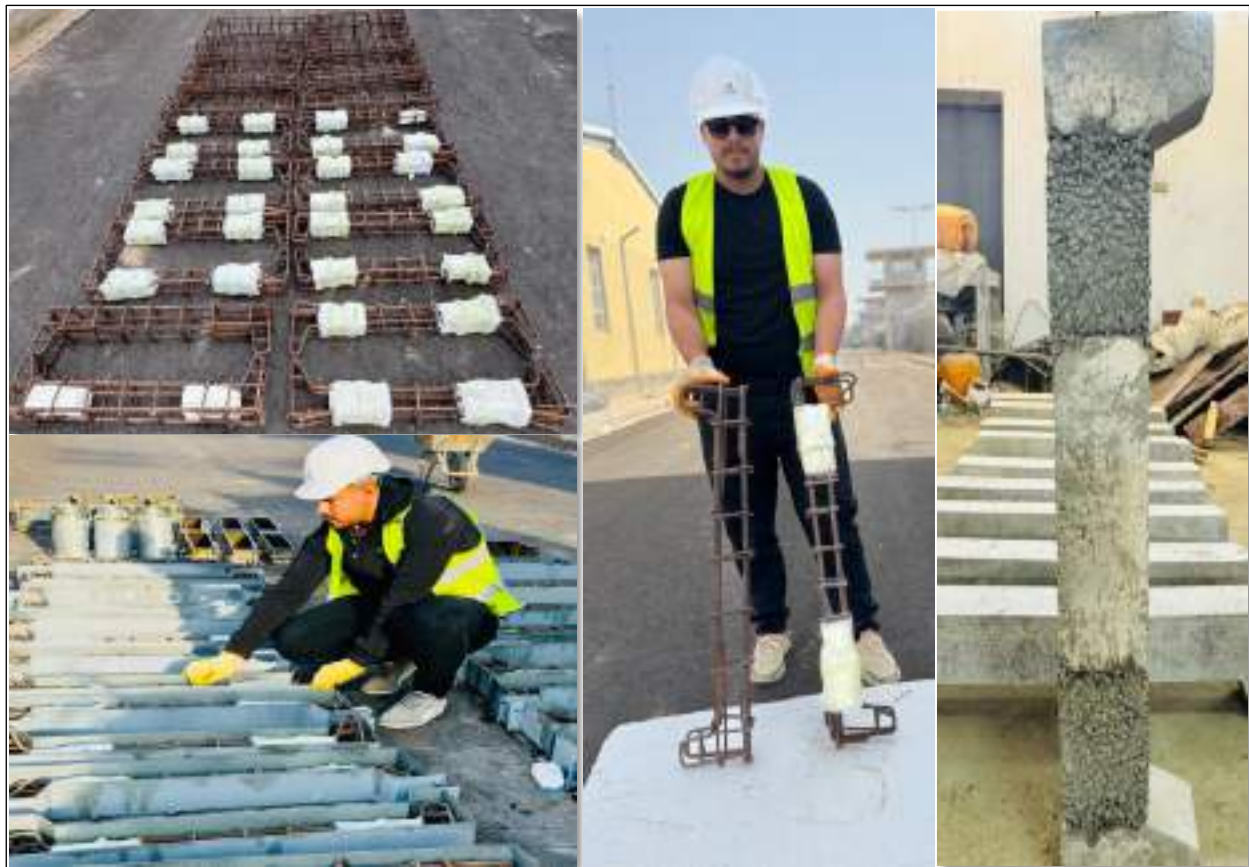


Figure 3.19 Honeycomb Zone Formation of Specimens.

3.5.5 Mix Proportion and Placement of NSC

The concrete was poured into the formwork at the Civil Engineering Laboratory at the University of Misan. Ready-mix normal-strength concrete ordered from a local concrete supplier was used, and the mix of NSC concrete was designed according to the American Method of Mix Proportions Selection (ACI Committee 211.1-91). Moreover, the detail of this mix is given in Table (3.15). The concrete was placed in three layers; each layer was compacted by applying a few seconds of vibrations using a mechanical vibrator to ensure even concrete dispersion in the formwork. After pouring the third layer, the concrete surface was finished with a wet trowel. The placement of the concrete into the formwork is shown in Fig. (3.20). Pouring the concrete into the sample molds was also required, see Fig. (3.21). A number of cube, cylinder and prism samples were cast and tested to determine the properties of the concrete. Standard procedures were used for the compaction of the conventional concrete for the cube, cylinder and prism molds in terms of the number of layers and rod. Six small cylinders with a 100 mm diameter were cast and tested under compression testing to obtain their compressive strength for 7 and 28-day strength. Three samples were tested at each age. Furthermore, six larger cylinders with a 150 mm diameter were cast for indirect tensile strength and six prisms 100 x 100 x 500 mm in size were cast for flexure strength testing. The indirect tensile, flexure strength, and other tests were conducted at 28 days. After pouring the concrete into the formworks and molds, a curing process was made to maintain a moist condition; therefore, the concrete hardening occurred gradually.

Table 3.15 Mix Proportion (Kg/m³).

Cement	Water	W/C	Sand	Gravel
470	200	0.43	675	1030



Figure 3.21 Pouring and Compacting Process of Concrete.



Figure 3.20 Concrete Casting into Sample molds.

3.5.6 Demolding and Curing Process of the Specimens

Continuing the casting process, all column specimens were placed under wet hessian rugs and covered with plastic sheets to maintain their moisture condition, as shown in Fig. (3.22). The curing process continued for 28 days. The small and large cylinders and cubes were taken out of the molds at one day and then stored in a curing tank until the 28-day testing. Finally, the prism samples were taken out of the molds after 2 days of casting and then placed in a curing tank until the 28-day testing. An extended period for demolding was required for the prisms as prism samples can be damaged more easily during demolding than cylinders.



Figure 3.22 Demolding and Curing Process of Specimens and Samples in Water Tank.

3.5.7 Mix Proportion and Process of HPFRC

The production of HPFRC involves the utilization of a high content of Portland cement, a very low water-to-cement ratio achieved by utilizing a high dosage of the most recent generation of superplasticizer, fine sand with a particle size ranging from 0.08 to 0.25 mm, and the inclusion of high reactivity silica fume. In this study, several mix proportions were evaluated to achieve the highest compressive strength according to (ASTM C109). The optimal mixture composition of HPFRC is presented in Table (3.16).

Table 3.16 Mix Proportions of HPFRC (Kg/m³).

Cement	Quartz Sand	Silica Fume	Water	Superplasticizer	Steel Fiber
900	775	200	198	27	156

The HPFRC specimens were subjected to trial mixes using a horizontal rotating mixer with a volume of 0.03 m³. The mixing process proposed in this work is illustrated in Fig. (3.23) and explained as follows:

1. Placing the sand into the mixer.
2. Dry mix silica fume and cement to distribute particles, then add to the mixer and mix for 5 minutes.
3. Super plasticizer was added to water and agitated, then added to the dry mix and mixed for 10 minutes.
4. The mixer was stopped and manual mixing was done for areas not reached by the blades.
5. The mixer performed. When flowable consistency is reached, steel fiber is gently added during mixer operation to ensure uniform dispersion for 5 minutes to produce reasonable fluidity.
6. The entire mixing process takes roughly 20 minutes.

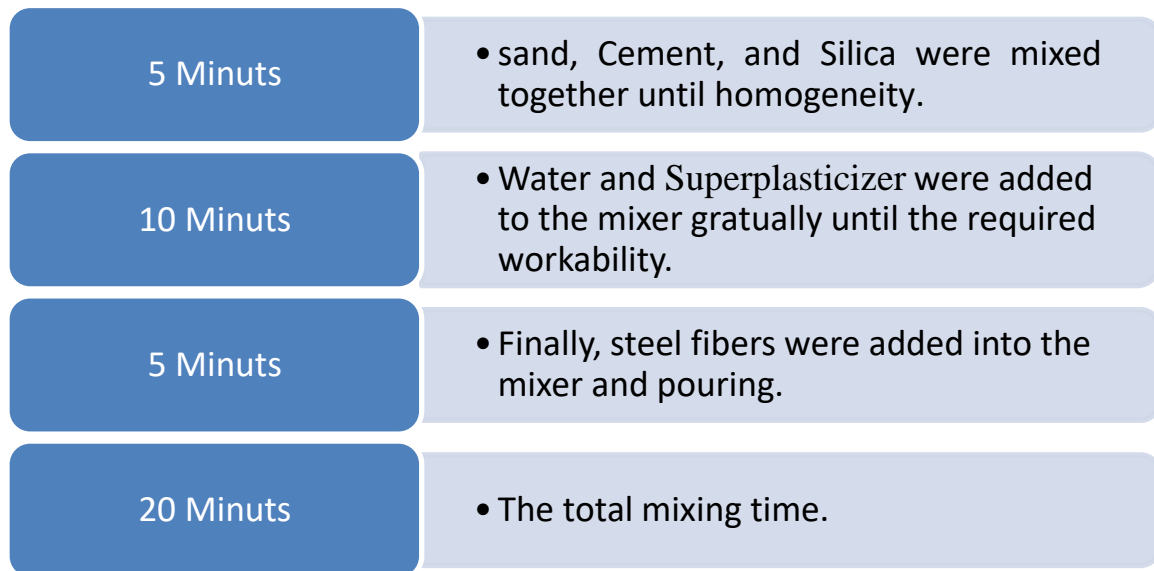


Figure 3.23 HPFRC Mixing Time Process.

3.6 Properties of NSC and HPFRC

Three types of tests, Compressive strength test, indirect tensile strength test, and modulus of rupture test, were undertaken on the concrete used in this study for casting the column specimens. The purpose of those tests was to determine the

mechanical of the concrete. The summary results of these tests are presented in Table (3.3). Moreover, the tests are matched to the specifications of ASTM and BS. The three tests are shown in Figs. (3.24-3.26), respectively.

Test of Compressive Strength

The compressive strength test was conducted in accordance with the standards (BS 1881: Part 116-1989) and (ASTM C39, 2019). A hydraulic compression machine with a maximum capacity of 2000 kN was used to test a total of 6 cubes measuring 150 mm and 6-cylinder specimens measuring 150×300 mm. The load was steadily and progressively applied at a consistent rate of 18 MPa per minute until failure ensued. The item can be found in the Constructional Materials Laboratory of the College of Engineering at Missan University. Figure 3.10 illustrates the compressive strength test. The compressive strength was determined by dividing the greatest load obtained during the test by the cross-sectional area of the specimen (P/A).

Test of Splitting tensile strength

The splitting test was conducted and evaluated in accordance with the ASTM C496 standard from 2011. A total of six cylinders measuring 150×300 mm was tested. Two bearing strips, each measuring 3.0 mm in thickness and 300 mm in length, were positioned above and below the specimen to create concentrated stress. This was done to apply a uniform load on the test surface of the cylinder, as depicted in **Fig. (3.10)**. The testing machine had a capacity of 2000 kN, and the load was applied steadily and without sudden impact until the cylinder failed. The expression of the “splitting tensile strength” was calculated by the equation:

$$f_{st} = \frac{2P}{\pi LD} \quad (3.1)$$

where f_{st} is splitting tensile strength in N/mm^2 , P is the load of compressive in N , D is the cylinder diameter in mm and L is the cylinder length in mm .

Modulus of Rupture Test (Flexural Strength)

Prisms made of concrete with dimensions of $100 \times 100 \times 500$ mm were created using the process outlined in ASTM C 78, 2019. 6 prisms were subjected to testing using a universal hydraulic machine with a maximum capacity of 2000 kN. The load was steadily and progressively raised at a steady pace until failure ensued. The item was accessible at the Constructional Materials Laboratory of the College of Engineering at Misan University. The flexural strength, measured as the modulus of rupture (M.O.R), was determined by analyzing the data acquired from a simple beam subjected to a two-point load.

The specimens' "Flexural strength" was determined with a precision of 0.01 MPa using the following formula:

- 1- To calculate the flexural strength, if a fracture occurs in the tension surface within the middle one-third of the span length, use the following formula:

$$f_{rt} = \frac{M_{max} Y_{max}}{I} = \frac{\frac{PL}{6} \cdot \frac{h}{2}}{\frac{bh^3}{12}} = \frac{PL}{bh^2} \quad (3.2)$$

where:

- f_r = The “modulus of rupture”.
- P = The maximum applied load, measured in Newtons.
- l = The distance between the centres, measured in millimetres.

- h = The mean depth of the specimen in millimetres.
 - b = the mean width of the specimen in millimetres.
- 2- If a fracture occurs outside the middle one-third of the span length by no more than 5%, the flexural strength is computed as follows:

$$F_{rt} = \frac{M_{max} Y_{max}}{I} = \frac{\frac{Pa}{2} \cdot \frac{h}{2}}{\frac{bh^3}{12}} = \frac{3Pa}{bh^2} \quad (3 - 3)$$

where a is the average tension surface prism distance between the failure crack and the nearest support.

- 3- If a fracture occurs outside the central one-third of the span length by more than 5%, the result is disregarded.

Table 3.17 Mechanical Properties of Test Results.

Type of Concrete	NSC	HPFRC
f_{cu} (MPa)	31	112.5
f_t (MPa)	3.67	13.4
f_r (MPa)	4.5	14.46
Slump (mm)	10	20

Where;

f_{cu} : compressive strength of cube at 28 days.

f_t : splitting tensile strength.

f_r : modulus of rupture.



Figure 3.24 The Compressive Strength Test.



Figure 3.25 Splitting Tensile Strength.



Figure 3.26 The Modulus of Rupture Test.

3.7 Strengthening of Column Specimens with HPFRC Jacketing and CFRP Wrapping.

3.7.1 Strengthening with HPFRC Jacketing

Before the strengthening process, the fabrication of the strengthened columns mainly includes the following steps:



Figure 3.27 HPFRC Strengthening Process.

1. Roughening the interface of the RC columns, and cleaning the concrete residue and powder on the interface.
2. Completing the secondary formwork erection for the column specimens, brushing the concrete interface treatment agent on the interface using Sikadure LB32 to ensure excellent adhesion between the normal concrete and HPFRC jackets then strengthening by HPFRC layer.

3. Use a tabletop electric vibrator to achieve optimal material properties, improved compaction, enhanced fiber dispersion, better surface finish, increased workability, and reliable defect detection.
4. Curing and testing of the strengthened specimens accordingly.
5. The above steps were repeated to cast jackets for all required specimens.

Furthermore, all steel formworks were well cleaned, and their internal surface was lightly oiled to prevent adhesion with hardened HPFRC. Steel formworks were manufactured with very accurate dimensions based on the required jacket thickness (15 and 30 mm) and the number of jacket faces (two and four). Strengthening steps are shown in Fig. (3.27).

3.7.1.1 Curing of Strengthened Specimens with HPFRC

After the casting process had been completed for one day, all of the formworks were opened, as depicted in Fig. (3.28). Following this, the specimens were immersed in a basin filled with water and kept at room temperature for a duration of 28 days. Following the completion of the 28-day period, samples are taken from the water, and the eccentric compression test is carried out.



Figure 3.28 Curing of HPFRC Jacketing Specimens.

3.7.2 Strengthening with CFRP Wrapping

Three column specimens were wrapped with CFRP sheets as strengthening material. Preparation was required before the wrapping process. The surface of the specimens was ground and cleaned with water and then left to dry. The CFRP was wrapped to the specimens by a wet lay-up procedure. The adhesive was prepared by mixing epoxy resin and slow hardener in a 1:4 ratio by the manufacturer's recommendation till the color is homogenous. The surface was coated first with a thin layer of epoxy resin (0.5-1 mm thickness), followed by the application of the first CFRP layer in a predefined orientation. An overlap of 100 mm was applied at the end of each strap in the transverse direction for all specimens. The wrapping configuration and wrapping process of the column specimens are shown in Fig. (3.29).

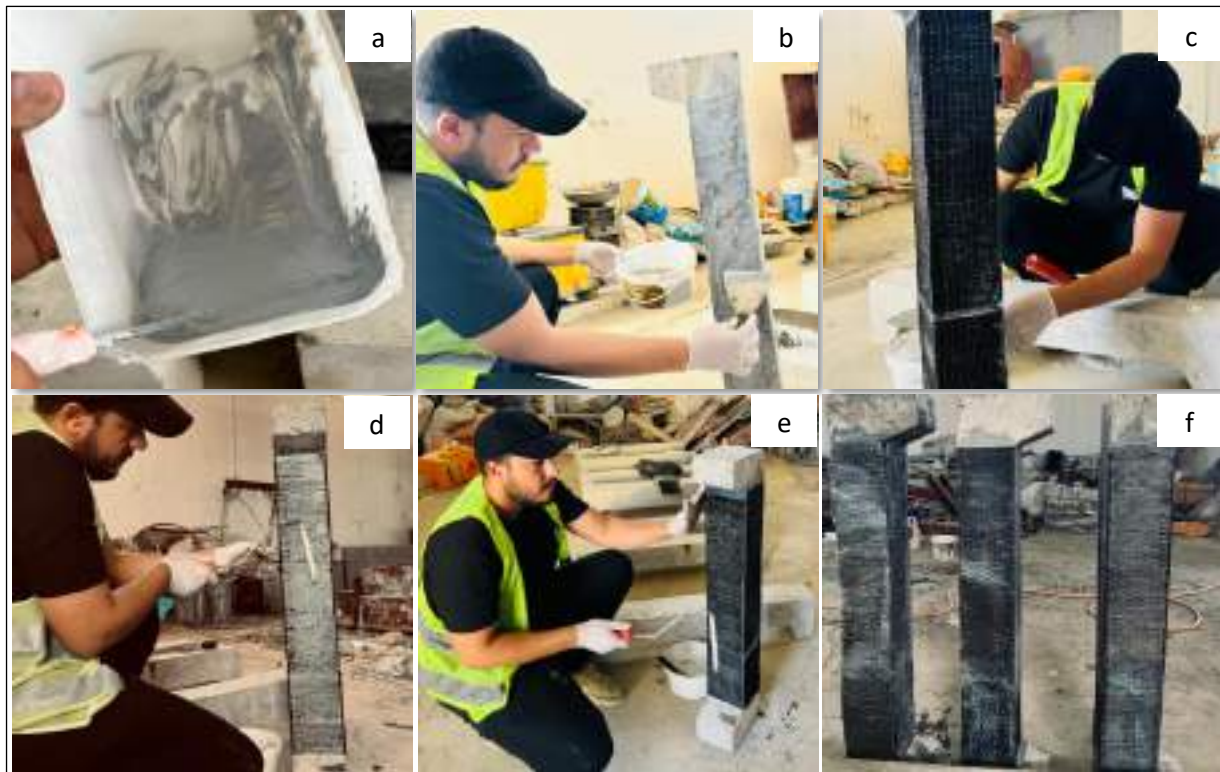


Figure 3.29 CFRP Wrapping Process.

3.7.2.1 Curing of Strengthened Specimens with CFRP

After that, the specimens that had been wrapped were laid out at room temperature for at least fourteen days to allow the epoxy glue to cure. Following that, the specimens were prepared to undergo compression and flexure testing, which was the next step in the testing process.

3.8 Painting the specimens after jacketing with HPFRC

Painting column specimens before testing was illustrated in Fig. (3.30) and serves several purposes like Identification, Visual Inspection, Measurement Accuracy and Aesthetics:



Figure 3.30 Painted Column Specimens.

3.9 Equipment and Instruments Used for Testing

3.9.1 Data logger series

The data logger system (GEODATALOG 30-WF6016) was used to record the strain gauge reading as shown in Fig. (3.31). The GEODATALOG 30-WF6016 is equipped with 16 channels for data obtaining, allowing the simultaneous measurement of multiple strain gauges or sensors. The data logger operates with a

power supply of 110-240 V at 50-60 Hz, single-phase. The data logger comes complete with DATACOMM software, which is installed on the personal computer. This software is specifically designed for PC data-obtaining systems, enabling the user to collect, monitor, and analyze the data obtained from the strain gauges.



Figure 3.31 Data Logger.

3.9.2 Deflection Measurement (LVDT)

A linear variable differential transformer (LVDT) was adopted as an instrument to measure the deflection in the tested column inside the test device with a capacity of 120 mm, as shown in Fig. (3.32). The concrete column was instrumented with two dial gauges with a magnetic base, the first one fixed vertically and the other fixed horizontally to denote the axial and lateral displacements. The accuracy of these dial gauges was 0.01 mm. A 0.000001mm transducer was added to the data logger series to save calculated data.



Figure 3.33 Installation of LDVT

3.9.3 Strain Gauge

Strain gauges were procured by Tokyo Sokki Kenkyujo Company Limited in Japan, as shown in Fig. (3.33). For the measurement of strains on the surface of the column, two strain gauges were digitally recorded by an electrical strain gauge and saved by a digital data collecting system. one strain gauge was positioned in the longitudinal direction, while the other was placed in the transverse direction of the column. The purpose of these strain gauges was to measure the strain experienced by the concrete under different loading conditions. The strain gauge was bonded using CN-E cyanoacrylate adhesive, which was cleaned and treated previously. The method of installation of the strain gauge is illustrated in Fig. (3.34). Since the readings were not recorded by the strain gauges for a certain number of specimens, the strain gauges results were neglected in this study.



Figure 3.35 Strain Gauge

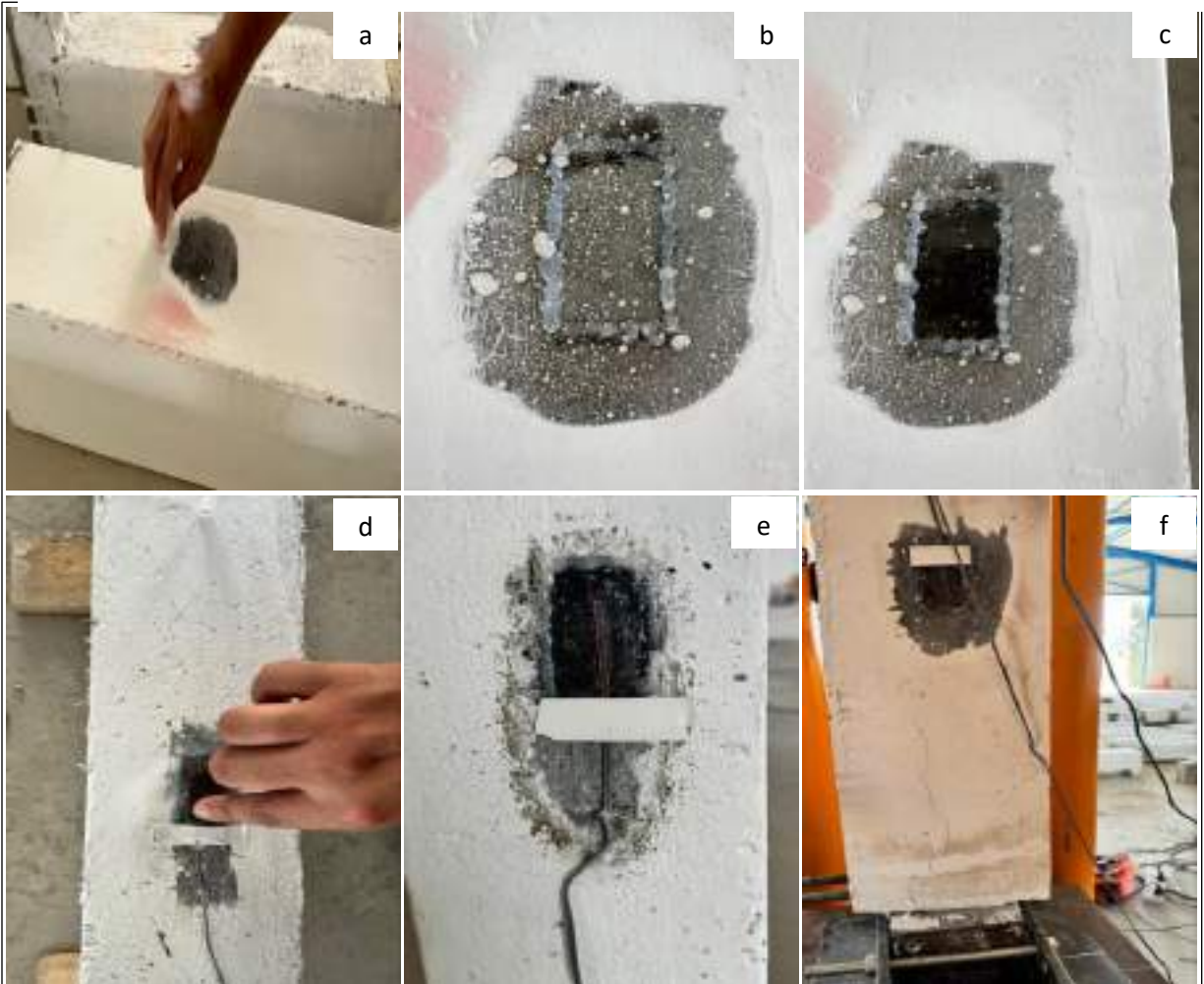


Figure 3.37 Steps of installation of Strain gage

3.9.4 Loading Head

Out of a total of thirty column specimens, twenty-nine were subjected to eccentric loading in this investigation. Two loading heads were specifically built to deliver eccentric loading to the column and prevent local failure at the corbel of the column specimen. One loading head was placed at the uppermost part of the specimen, while the other was placed at the lowermost part, as shown in Fig. (3.35).



Figure 3.38 Constructed Loading Head.

3.10 Column Specimens Testing Procedure

Prior to testing, it was customary to clean the surface of the column specimen and apply a coating to enhance crack visibility and clarify the crack path. All column specimens were tested by the ALFA Testing Machine with a maximum compressive capacity of 5000 kN. Afterward, the material was placed in a vertical position for testing. The centerline, supports, line loads, and LVDT were securely fastened in their respective positions. All the necessary equipment for conducting the testing was assembled as depicted in Fig. (3.36). The load was applied with a

small increment of about (8 kN) with an average of the ultimate applied load and the data logger to take the measurement each second. Cracks were found and drawn on test column faces. Visual concrete crack positions and loads were recorded. We tracked the initial crack width with loading. We recorded lateral deflections versus loads simultaneously for each load increment. Vertical dial gauges with 0.001 mm graduation and 50 mm needle length installed at the specimens' bottom bearing plates recorded the columns' axial deformation.

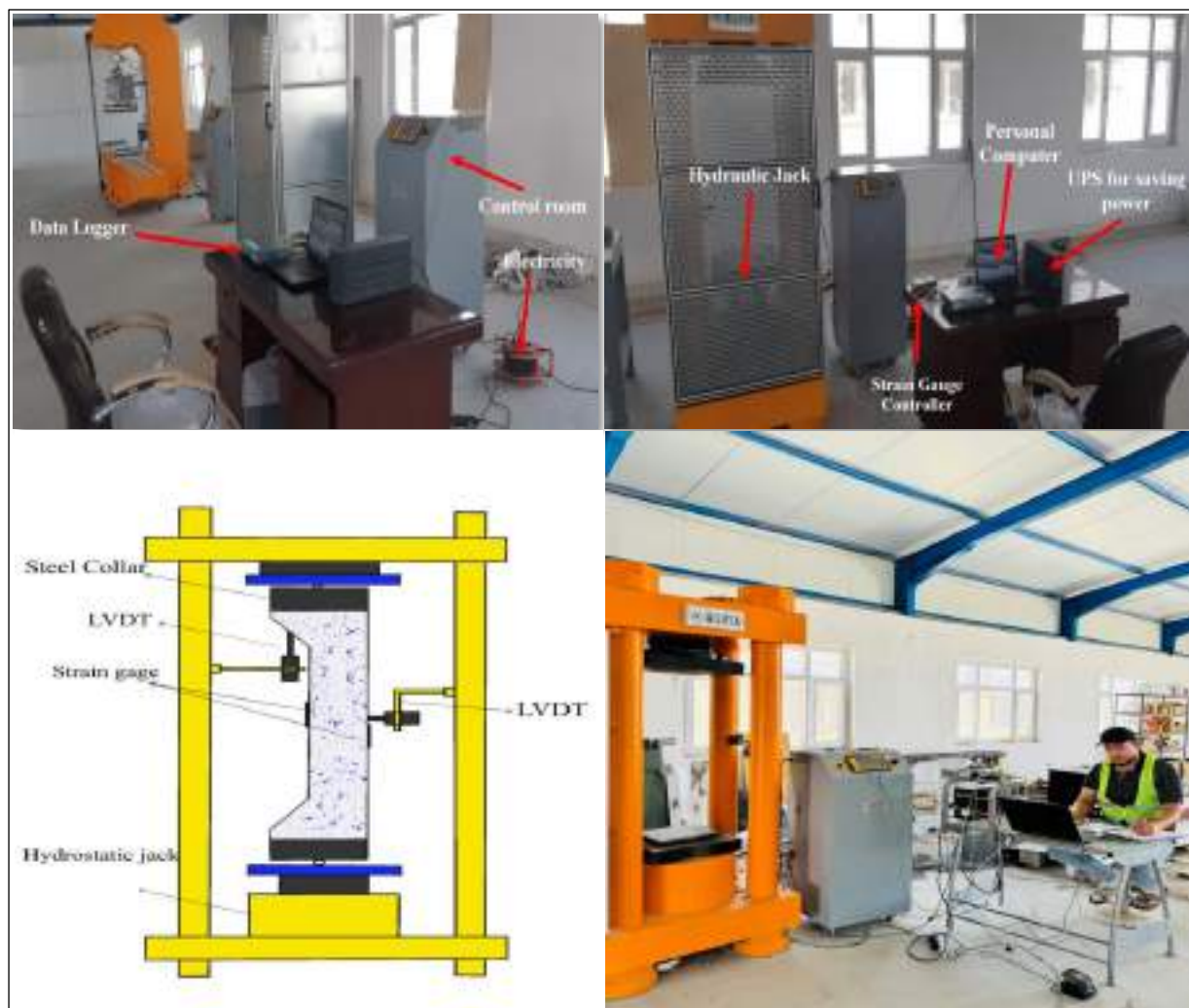


Figure 3.39 Setup of Typical Tested Specimens

Testing proceeded until the RC column's load capacity decreased with deformation. To study the behavior of RC columns under concentric and eccentric stresses, this study took into account three eccentricities (e): 0, 50, and 100 mm. The size and placement of the bearing steel plate were chosen so that the distance between the plate's center lines and the column section equals the desired eccentricity to obtain the necessary eccentricity value.

CHAPTER FOUR: RESULT AND DISCUSSION

4.1 General

In this study, a total of thirty reinforced concrete (RC) column specimens were created and examined. One specimen was subjected to axial compression load, while ninety-two specimens were subjected to eccentric loading, as described in Chapter Three. The specimens experienced testing at the Civil Engineering Laboratory located at The College of Engineering at Misan University. The **ALFA 5000 kN** compression testing machine was utilized to apply force. The data acquisition system, in connection with the testing apparatus, recorded the applied load, displacement, and strain. Several parameters are studied as follows:

- Load eccentricity (e).
- Jacket thickness.
- Strengthening face or side.
- The honeycomb damage ratio (%).
- Representing the honeycomb zone.

The effects of these parameters on the load-displacement relationship, crack pattern, modes of failure, and the ultimate loads are demonstrated. The results show load capacity, ductility, stiffness, toughness, and moment capacity behavior for all strengthened columns and compare them with the control specimen.

This chapter provides a detailed description of the experimental result study conducted on the compression testing of the column specimens. The results of the investigation are examined to provide a brief overview of how different parameters

impact the performance of square RC columns strengthened with HPFRC under eccentric loads.

4.2 Experimental Results

Every specimen underwent testing until it reached the point of failure. The load and displacement data were obtained by a data logger that was linked to the test equipment. The subsequent sections will examine the test findings of columns that were strengthened and those that were not strengthened. The efficiency of strengthening column specimens was evaluated by comparing the ultimate load, ultimate displacement, ultimate moment, fracture pattern and failure mechanism, ductility, stiffness, and toughness. The summary of the experimental program is illustrated in Table (4.1).

Table 4.1 The experimental results of specimens.

Group	Column ID	Pu (kN)	Ultimate Disp. (mm)		Change Load Carrying Capacity (%)	Stiffness (kN/mm)	Toughness (kN.mm)	Ductility Index
			Axial at top	Lateral at mid				
a	C1	317	9.00	0.00	-	35.22	2369.0	1.1
	C2	233	8.50	11.00	-	27.41	1601.0	1.3
	C3	115	8.00	10.25	-	14.38	777.0	1.0
	C4	425	7.50	10.50	-	56.67	1788.0	1.3
	C5	320	7.25	11.00	-	44.14	3069.0	1.4
	C6	450	7.00	10.25	-	64.29	3438.0	1.8
	C7	304	6.75	9.50	-	45.04	1381.0	1.0
b	C8	295	6.30	11.00	156.52	46.83	1218.3	1.3
	C9	199	5.75	10.25	73.04	34.61	961.0	1.2
	C10	315	4.70	9.50	173.91	67.02	1257.5	1.1
	C11	290	5.50	9.00	152.17	52.73	1120.0	1.1
c	C12	230	6.00	12.00	100.00	38.33	1145.0	1.2
	C13	140	5.00	11.50	21.74	28.00	745.3	1.7
	C14	330	4.60	10.50	186.96	71.74	1369.0	1.3
	C15	194	5.30	9.75	68.70	36.60	932	1.7

Continue

d	C16	215	6.00	11.00	86.96	35.83	987	1.1
	C17	125	6.25	10.50	8.70	20.00	841	2.1
	C18	401	5.3	10.25	72.10	75.66	2017	1.4
	C19	250	5.00	9.00	7.30	62.40	1141	1.5
e	C20	335	5.75	12.50	191.30	58.26	1735	1.3
	C21	270	4.80	11.00	134.78	56.25	1211	1.5
	C22	401	4.30	10.75	72.10	93.26	1545	1.3
	C23	312	5.50	9.50	33.91	45.45	1451	1.1
f	C24	313	5.70	11.50	172.17	54.91	1543	1.3
	C25	200	6.0	13.00	73.91	33.33	1004	1.2
	C26	520	5.00	10.00	352.17	104.00	2669	1.6
	C27	290	5.40	10.75	152.17	53.70	1460	1.4
g	C28	256	6.75	13.50	9.87	37.93	1780	1.5
	C29	125	5.60	11.50	8.70	22.32	641	1.4
	C30	132	6.20	13.25	14.78	21.29	686	1.6

4.2.1 Mode of Failure and Load-Displacement Relation

The crack paths and failure modes and the load versus displacement curves of the tested column specimens are illustrated in Figs. (4.1 - 4.7) respectively.

Group (a) consists of seven unstrengthened column specimens [C1 to C7]. The columns [C1, C3, C4, and C5] have the same failure mode approximately, damage appeared at the bottom end of the specimens when the ultimate load reached (317, 115, 425, and 320) kN respectively as a compression failure with an axial displacement of (9, 8, 7.5, and 7.25) mm respectively and a lateral displacement of (0, 10.25, 10.5, and 11) mm respectively. The columns [C2 and C6] have the same failure mode as well, failing in compression at the top end of the specimens with cover deterioration when the ultimate load reached (233 and 450) kN. They recorded an axial displacement of (8.5 and 7) mm and a lateral displacement of (11 and 10.25) mm. Finally, the column [C7] failed in compression at the middle part of the specimen at the compression side with the

appearance of small cracks along the column surface with an ultimate load of 304 kN and an axial and a lateral displacement of (6.75 and 9.5) mm.

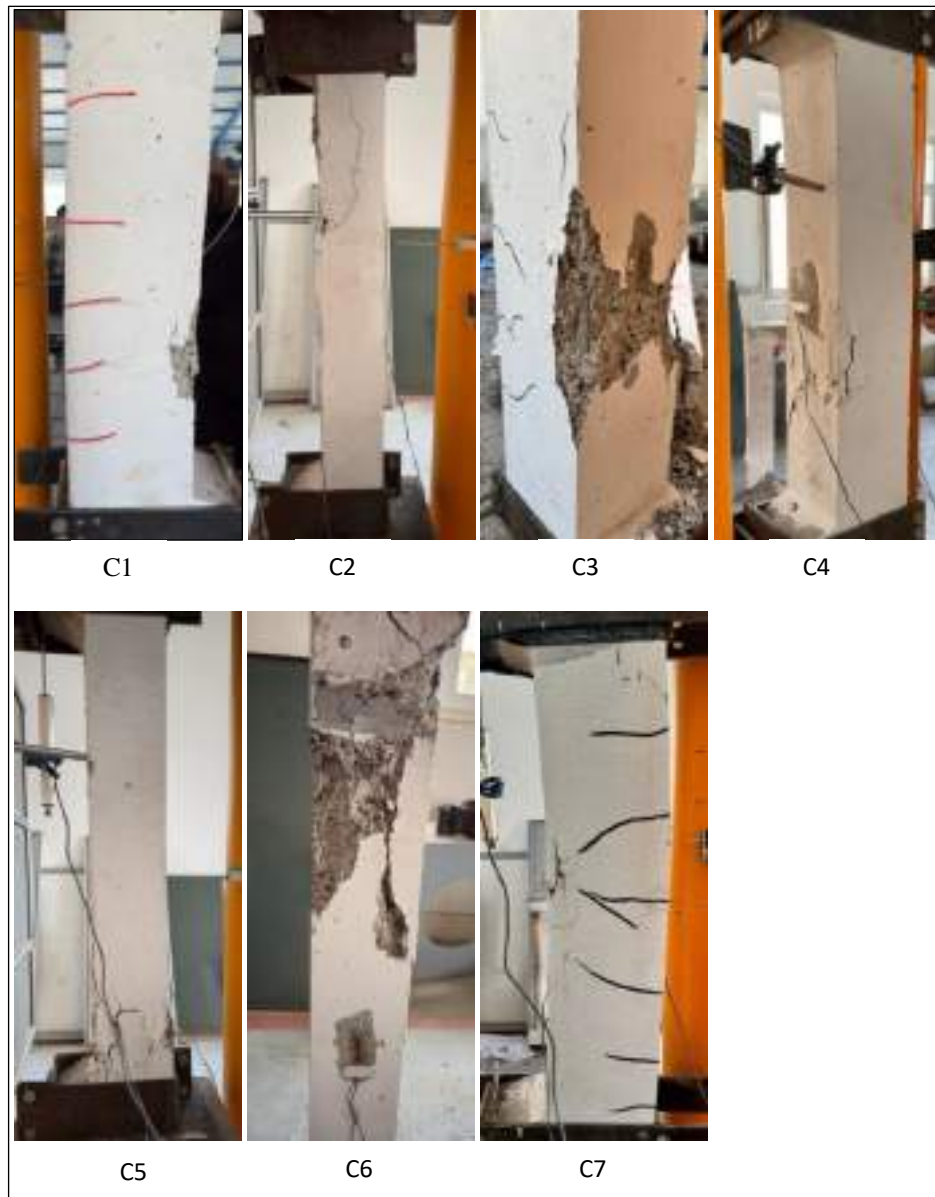


Figure 4.1 Mode Failure and Cracks Pattern for Group a Reference columns.

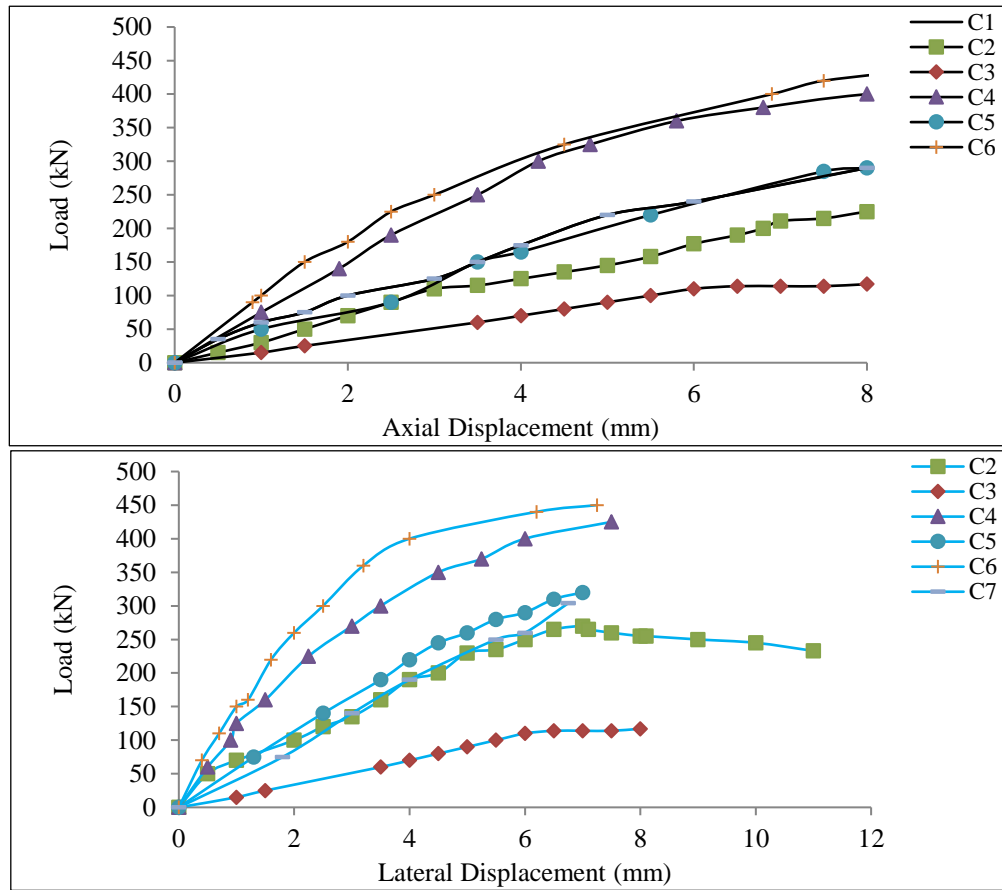


Figure 4.2 Load-Displacement Curve for Group a Reference columns.

Group (b) consists of four strengthened HPFRC column specimens [C8 to C11]. The honeycomb defect ratio of these specimens was 0%. The failure of the column specimens was caused by cracks that ran horizontally along the height of the column and cracks that ran diagonally at the extremities of the effective length of the specimens. Failure started with the appearance of microscopic cracks on the surface of the HPFRC jacket, and it proceeded with the deterioration of the column substrate. Finally, the failure of the specimens occurred as a result of the compression of the material. The ultimate load of specimens [C8, C9, C10, and

C11] were (295, 199, 315, and 290) kN, respectively. Moreover, they recorded an axial displacement of (6.3, 5.75, 4.7, and 5.5) mm, respectively, and a lateral displacement of (11, 10.25, 9.5, and 9) mm. The specimen C10 gained the highest load capacity due to the strengthening with HPFRC in comparison with the reference C3.

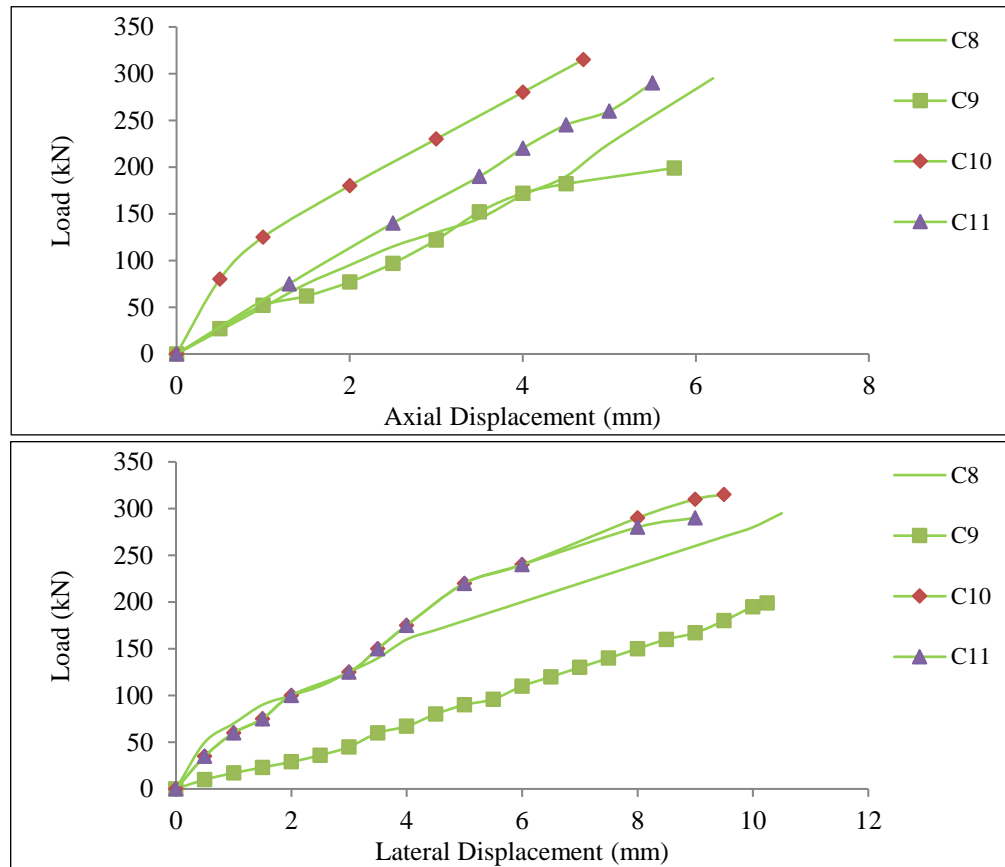


Figure 4.3 Load-Displacement Curve for Group b 0% Defect Ratio.

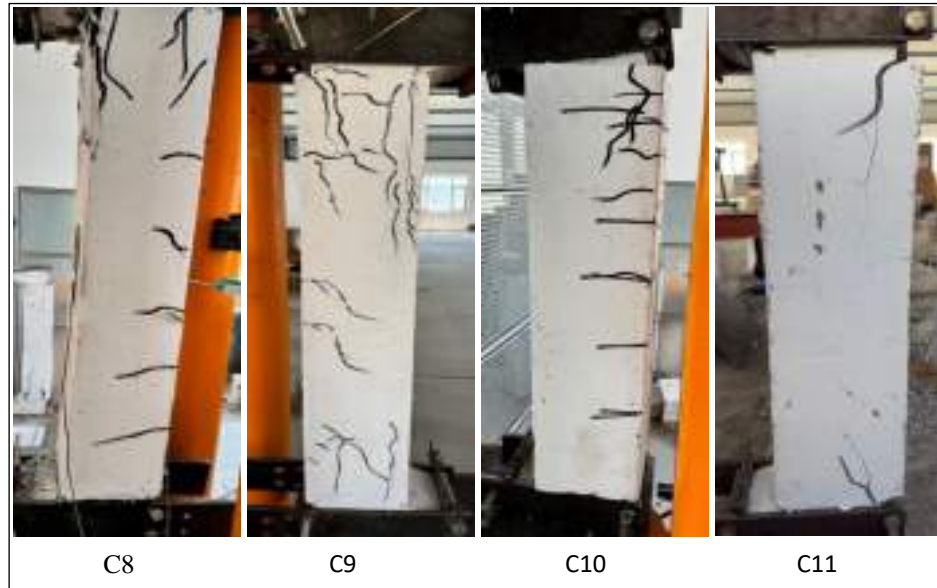


Figure 4.4 Mode Failure and Cracks Pattern for Group b 0% Defect Ratio.

Group (c) consists of four strengthened HPFRC column specimens [C12 to C15]. The honeycomb defect ratio of these specimens was 35%, represented by foam material. The column [C12] failed locally by compression at the upper part of the specimens at the compression side without detachment of the new HPFRC layer, accompanied by small cracks that were checked by visible eye. The ultimate load capacity was 230 kN and the axial and lateral displacement were of (6 and 12) mm. The column specimen [C13], the first crack started at the bottom of the specimen and the number of cracks started increasing gradually. Up to 90% of the maximum load-carrying capacity was loaded, the outside of the jacket developed warning indicators before collapse. The ultimate load capacity was 140 kN, and the axial and a lateral displacement of (5 and 11.5) mm. A similar pattern of group (b) was observed in the column specimen [C14].



Figure 4.5 Mode Failure and Cracks Pattern for Group c 35% Defect Ratio Foam.

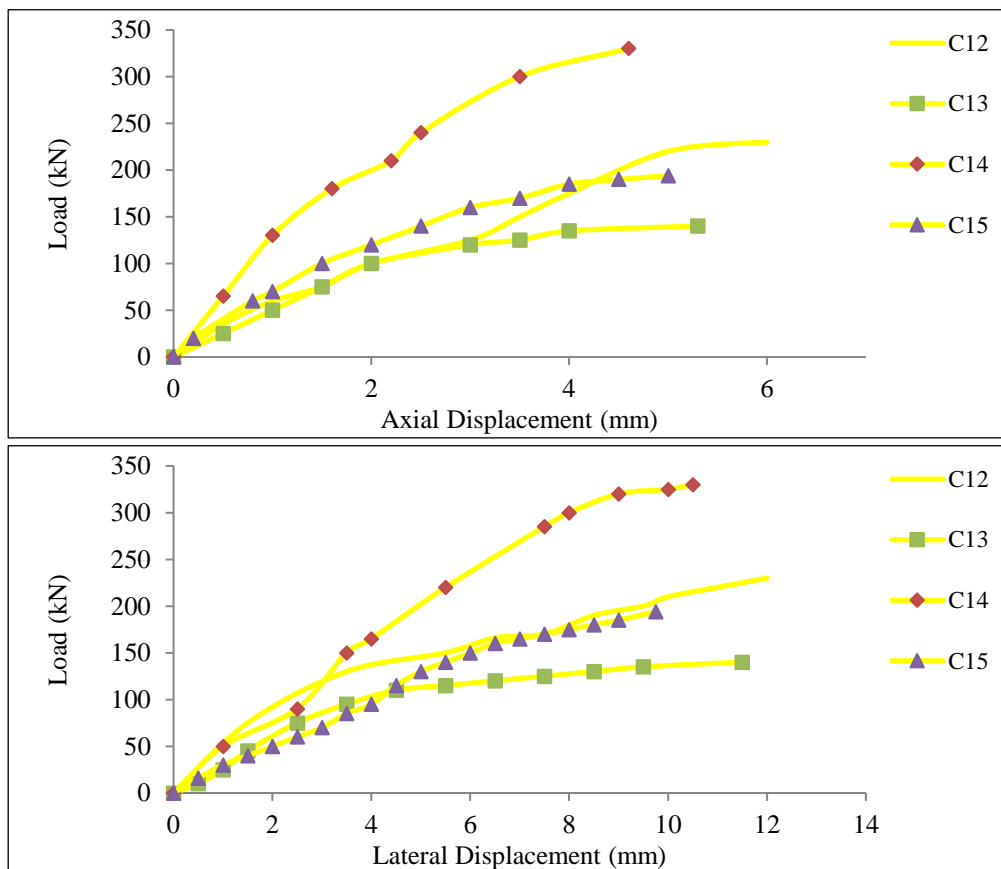


Figure 4.6 Load-Displacement Curve for Group c 35% Defect Ratio.

The HPFRC jackets and concrete substrate developed vertical cracks in the area of the honeycomb fault on top of the column specimen [C15] when its resistance reached its maximum value of 194 kN and maximum axial and lateral displacement of (5.3 and 9.75) mm. Therefore, the main failure mode of this column was shearing failure.

Group (d) consists of four strengthened HPFRC column specimens [C16 to C19]. The honeycomb defect ratio of these specimens was 70%, represented by foam material. The columns [C16 and C17] exhibited failure by compression and spalling of the concrete at both ends. The specimens failed because of vertical and horizontal cracks along the height of the column on both sides. Failure started with the appearance of microscopic cracks on the surface of the HPFRC jacket and then progressed to the substrate layer. Then, the specimens failed due to compression. According to the test results, they recorded an ultimate load of (215 and 125) kN, an axial displacement of (6 and 6.25) mm, respectively, and a lateral displacement of (11 and 10.5) mm. The damage to column [C18] appeared at the bottom end of the specimen. The steel of the stirrups started to yield, and cracks were initiated by increasing the compressive load. Then, the vertical reinforcement started to buckle and yield at the ultimate load of 401 kN. This column recorded the highest load capacity in this group in comparison to reference [C2] due to the effect of eccentricity (50 mm) and the strengthening thickness (30 mm). On the contrary, the column [C19], failed at the upper end of the specimen compressively with the appearance of small cracks on the surface of the column as well as deteriorated the cover of the column until reaching the maximum load of 250 kN with a maximum axial and lateral displacement of (5 and 9) mm.

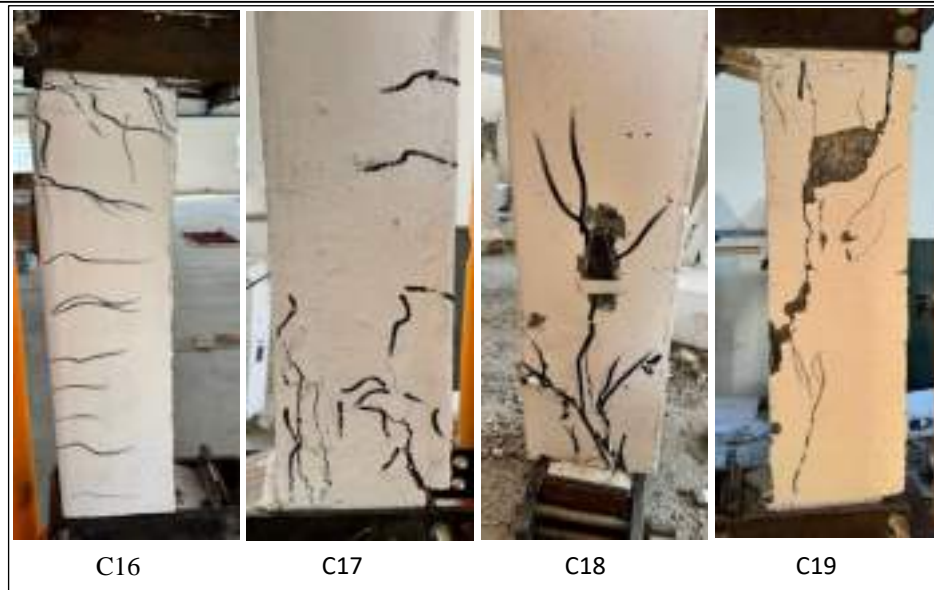


Figure 4.7 Mode Failure and Cracks Pattern for Group d 70% Defect Ratio Foam.

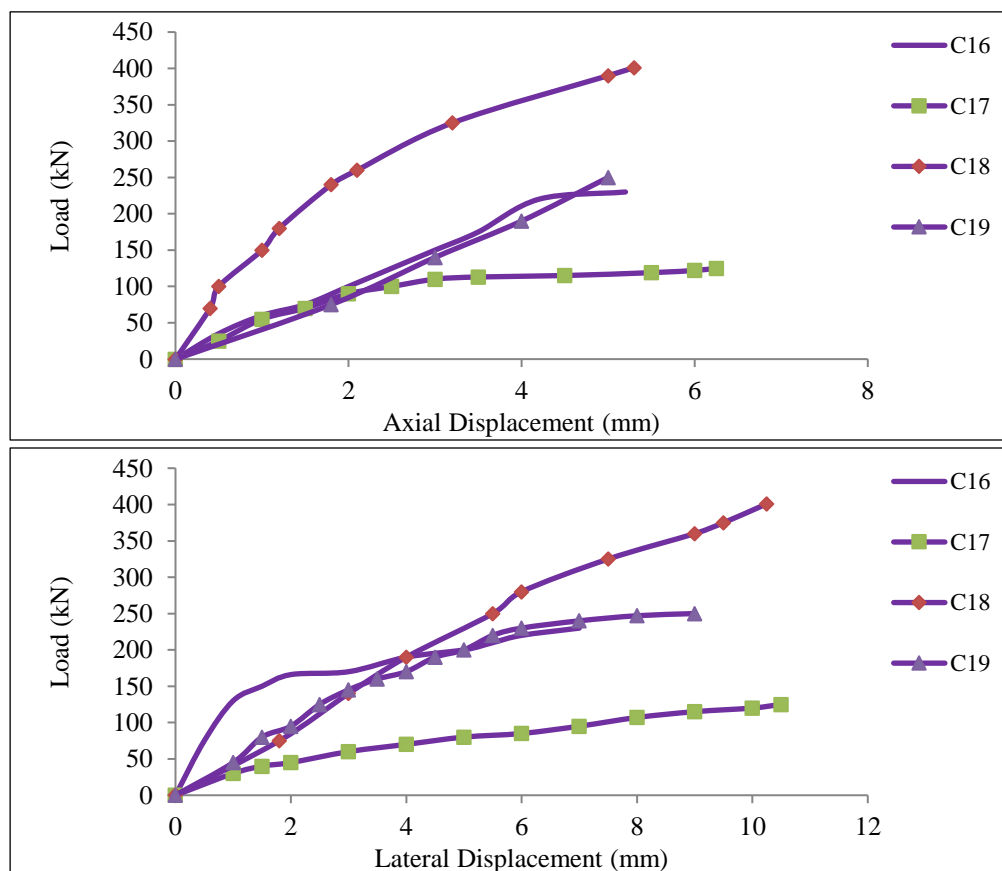


Figure 4.8 Load-Displacement Curve for Group d 70% Defect Ratio.

Group (e) consists of four strengthened HPFRC column specimens [C20 to C23]. The honeycomb defect ratio of these specimens was 70%, represented by foam material such as in groups (c and d). The column [C20] exhibited the same mode failure of specimens [C16 and C17] but the difference in the gaining of ultimate load, where recorded of 335 kN and maximum axial and lateral displacement of (5.75 and 12.5) mm. The column [C21] exhibited failure at a load value above that of the control column. Upon the initiation of cracks on both sides of the upper base at the front and back, the ultimate load was 270 kN, and the concrete substrate displayed diagonal shear cracks in the top and bottom portion of the honeycomb defect zone of the column upon reaching the maximum failure load. Consequently, the primary mechanism of failure for this column was shear failure. The columns [C22 and C23] failed at the end-top of the column at the compression zone due to the stresses focused in this section, with visible cracks appearing parallel to the column axis on the outer surface of the column. Eventually, crushing the concrete and steel achieved the yield strain.

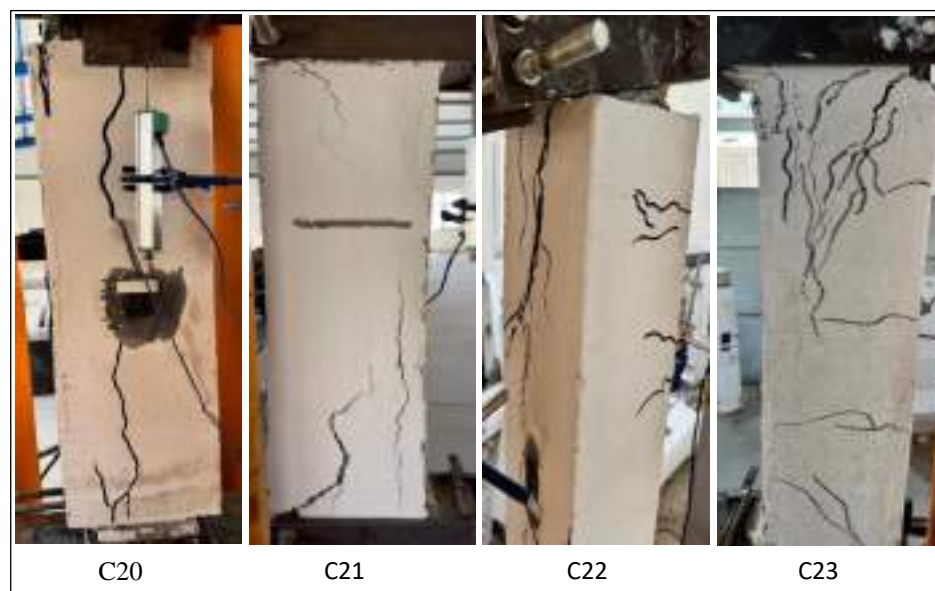


Figure 4.9 Mode Failure and Cracks Pattern for Group e 70% Defect Ratio Foam.

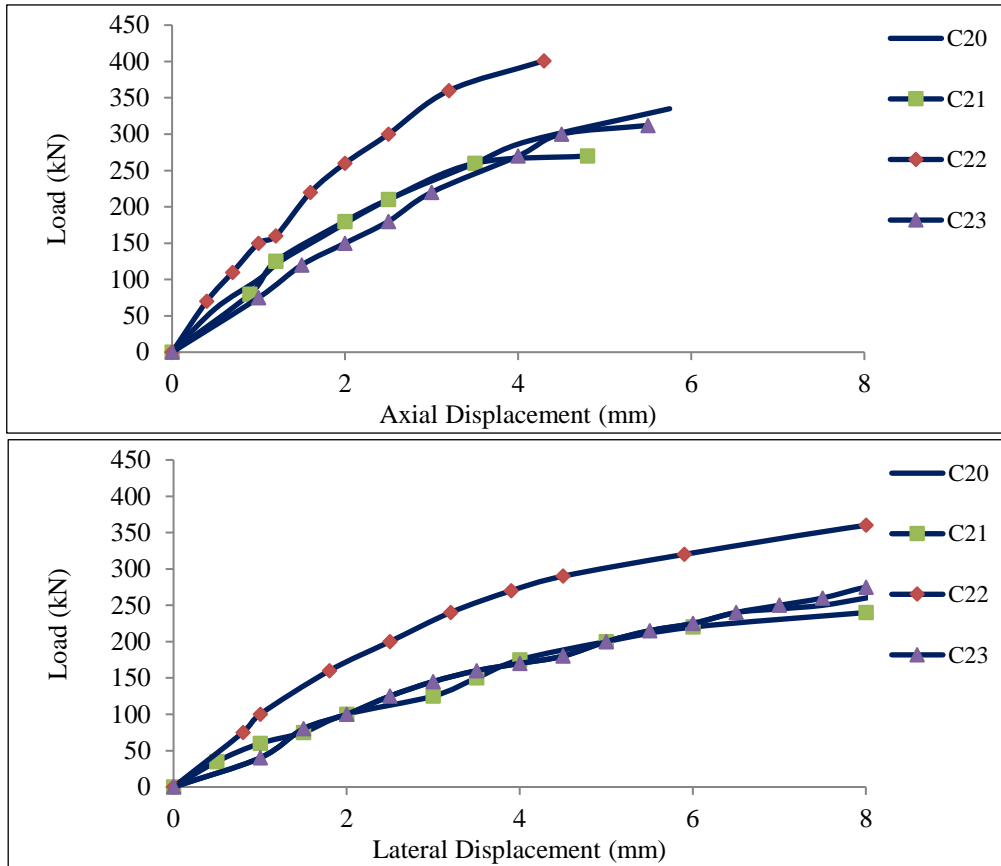


Figure 4.10 Load-Displacement Curve for Group e 70% Defect Ratio.

Group (f) consists of four strengthened HPFRC column specimens [C24 to C27]. The honeycomb defect ratio of these specimens was 70%, represented by weak-strength concrete. The failure of columns [C24, C25, and C26] strengthened only with a HPFRC jacket occurred by vertical cracks along the height of the column. failure began with emerging small cracks on the surface of the HPFRC jacket and then continued by the rupturing of the substrate. The location of the substrate rupture in most of the specimens occurred around the end-height of the specimens. started to fail after the failure of the HPFRC jacket with some vertical and diagonal cracks, and the failure of the specimens happened due to the crushing. The maximum load of these specimens was recorded (313, 200, and 520) kN with an axial and lateral displacement of (5.7, 6, and 5) mm respectively, and (11.5, 13,

and 10) mm respectively. The column [C26] gained the largest load capacity in comparison to the reference C3. The column [C27] failed mainly due to compression failure. The cracks were propagated above the lower corbel, in which crushing of large portions of the concrete cover on the compression side occurred with notice before failure.

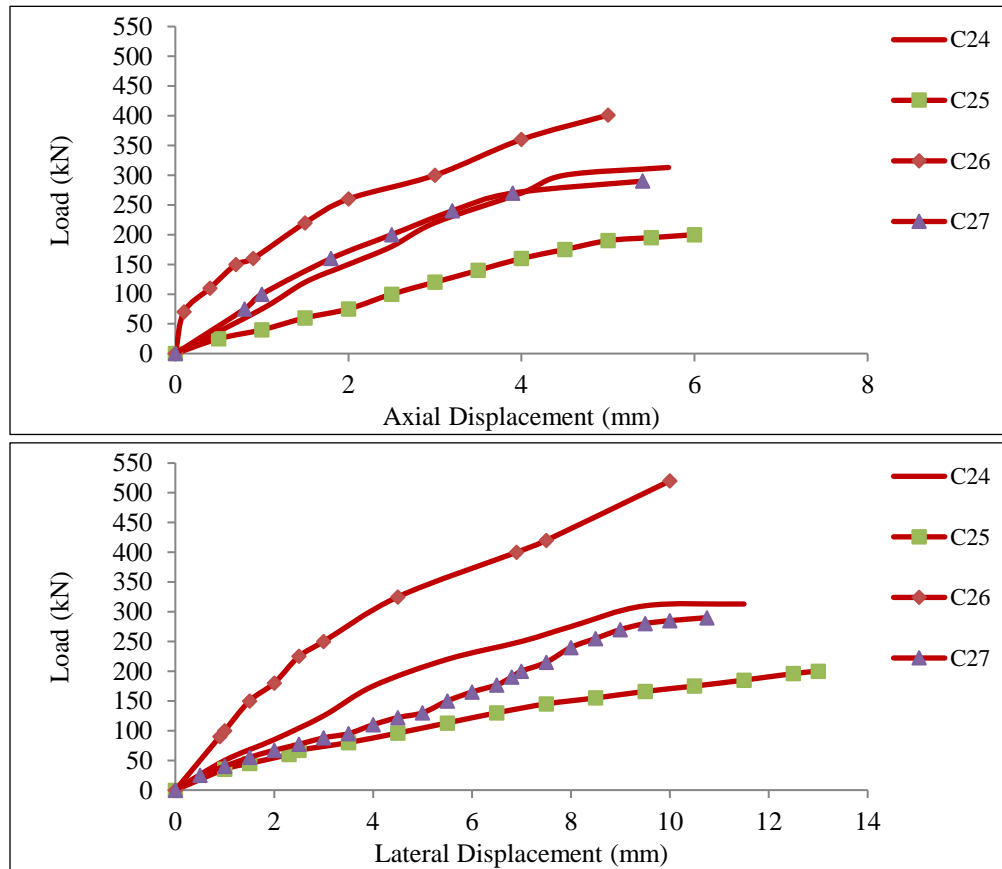


Figure 4.11 Load-Displacement Curve for Group f 70% Defect Ratio.



Figure 4.12 Mode Failure and Cracks Pattern for Group f 70% Defect Ratio WSC.

Group (g) consists of three strengthened CFRP column specimens [C28 to C30]. For the column specimens [C28, C29, and C30] strengthened with CFRP sheets, snapping sounds were heard before the ultimate failure, revealing the rupture of CFRP composites. This type of failure was explosive but not sudden, and the CFRP composites failed due to the expanded concrete. According to the results, these column specimens recorded the ultimate load of (256, 125, and 132) kN, respectively, with an axial and lateral displacement of (6.75, 5.6, and 6.2) mm and (13.5, 11.5, and 13.25) mm, respectively.

In general, the effect of fibers in tested columns makes the crack extension slower and the specimen still maintains greater rigidity. Tensile cracks propagated with an increase of applied load.



Figure 4.13 Mode Failure and Cracks Pattern for Group g 70% Defect Ratio.

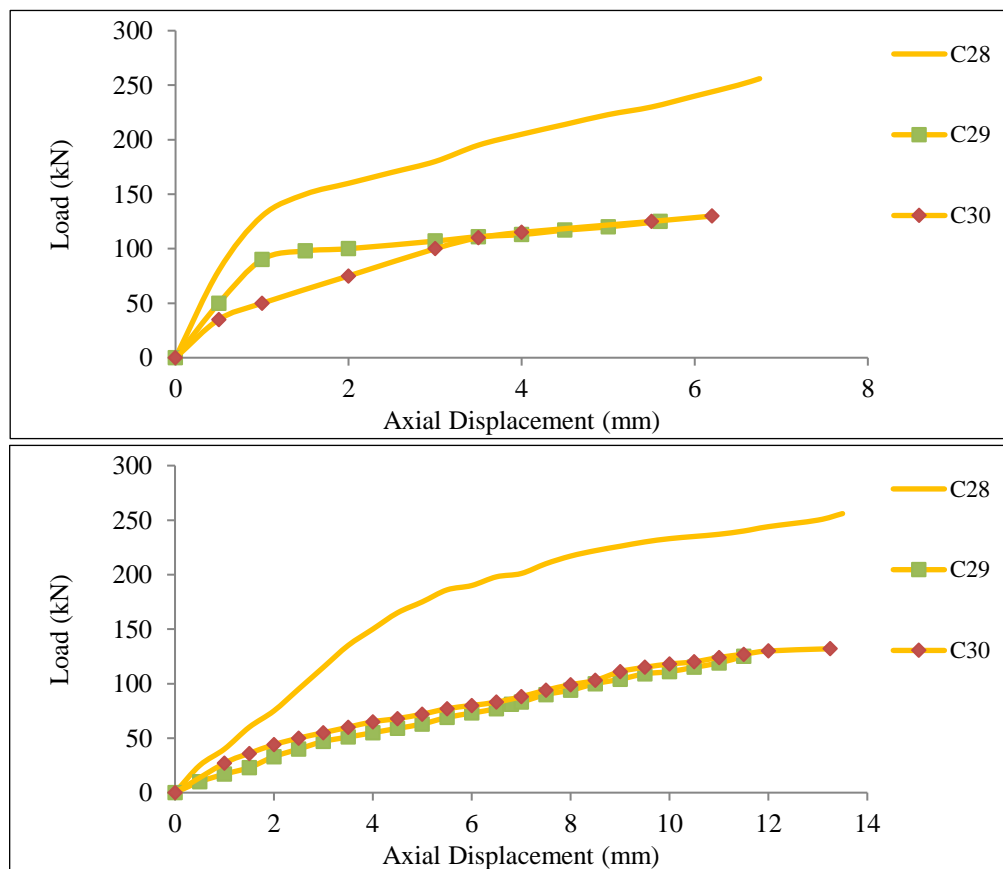


Figure 4.14 Load-Displacement Curve for Group g 70% Defect Ratio.

4.3 Discussion of Experimental Results

4.3.1 Load-Displacement Relationships

As described above, the strengthened columns proved an increase in the load-carrying capacity, ductility, stiffness, and toughness. The full casting scheme using HPFRC jacketing was more effective than bonding laminates. The slope of strengthened columns is higher than that of the control specimen at different eccentricities. It was found that the load-displacement response was bilinear up to the ultimate load and could be divided into uncracked and cracked stages. All specimens showed the same behavior in the uncracked stage, while the post-cracking behavior appeared to be different.

As can be seen the loading to axial and lateral displacement for the reference columns, HPFRC jacketed columns led to the ductile behavior of the strengthened columns as a result of the presence steel fibers. It can be seen that the load-lateral displacement curve behaved linearly from the initial loading up to the maximum load; this stage increased with increasing HPFRC jackets.

The post-peak region became more obvious with increasing the eccentricity as the flexural behaviors govern in the columns. The lateral deflection is decreased with increasing HPFRC thickness. The strengthened specimens exhibited much stiffer responses and lower deflection than the control specimen. The results show that increasing the thickness of HPFRC jacketing causes a decrease in displacements at the same load.

4.3.2 Axial Load Capacity

The ultimate load and the corresponding displacement for all specimens are summarized in Table (4.1). From this table, it can be seen that for all the specimens strengthening with HPFRC, the load ratio P_{cs}/P_{co} is always larger than one. Results

show that the gain in column strength decreased with a nominal increase in eccentricity. The full casting that used a HPFRC jacket was highly effective as a strengthening scheme. The thickness of the HPFRC jackets moderately improved the efficiency of strengthening columns. The gain in strength of strengthened columns is proportional to the thickness of the HPFRC jacket. This was also confirmed by authors [58-59]. As shown in Table (4.1), increasing the thickness of the HPFRC jacket from 15 mm to 30 mm with 0.00 % honeycomb defect ratio (C8 and C10) resulted in an increase in gain of column strength from 156.2% to 173.91%, and for specimens (C9 and C11) increase in gain of column strength ranged from 73.04% to 152.17%. Moreover, the specimens with a 35 % honeycomb defect ratio (C12 and C14) resulted in an increase in gain of column strength from 100% to 186.96%, and for specimens (C13 and C15) an increase in gain of column strength from 21.74% to 68.7%. Meanwhile, the gain in strength for specimens (C16 and C20) with a 70 % honeycomb defect ratio increased from 86.96% to 191.3%, respectively. In addition, the results indicated that the load capacity of strengthened columns with HPFRC laminates on 4-sides was higher than that of strengthened columns with HPFRC laminate on both tension and compression sides. The improvement in column strength is attributed to the increased thickness of the UHPFC jacketing, which results in an increase in the cross-sectional dimensions, as well as higher mechanical properties (compressive and tensile strengths) of HPFRC as a result of the presence of steel fiber. The roughening of the column surface improves the bond strength between the column core and HPFRC layers, leading to a higher increase in column strength. The gaining strength of the strengthening column specimens is shown in Figs. (4-14 to 4.19).

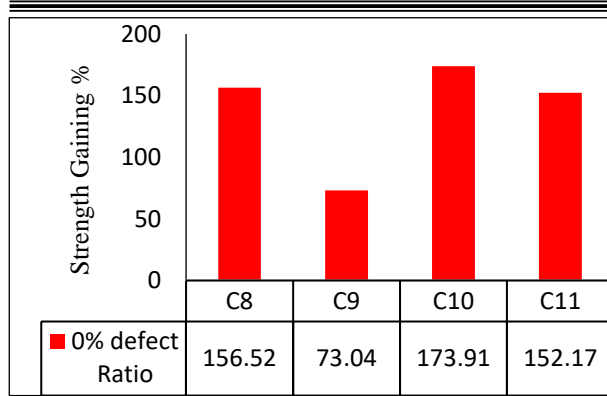


Figure 4.17 Gaining in Strength for group b.

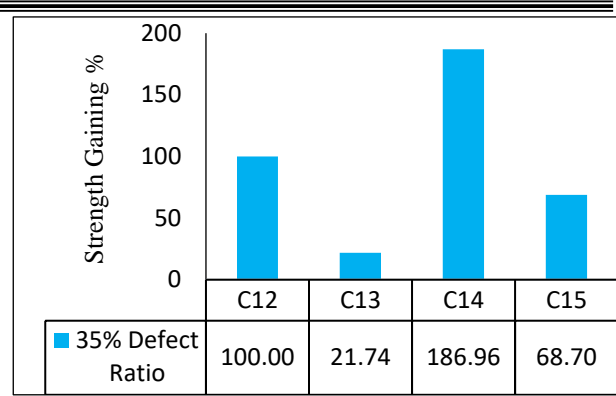


Figure 4.18 Gaining in Strength for group c.

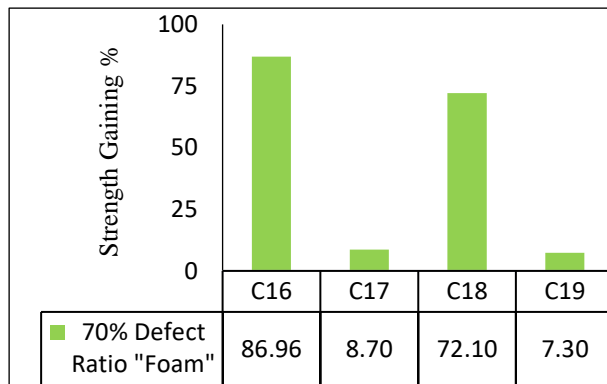


Figure 4.16 Gaining in Strength for group d.

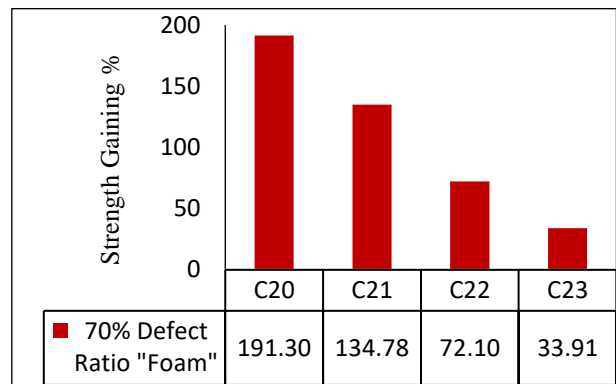


Figure 4.15 Gaining in Strength for group e.

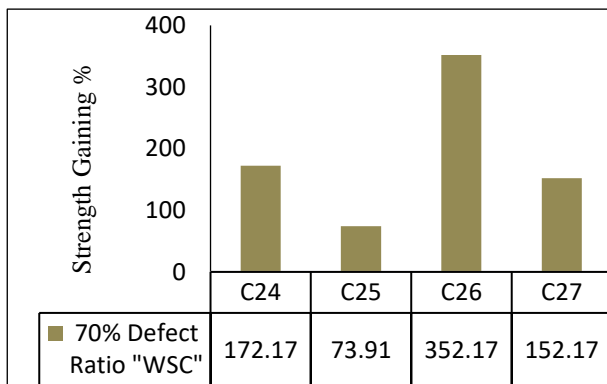


Figure 4.19 Gaining in Strength for group f.

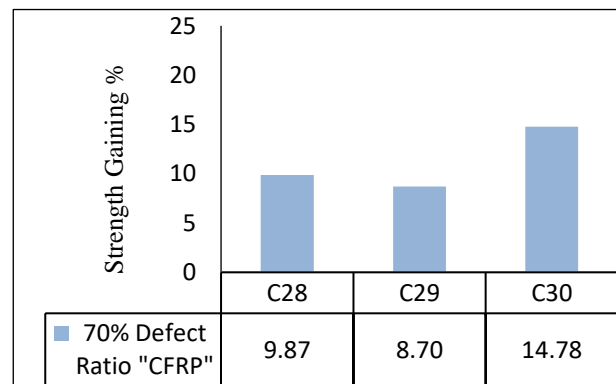


Figure 4.20 Gaining in Strength for group g.

4.3.3 Ductility Index

Ductility is defined as the measure of a material's capacity to undergo plastic deformation before fracture, and for a column subjected to an axial load, it is a measure of how much loss of load-carrying capacity occurs under increasing axial deformation once the cover region begins to fail. The ductility index is associated with the material's ability to stretch or elongate, while stiffness is related to the material's resistance to bending or flexing. The ductility of the tested columns was computed using the approach developed by considering a displacement ductility ratio as an index; these approaches were proposed by [65]. They defined the displacement ductility as the ratio between the displacement at peak load (Δu) and the yield displacement (Δy), as presented in Fig. (4.20). The notional yield displacement (Δy) is defined as the intersection of a line passing through a point on the load-displacement curve corresponding to 75% of the maximum applied load on the specimen ($0.75P_u$) extended to intersect with the horizontal line at (P_u). The displacement ductility index ($\Delta \mu$) can be calculated according to the equation below.

$$\Delta \mu = \Delta u / \Delta y \text{ ----- (4-1).}$$

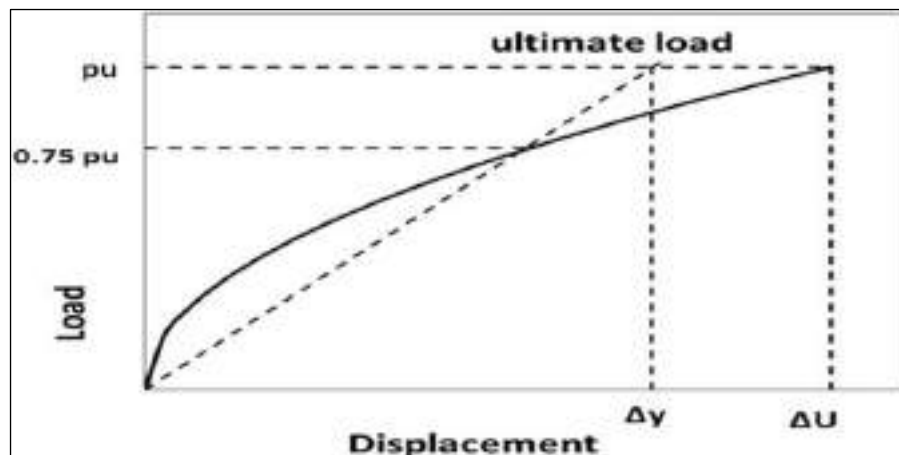


Figure 4.21 Determination Procedures of Column Ductility Displacement.

The results of the ductility index of columns are listed in Table (4.2) and Figs. (4.21 – 4.26)

Table 4.2 Ductility index of column specimens.

Group	Column ID	Δ_y mm	Δ_u mm	$\Delta\mu$
Group a	C1	7.95	9.00	1.13
	C2	6.50	8.50	1.31
	C3	7.85	8.00	1.02
	C4	5.92	7.50	1.27
	C5	5.20	7.25	1.39
	C6	3.95	7.00	1.77
	C7	6.50	6.75	1.04
Group b	C8	5.00	6.30	1.26
	C9	4.65	5.75	1.24
	C10	4.20	4.70	1.12
	C11	5.20	5.50	1.06
Group c	C12	5.20	6.00	1.15
	C13	3.00	5.00	1.67
	C14	3.50	4.60	1.31
	C15	3.03	5.30	1.75
Group d	C16	5.50	6.00	1.09
	C17	2.95	6.25	2.12
	C18	3.70	5.30	1.43
	C19	3.78	5.50	1.46
Group e	C20	4.40	5.75	1.31
	C21	3.20	4.80	1.50
	C22	3.35	4.30	1.28
	C23	4.40	5.00	1.14
Group f	C24	4.37	5.70	1.30
	C25	5.00	6.00	1.20
	C26	3.13	5.00	1.60
	C27	3.74	5.40	1.44
Group g	C28	4.50	6.75	1.50
	C29	4.00	5.60	1.40
	C30	3.95	6.20	1.57

The results showed that increasing (the thickness, and the number of sides) of the HPFRC jacket improves ductility because the HPFRC-contented steel fibers enhance the ductility, prevent sudden failure, and delay the appearance of cracks in columns.

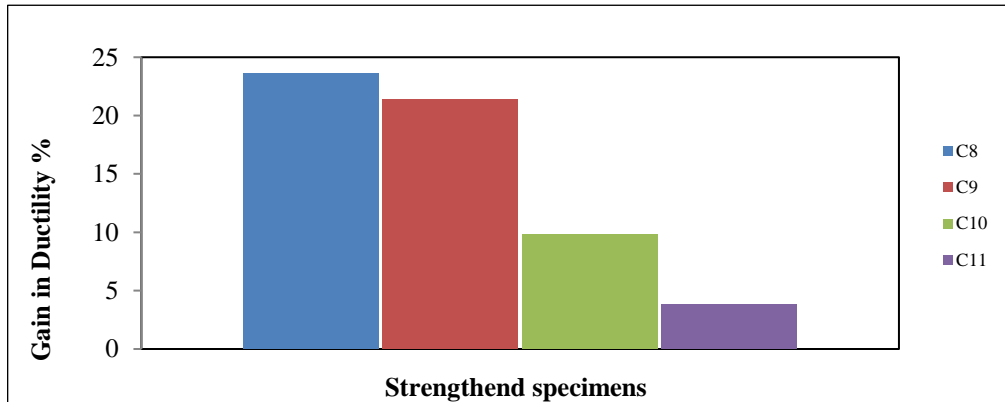


Figure 4.22 Gaining in Ductility for Group b.

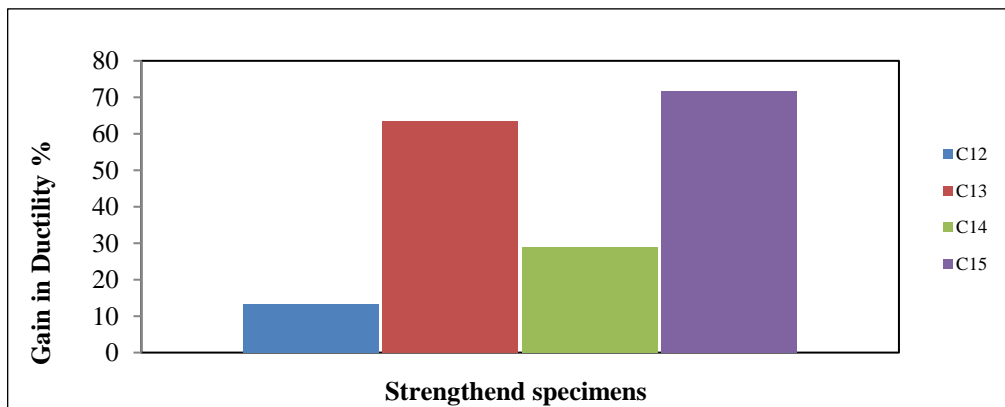


Figure 4.23 Gaining in Ductility for Group c.

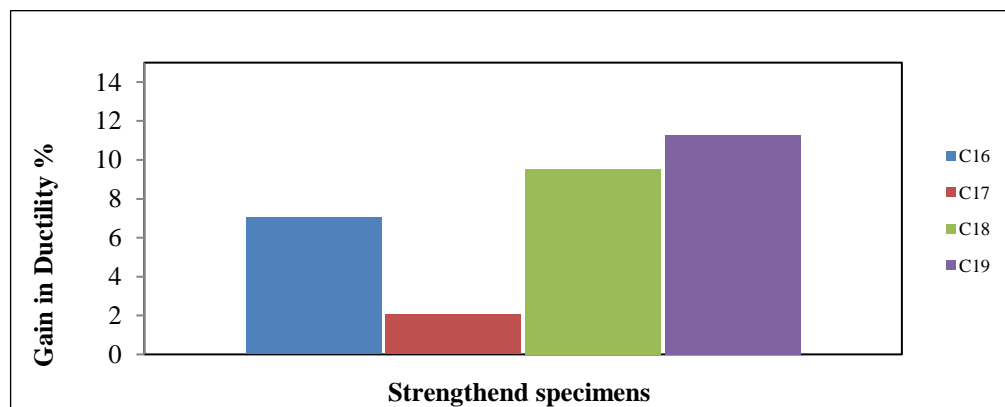


Figure 4.24 Gaining in Ductility for Group d.

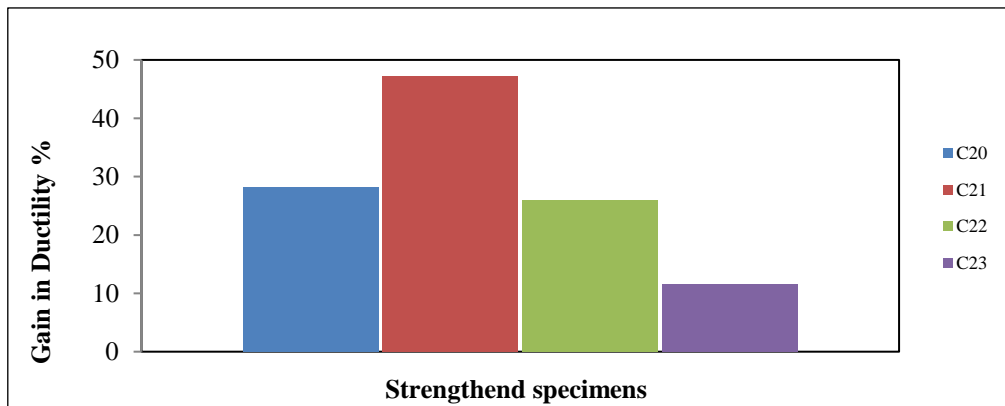


Figure 4.25 Gaining in Ductility for Group e.

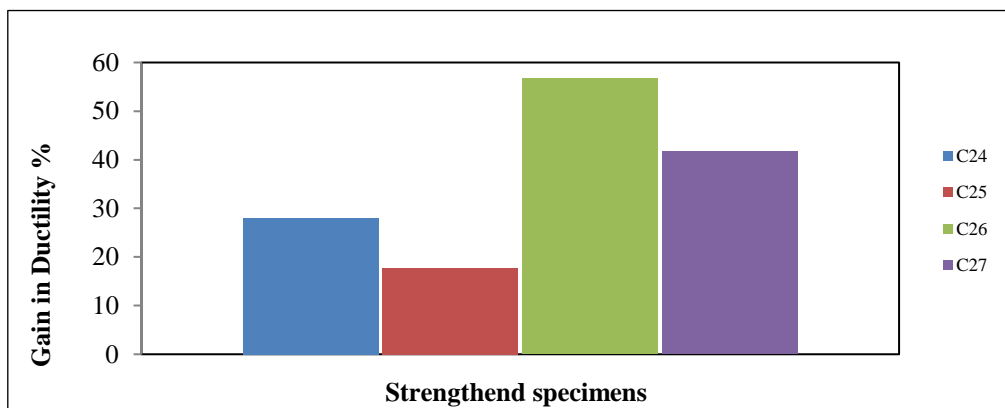


Figure 4.26 Gaining in Ductility for Group g.

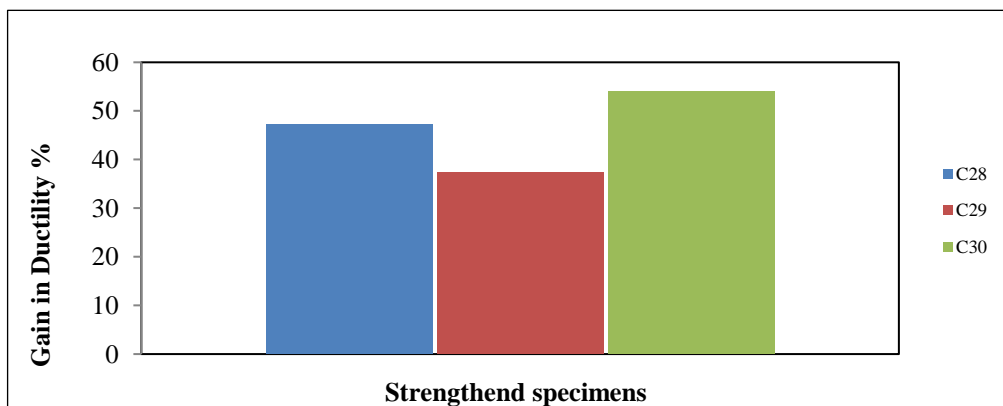


Figure 4.27 Gaining in Ductility for Group f.

4.3.4 Stiffness

Stiffness is defined as the resistance of a column to elastic deformation when the load is applied. Technically, the greater of the modulus of elasticity for an elastic solid, the greater its stiffness. In the last decade, various displacement-based design (DBD) approaches have been proposed to better control the displacements of structures during earthquakes and thereby enable performance-based seismic design proposed two procedures to determine the stiffness of reinforced concrete columns, that are commonly utilized secant stiffness (K_s) and initial stiffness (K_{in}). Secant stiffness of RC columns, which is also called effective stiffness is defined as the ratio of the maximum applied load on the specimen (P_u), to the maximum displacement (Δ_u). Initial stiffness is determined by a simple approach, in which a secant passing through a point on the load-displacement envelope corresponding to 70% of the maximum applied load on the specimen ($0.7P_u$) is extended to intersect with the horizontal line at (P_u).

The results of the secant and initial stiffness columns are shown in Table (4.3) and Figs. (4.27 – 4.32). It showed that the increase in the thickness of the HPFRC jacketing and the number of strengthening sides led to an increase in the initial stiffness and the secant stiffness due to an increase in the size of columns, improvement in the modules of elasticity, which led to the reduction of cracks and increased the stiffness of columns.

Table 4.3 Stiffness of column specimens.

Group	Column ID	Secant stiffness (Ks)		
		Pu (kN)	Δ_u mm	Ks kN/mm
a	C1	317	9.00	35.22
	C2	233	8.50	27.41
	C3	115	8.00	14.38
	C4	425	7.50	56.67
	C5	320	7.25	44.14
	C6	450	7.00	64.29
	C7	304	6.75	45.04
c	C8	295	6.3	46.83
	C9	199	5.75	34.61
	C10	315	4.70	67.02
	C11	290	5.50	52.73
b	C12	230	6.00	38.33
	C13	140	5.00	28.00
	C14	330	4.60	71.74
	C15	194	5.30	36.60
d	C16	215	6.00	35.83
	C17	125	6.25	20.00
	C18	401	5.30	75.66
	C19	312	5.00	62.40
e	C20	335	5.75	58.26
	C21	270	4.80	56.25
	C22	401	4.30	93.26
	C23	250	5.50	45.45
f	C24	313	5.70	54.91
	C25	200	6.00	33.33
	C26	520	5.00	104.00
	C27	290	5.40	53.70
g	C28	256	6.75	37.93
	C29	125	5.60	22.32
	C30	132	6.20	21.29

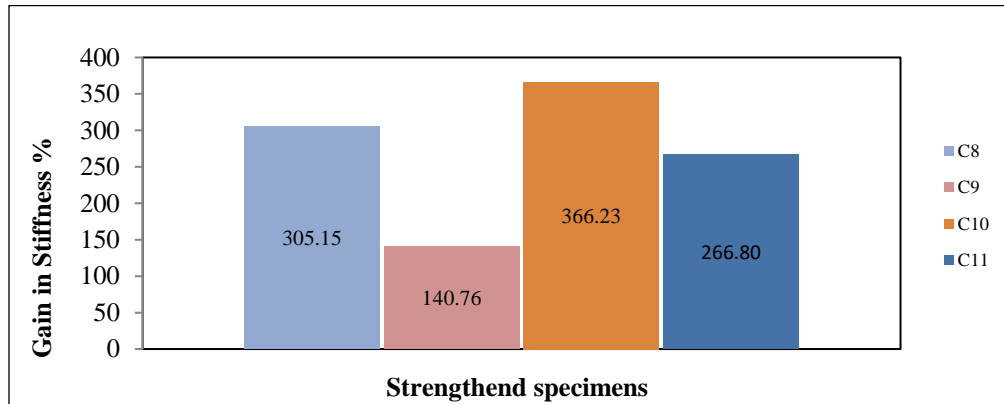


Figure 4.28 Gaining in stiffness for group b.

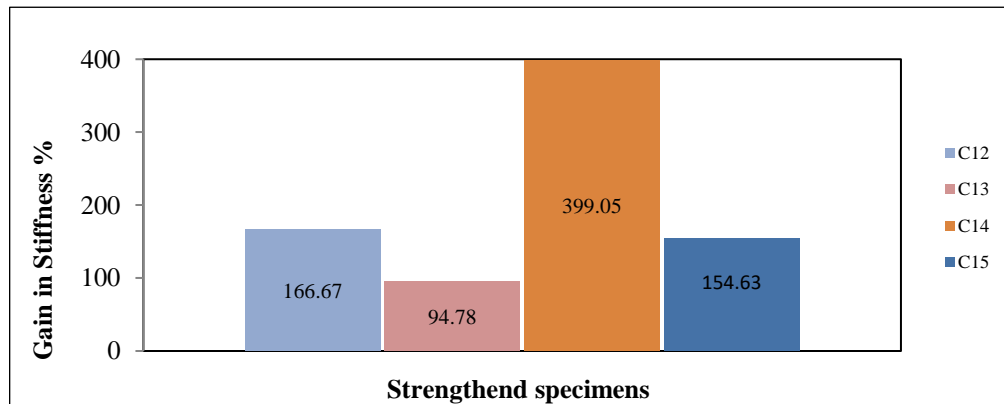


Figure 4.29 Gaining in Stiffness for Group c.

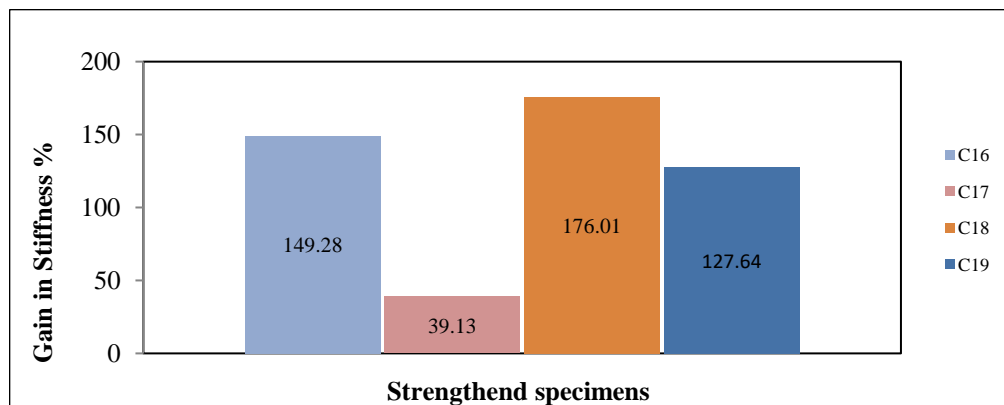


Figure 4.30 Gaining in Stiffness for Group d.

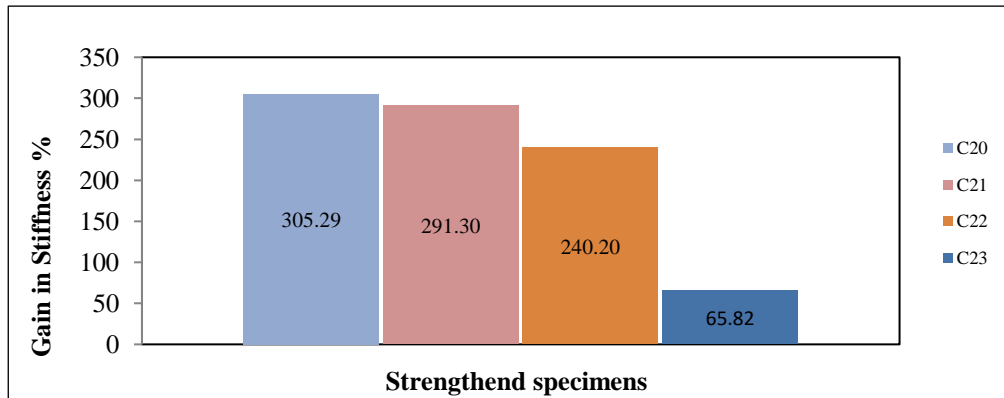


Figure 4.31 Gaining in Stiffness for Group e.

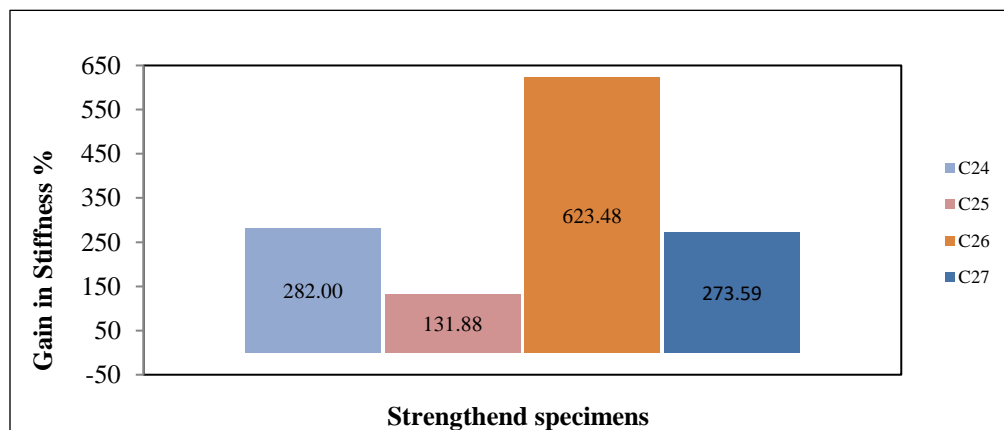


Figure 4.32 Gaining in Stiffness for Group f.

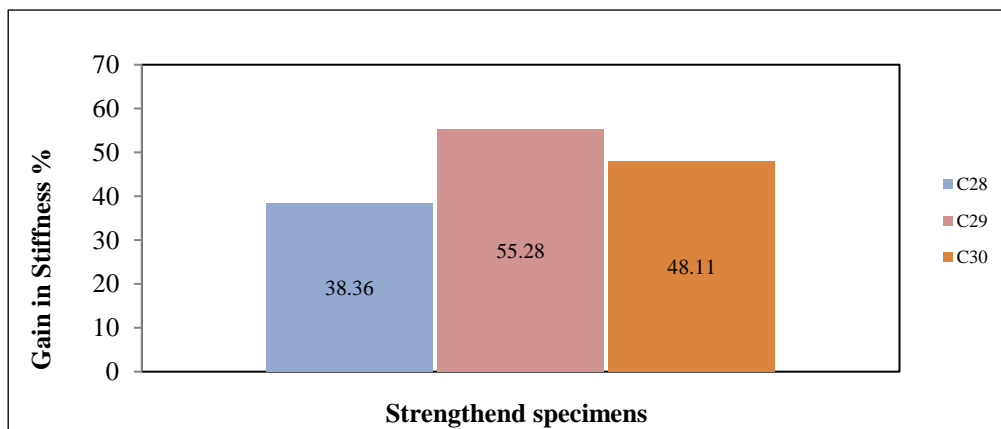


Figure 4.33 Gaining in Stiffness for Group g.

The stiffness of strengthened columns is higher than that of the control specimens. The percentage of gain in stiffness is inversely proportional to the eccentricity ratio (e/t). The thickness of HPFRC jackets has an eminent effect on the percentage of gain in stiffness. A comparison of the result of strengthened columns specimens clarified that increasing the thickness of the HPFRC jacket from 15 mm to 30 mm with 0.00 % honeycomb defect ratio (C8 and C10) resulted in an increase in gain of column stiffness from 225.74% to 366.23%, and for specimens (C9 and C11) increase in gain of column stiffness from 140.76% to 266.80%. Moreover, the specimens with 35 % honeycomb defect ratio (C12 and C14) resulted in an increase in gain of column stiffness from 166.67% to 399.05%, and for specimens (C13 and C15) increase in gain of column stiffness from 94.78% to 154.63%. While the gain in stiffness for specimens (C16 and C20) with 70 % honeycomb defect ratio increased from 149.28% to 305.29%, respectively. Moreover, the values of the stiffness increase with the increase of the size of the treated honeycomb because the ultimate strength increases when the honeycombed specimens are treated with materials of high strength, as mentioned in (chapter 3).

4.3.5 Toughness

Toughness is the ability of a column to absorb energy without rupture. Toughness is the area under the load-deflection curve until the maximum load is reached, which represents the energy absorption of the concrete column that could be sustained before a significant decrease in the load bearing capacity can be recorded. The thickness of the jacket and the number of strengthening sides increased the energy absorption capacity of the column specimens. The result of the toughness of columns tested was shown in Figs. (4.33 – 4.38). The toughness factor (TF) is the ratio of the toughness of strengthened columns to that of un-strengthened columns or the control specimen. The T.F of strengthened columns is

higher than that of the control specimens. The TF of strengthened columns with full casting using HPFRC jackets is higher than that of strengthened columns that used bonding laminates. HPFRC thickness and strengthening scheme had a great effect on the T.F of test specimens. A comparison of the result of strengthened columns specimens clarified that increasing the thickness of the HPFRC jacket from 15 mm to 30 mm with 0.00 % honeycomb defect ratio (C8 and C10) resulted in an increase in the gain of column T.F from 1.57 to 1.62 and for specimens (C9 and C11) increase in the gain of column T.F from 1.24 to 1.44. Moreover, the specimens with 35 % honeycomb defect ratio (C12 and C14) resulted in an increase in the gain of column T.F from 1.47 to 1.76 and for specimens (C13 and C15) an increase in gain of column T.F from 0.96 to 1.2. While the gain in stiffness for specimens (C16 and C20) with 70 % honeycomb defect ratio increased from 1.27 to 2.23.

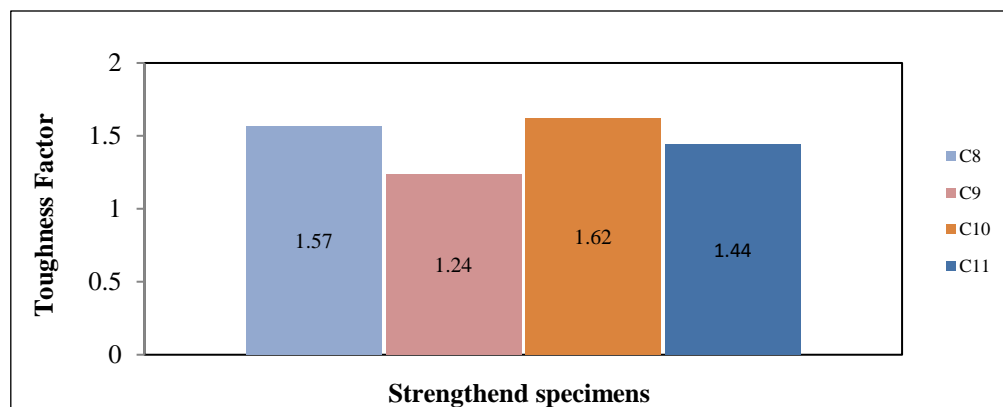


Figure 4.34 Toughness Factor for Group b.

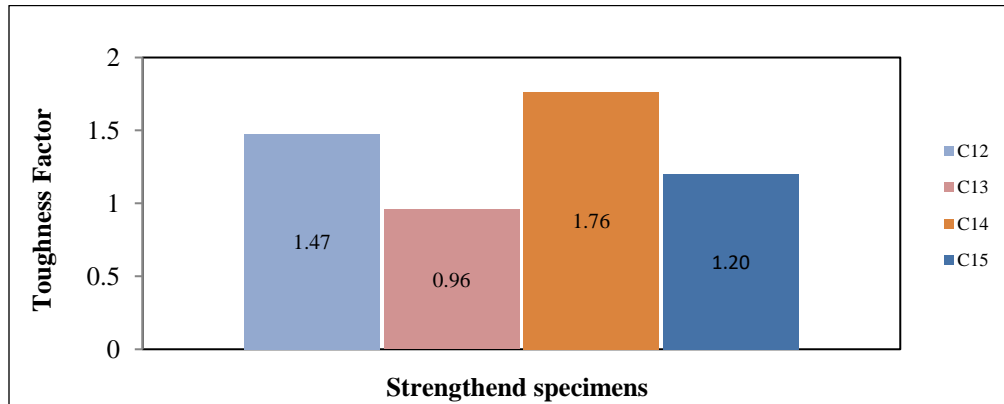


Figure 4.35 Toughness Factor for Group c.

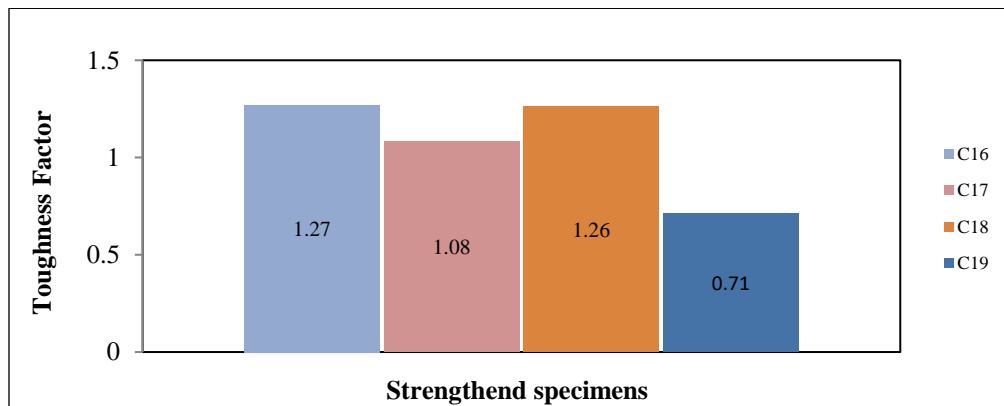


Figure 4.36 Toughness Factor for Group d.

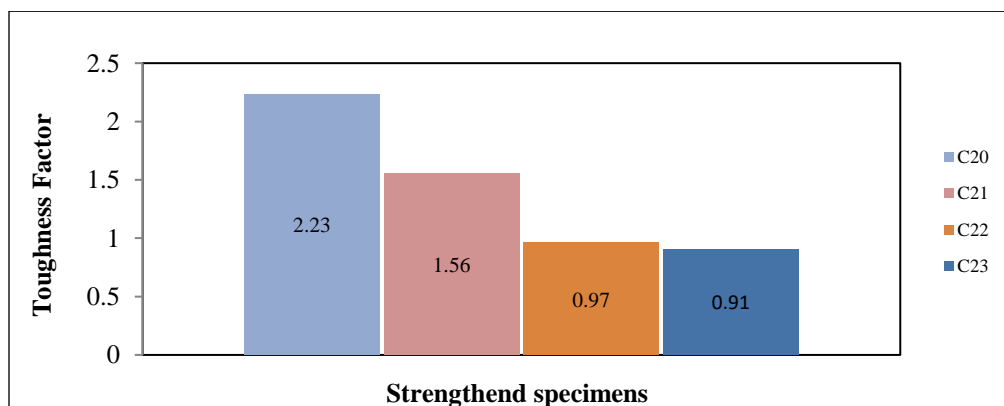


Figure 4.37 Toughness Factor for Group e.

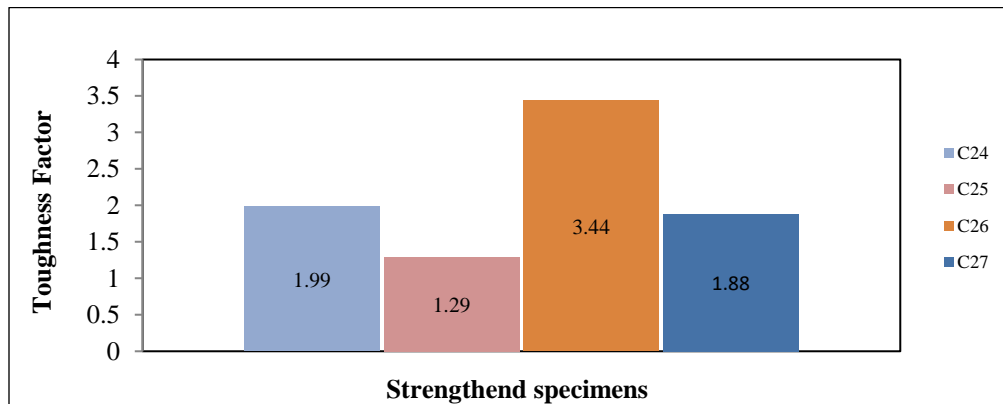


Figure 4.38 Toughness Factor for Group f.

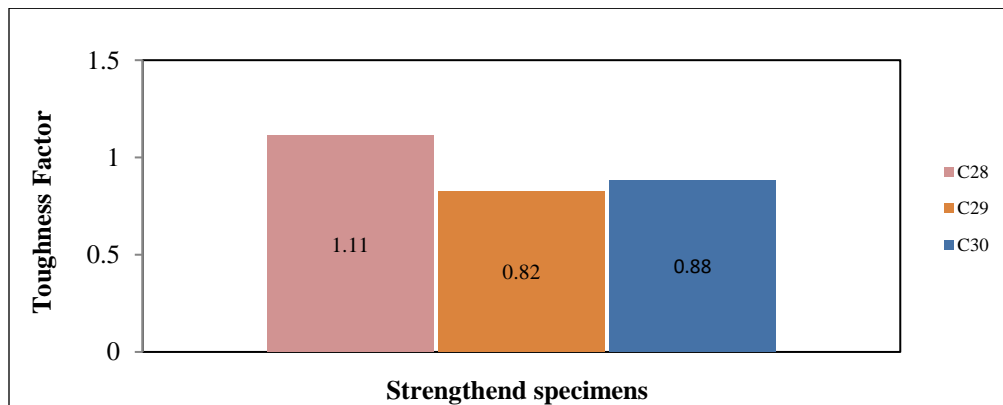


Figure 4.39 Toughness Factor for Group g.

4.3.6 Effect of Side Numbers of Strengthening and Jacket Thickness on Load Carrying Capacity of RC Columns

This section investigated the number of strengthening faces (two or four) and the jacket thickness (15 or 30) mm. The designation of specimens is used such that the first number indicates the strengthening face and the second number indicates the jacket thickness of HPFRC layers.

Table (4.1) illustrates the effect of increasing the number of strengthening faces and the jacket thickness on the behavior of strengthened concrete columns with HPFRC jackets. It can be seen from this table that when all other parameters

are the same, the increase in the number of strengthening faces (from two sides to 4 sides) and jacket thickness (from 15 mm to 30 mm) leads to a greater increase in ultimate strength and enhancement of the corresponding displacement of the strengthened columns with HPFRC jackets.

Fig. (4.40) shows the effect on ultimate strength; it can be seen that the gain in ultimate strength increases with the increase of strengthening face and jacket thickness. It increased by about (73.04% and 152.17) for columns that strengthened from two-facing and about (156.52% and 173.91%) for columns strengthened from four-facing with HPFRC jacket thickness (15 mm and 35 mm) respectively compared with the control specimen. This occurs because of the enlargement of the section size and the increased compressive strength of HPFRC, which causes a decrease in the neutral axis of stresses and increases the compression area of the column section.

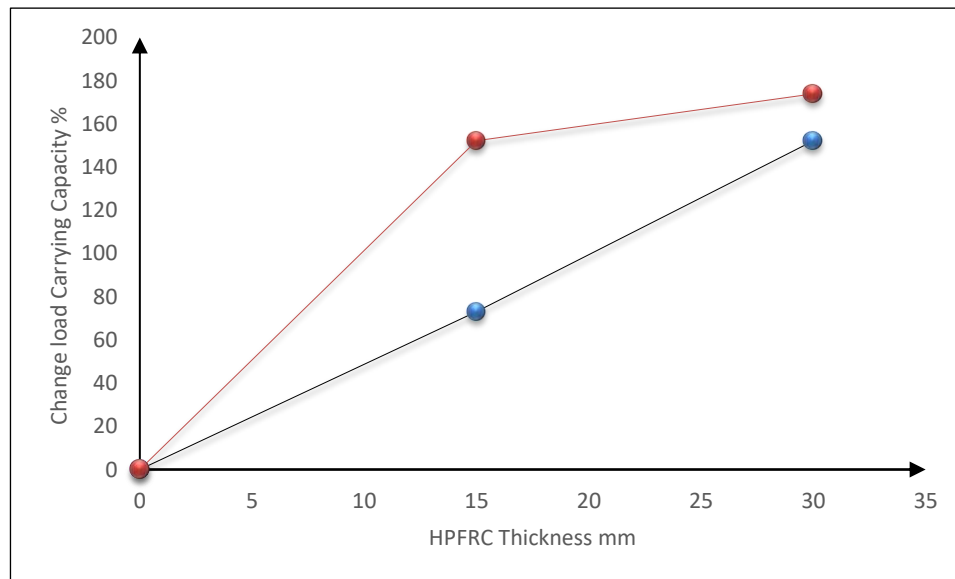


Figure 4.40 Effect of Strengthening face and Jacket Thickness on Load capacity.

4.3.7 Effect of CFRP on Load Carrying Capacity of RC Columns

The experimental results of columns wrapped with one layer of CFRP are presented in Table (4.1). Three columns were tested for failure under eccentric loading with different eccentricities. Column C28 was tested under an eccentric 50 mm loading with a honeycomb defect ratio of 70% represented by the foam material while, columns C29 and C30 were tested under an eccentric 100 mm loading with a honeycomb defect ratio of 70% represented by the foam material and WSC, respectively.

The results showed that the CFRP-wrapped layers are improving the load-carrying capacity of the strengthened specimens in comparison to the control specimen. The load-carrying capacity was increased by (8.70%, 9.87%, and 14.78%) for the specimens (C28:C30) related to the control specimen as shown in Fig. (4.20). The CFRP wrapping enhanced the performance of the columns by increasing the column ductility. On the other hand, the effectiveness of CFRP wrapped layer was lower than the UHPCFRC jacketing in strengthening the honeycomb-damaged columns.

Chapter Five: Conclusions & Recommendations

5.1 Summary

This thesis presents an experimental study on the strengthening of RC columns by HPFRC under eccentric loadings under the effect of honeycomb failure. The experimental program consisted of thirty RC columns. Twenty columns were strengthened with HPFRC, and three columns were strengthened with CFRP. While seven of them are unstrengthened as control. All columns have a square cross-section of 120 x 120 mm, whereas their height, including corbel heads, is 950 mm. The dimensions of the top and bottom corbels are 100 x 120 x 200 mm. The columns are reinforced with 4 $\Phi 10$ as longitudinal reinforcement and $\Phi 8$ mm bars stirrups spaced at 100 mm spacing. Several variables, such as eccentricity ratio (e/t), the thickness of the strengthening layer, the honeycomb ratio, and strengthening schemes, are considered.

5.2 Conclusion

The following findings can be extracted from experimental investigations.

1. The HPFRC technique provides an effective technique for strengthening RC columns under eccentric loadings.
2. Full casting with HPFRC jacketing schemes was more effective than laminate schemes.
3. The HPFRC thickness has a significant influence on the amount of gain in axial load capacity, ductility, stiffness, and toughness of strengthened columns. Increasing the HPFRC thickness from 15 mm to 30 mm with a 100 mm eccentricity ratio (C12 and C14) resulted in an increase in stiffness from 38.33 to 71.74 kN/mm and in TF from 1.47 to 1.76.

4. HPFRC was significant in enhancing the load capacity and ductility for the strengthening columns. 156.2%, 173.91%, and 186.96% are the gain of axial load for columns C8, C10 and C14 which were tested under eccentric loadings.
5. For UHPRFC jackets, the better roughening of the column surface and the bond between the HPFRC mixture and column surface must be ensured to achieve the suitable strength of the strengthening columns.
6. HPFRC jacketing is more efficient under eccentric axial loads for four faces than for two faces with the same strengthening thickness.
7. The fibers had an effective role in delaying the appearance of cracks because of their work as a bridge that prevents the cracks and then enhances the ductility.
8. All treated specimens of RC columns failed locally and had pure compression and crushing failures. Furthermore, the failure location indicates that it was not within the treated area.
9. The experimental results showed that the strength of the treated columns has been fully restored, and exceeds the strength of the control column based on the honeycomb defect's shape, size, and location.
10. It was observed that the stiffness and ductility index of the rehabilitated honeycombed columns were too much affected by the presence of the honeycombed zone inside the columns, therefore, the reliance on the stiffness and ductility index, as often adopted when load testing is used, as an aid in assessment work can lead to safe assessment results because it supports and clearly shows the behavior of specimens.
11. The column strengthened with HPFRC Showed more effectiveness than CFRP in load capacity, ductility and stiffness but inversely in cost.

5.3 Recommendation

The following recommendations are suggested for future experimental and numerical work.

1. Behavior of Strengthened RC Columns using HPFRC under lateral loads.
2. Strengthening of Slender RC Columns using HPFRC under Concentric and Eccentric Loading.
3. Strengthening of fire exposure RC Columns using HPFRC.
4. Studying the strengthening of columns after being loaded to represent the column condition in real life.
5. Studying the behavior of the circular cross-section area columns strengthening with HPFRC under different load conditions.

Appendices

Appendix A

Material Properties

A.1. Data Sheet of Quartz Sand

Safety Data Sheet

Sikadur®-504 Aggregate

Revision Date 08/16/2022



Print Date 08/16/2022

SECTION 1. IDENTIFICATION

Product name	: Sikadur®-504 Aggregate
Company name	: Sika Corporation 201 Polito Avenue Lyndhurst, NJ 07071 USA www.sikausa.com
Telephone	: (201) 933-8800
Telefax	: (201) 804-1076
E-mail address	: ehs@sika-corp.com
Emergency telephone	: CHEMTREC: 800-424-9300 INTERNATIONAL: +1-703-527-3867
Recommended use of the chemical and restrictions on use	: For further information, refer to product data sheet.

SECTION 2. HAZARDS IDENTIFICATION

GHS classification in accordance with the OSHA Hazard Communication Standard (29 CFR 1910.1200)

Carcinogenicity (Inhalation)	: Category 1A
Specific target organ toxicity - single exposure	: Category 3 (Respiratory system)
Specific target organ toxicity - repeated exposure	: Category 1 (Lungs)

GHS label elements

Hazard pictograms	:  
-------------------	---

Signal Word	: Danger
Hazard Statements	: H335 May cause respiratory irritation. H350 May cause cancer by inhalation. H372 Causes damage to organs (Lungs) through prolonged or repeated exposure.
Precautionary Statements	: Prevention:

Safety Data Sheet

Sikadur®-504 Aggregate

Revision Date 08/16/2022



Print Date 08/16/2022

P201 Obtain special instructions before use.
P202 Do not handle until all safety precautions have been read and understood.
P260 Do not breathe dust.
P264 Wash skin thoroughly after handling.
P270 Do not eat, drink or smoke when using this product.
P271 Use only outdoors or in a well-ventilated area.
P280 Wear protective gloves/ protective clothing/ eye protection/ face protection.

Response:

P304 + P340 + P312 IF INHALED: Remove person to fresh air and keep comfortable for breathing. Call a POISON CENTER/ doctor if you feel unwell.
P308 + P313 IF exposed or concerned: Get medical advice/ attention.

Storage:

P403 + P233 Store in a well-ventilated place. Keep container tightly closed.
P405 Store locked up.

Disposal:

P501 Dispose of contents/ container to an approved waste disposal plant.

Additional Labeling

There are no ingredients with unknown acute toxicity used in a mixture at a concentration $\geq 1\%$.

Other hazards

None known.

SECTION 3. COMPOSITION/INFORMATION ON INGREDIENTS

Mixtures

Components

Chemical name	CAS-No.	Classification	Concentration (% w/w)
Quartz (SiO ₂) >5µm	14808-60-7	Carc. 1A; H350I STOT RE 1; H372 STOT SE 3; H335	$\geq 90 - \leq 100$
aluminium oxide	1344-28-1		$\geq 1 - \leq 5$

Actual concentration is withheld as a trade secret

SECTION 4. FIRST AID MEASURES

General advice : Move out of dangerous area.
Consult a physician.
Show this material safety data sheet to the doctor in attendance.

If inhaled : Move to fresh air.

Safety Data Sheet

Sikadur®-504 Aggregate



Revision Date 08/16/2022

Print Date 08/16/2022

- Consult a physician after significant exposure.
- | | |
|---|---|
| In case of skin contact | : Take off contaminated clothing and shoes immediately.
Wash off with soap and plenty of water.
If symptoms persist, call a physician. |
| In case of eye contact | : Remove contact lenses.
Keep eye wide open while rinsing.
If eye irritation persists, consult a specialist. |
| If swallowed | : Clean mouth with water and drink afterwards plenty of water.
Do not induce vomiting without medical advice.
Do not give milk or alcoholic beverages.
Never give anything by mouth to an unconscious person. |
| Most important symptoms and effects, both acute and delayed | : Prolonged exposure can cause silicosis.
Irritant effects
Cough
Respiratory disorder
May cause respiratory irritation.
May cause cancer by inhalation.
Causes damage to organs through prolonged or repeated exposure. |
| Notes to physician | : Treat symptomatically. |

SECTION 5. FIRE-FIGHTING MEASURES

- | | |
|--|---|
| Suitable extinguishing media | : Use extinguishing measures that are appropriate to local circumstances and the surrounding environment. |
| Further information | : Collect contaminated fire extinguishing water separately. This must not be discharged into drains.
Fire residues and contaminated fire extinguishing water must be disposed of in accordance with local regulations. |
| Special protective equipment for fire-fighters | : In the event of fire, wear self-contained breathing apparatus. |

SECTION 6. ACCIDENTAL RELEASE MEASURES

- | | |
|---|--|
| Personal precautions, protective equipment and emergency procedures | : Use personal protective equipment.
Avoid breathing dust.
Deny access to unprotected persons. |
| Environmental precautions | : Try to prevent the material from entering drains or water courses.
If the product contaminates rivers and lakes or drains inform respective authorities.
Local authorities should be advised if significant spillages cannot be contained. |

Safety Data Sheet

Sikadur®-504 Aggregate



Revision Date 08/16/2022

Print Date 08/16/2022

Methods and materials for containment and cleaning up : Pick up and arrange disposal without creating dust.
Keep in suitable, closed containers for disposal.

SECTION 7. HANDLING AND STORAGE

Advice on protection against fire and explosion : Avoid dust formation.
Provide appropriate exhaust ventilation at places where dust is formed.

Advice on safe handling : Avoid formation of respirable particles.
Avoid exceeding the given occupational exposure limits (see section 8).
Do not get in eyes, on skin, or on clothing.
For personal protection see section 8.
Smoking, eating and drinking should be prohibited in the application area.
Follow standard hygiene measures when handling chemical products.

Conditions for safe storage : Store in original container.
Keep in a well-ventilated place.
Observe label precautions.
Store in accordance with local regulations.

Further information on storage stability : Keep in a dry place.
No decomposition if stored and applied as directed.

SECTION 8. EXPOSURE CONTROLS/PERSONAL PROTECTION

Ingredients with workplace control parameters

Components	CAS-No.	Value type (Form of exposure)	Control parameters / Permissible concentration	Basis
Quartz (SiO ₂) >5µm	14808-60-7	TWA (Respirable particulate matter)	0.025 mg/m ³	ACGIH
		TWA (Respirable dust)	0.05 mg/m ³	OSHA Z-1
		TWA (respirable)	10 mg/m ³ / %SiO ₂ +2	OSHA Z-3
		TWA (respirable)	250 mppcf / %SiO ₂ +5	OSHA Z-3
		TWA (respirable dust fraction)	0.1 mg/m ³	OSHA P0
		TWA (Respirable particulate matter)	0.025 mg/m ³ (Silica)	ACGIH
		PEL (respirable)	0.05 mg/m ³	OSHA CARC

Safety Data Sheet

Sikadur®-504 Aggregate



Revision Date 08/16/2022

Print Date 08/16/2022

		TWA (respirable dust fraction)	0.1 mg/m3	OSHA P0
		TWA (Respirable particulate matter)	0.025 mg/m3	ACGIH
		TWA (Respirable particulate matter)	0.025 mg/m3 (Silica)	ACGIH
aluminium oxide	1344-28-1	TWA (total dust)	15 mg/m3	OSHA Z-1
		TWA (respirable fraction)	5 mg/m3	OSHA Z-1
		TWA (Total dust)	10 mg/m3	OSHA P0
		TWA (respirable dust fraction)	5 mg/m3	OSHA P0
		TWA (Respirable particulate matter)	1 mg/m3 (Aluminum)	ACGIH

The above constituents are the only constituents of the product which have a PEL, TLV or other recommended exposure limit. At this time, the other constituents have no known exposure limits.

Particles of nuisance dust

Form of exposure	Value type	Control parameters	Basis
total dust	TWA	15 mg/m3	OSHA Z-3
respirable fraction	TWA	5 mg/m3	OSHA Z-3

Engineering measures

Use of adequate ventilation should be sufficient to control worker exposure to airborne contaminants. If the use of this product generates dust, fumes, gas, vapor or mist, use process enclosures, local exhaust ventilation or other engineering controls to keep worker exposure below any recommended or statutory limits.

Personal protective equipment

Respiratory protection

Use a properly fitted NIOSH approved air-purifying or air-fed respirator complying with an approved standard if a risk assessment indicates this is necessary.

The filter class for the respirator must be suitable for the maximum expected contaminant concentration (gas/vapor/aerosol/particulates) that may arise when handling the product. If this concentration is exceeded, self-contained breathing apparatus must be used.

Safety Data Sheet

Sikadur®-504 Aggregate



Revision Date 08/16/2022

Print Date 08/16/2022

- | | |
|--------------------------|--|
| Hand protection | : Chemical-resistant, impervious gloves complying with an approved standard should be worn at all times when handling chemical products if a risk assessment indicates this is necessary. |
| Eye protection | : Safety eyewear complying with an approved standard should be used when a risk assessment indicates this is necessary. |
| Skin and body protection | : Choose body protection in relation to its type, to the concentration and amount of dangerous substances, and to the specific work-place. |
| Hygiene measures | :
Avoid contact with skin, eyes and clothing.
Wash hands before breaks and immediately after handling the product.
Remove contaminated clothing and protective equipment before entering eating areas.
Avoid breathing dust. |

SECTION 9. PHYSICAL AND CHEMICAL PROPERTIES

- | | |
|--|-----------------------|
| Appearance | : granular powder |
| Color | : tan, gray, white |
| Odor | : odorless |
| Odor Threshold | : No data available |
| pH | : 6 - 8 |
| Melting point/range | : 3,110 °F / 1,710 °C |
| Boiling point/boiling range | : 4,046 °F / 2,230 °C |
| Flash point | : Not applicable |
| Evaporation rate | : No data available |
| Flammability (solid, gas) | : No data available |
| Upper explosion limit / Upper flammability limit | : No data available |
| Lower explosion limit / Lower flammability limit | : No data available |
| Vapor pressure | : No data available |
| Relative vapor density | : No data available |
| Density | : 2.65 g/cm3 |

Safety Data Sheet

Sikadur®-504 Aggregate



Revision Date 08/16/2022

Print Date 08/16/2022

Solubility(ies)	
Water solubility	: negligible
Solubility in other solvents	: No data available
Partition coefficient: n-octanol/water	: No data available
Autoignition temperature	: No data available
Decomposition temperature	: No data available
Viscosity	
Viscosity, dynamic	: No data available
Viscosity, kinematic	: Not applicable
Explosive properties	: No data available
Oxidizing properties	: No data available
Volatile organic compounds (VOC) content	: Not applicable

SECTION 10. STABILITY AND REACTIVITY

Reactivity	: No dangerous reaction known under conditions of normal use.
Chemical stability	: The product is chemically stable.
Possibility of hazardous reactions	: Stable under recommended storage conditions.
Conditions to avoid	: No data available
Incompatible materials	: No data available
Hazardous decomposition products	: No decomposition if stored and applied as directed.

SECTION 11. TOXICOLOGICAL INFORMATION

Not classified based on available information.

Skin corrosion/irritation

Not classified based on available information.

Serious eye damage/eye irritation

Not classified based on available information.

Respiratory or skin sensitization

Skin sensitization

Not classified based on available information.

Safety Data Sheet

Sikadur®-504 Aggregate



Revision Date 08/16/2022

Print Date 08/16/2022

Respiratory sensitization

Not classified based on available information.

Germ cell mutagenicity

Not classified based on available information.

Carcinogenicity

May cause cancer by inhalation.

IARC	Group 1: Carcinogenic to humans Quartz (SiO ₂) (Silica dust, crystalline)	14808-60-7
OSHA	OSHA specifically regulated carcinogen Quartz (SiO ₂) (crystalline silica)	14808-60-7
NTP	Known to be human carcinogen Quartz (SiO ₂) (Silica, Crystalline (Respirable Size))	14808-60-7

Reproductive toxicity

Not classified based on available information.

STOT-single exposure

May cause respiratory irritation.

STOT-repeated exposure

Causes damage to organs (Lungs) through prolonged or repeated exposure.
Prolonged exposure can cause silicosis.

Aspiration toxicity

Not classified based on available information.

Further information

Product:

Quartz (14808-60-7): This classification is relevant when exposed to Quartz (silicon dioxide) in dust or powder form only, including cured product that is subject to sanding, grinding, cutting, or other surface preparation activities.

SECTION 12. ECOLOGICAL INFORMATION

Ecotoxicity

No data available

Persistence and degradability

No data available

Bioaccumulative potential

No data available

Safety Data Sheet

Sikadur®-504 Aggregate



Revision Date 08/16/2022

Print Date 08/16/2022

Mobility in soil

No data available

Other adverse effects

Product:

Additional ecological information : Do not empty into drains; dispose of this material and its container in a safe way.

SECTION 13. DISPOSAL CONSIDERATIONS

Disposal methods

Waste from residues : Disposal of this product, solutions and any by-products should at all times comply with the requirements of environmental protection and waste disposal legislation and any regional local authority requirements.

Contaminated packaging : Empty containers should be taken to an approved waste handling site for recycling or disposal.

SECTION 14. TRANSPORT INFORMATION

International Regulations

IATA-DGR

Not regulated as a dangerous good

IMDG-Code

Not regulated as a dangerous good

Domestic regulation

49 CFR

Not regulated as a dangerous good

SECTION 15. REGULATORY INFORMATION

TSCA list : All chemical substances in this product are either listed on the TSCA Inventory or are in compliance with a TSCA Inventory exemption.

CERCLA Reportable Quantity

This material does not contain any components with a CERCLA RQ.

SARA 304 Extremely Hazardous Substances Reportable Quantity

This material does not contain any components with a section 304 EHS RQ.

SARA 302 Extremely Hazardous Substances Threshold Planning Quantity

This material does not contain any components with a section 302 EHS TPQ.

SARA 311/312 Hazards

: Carcinogenicity
Specific target organ toxicity (single or repeated exposure)

Safety Data Sheet

Sikadur®-504 Aggregate



Revision Date 08/16/2022

Print Date 08/16/2022

SARA 313


: The following components are subject to reporting levels established by SARA Title III, Section 313:

aluminium oxide 1344-28-1 >= 1 - < 5 %

Clean Air Act

This product does not contain any hazardous air pollutants (HAP), as defined by the U.S. Clean Air Act Section 112 (40 CFR 61).

California Prop. 65

 **WARNING:** This product can expose you to chemicals including Quartz (SiO₂) >5µm, which is known to the State of California to cause cancer. For more information go to www.P65Warnings.ca.gov.

SECTION 16. OTHER INFORMATION

Full text of other abbreviations

ACGIH	: USA. ACGIH Threshold Limit Values (TLV)
OSHA CARC	: OSHA Specifically Regulated Chemicals/Carcinogens
OSHA P0	: USA. Table Z-1-A Limits for Air Contaminants (1989 vacated values)
OSHA Z-1	: USA. Occupational Exposure Limits (OSHA) - Table Z-1 Limits for Air Contaminants
OSHA Z-3	: USA. Occupational Exposure Limits (OSHA) - Table Z-3 Mineral Dusts
ACGIH / TWA	: 8-hour, time-weighted average
OSHA CARC / PEL	: Permissible exposure limit (PEL)
OSHA P0 / TWA	: 8-hour time weighted average
OSHA Z-1 / TWA	: 8-hour time weighted average
OSHA Z-3 / TWA	: 8-hour time weighted average

Notes to Reader

The information contained in this Safety Data Sheet applies only to the actual Sika Corporation ("Sika") product identified and described herein. This information is not intended to address, nor does it address the use or application of the identified Sika product in combination with any other material, product or process. All of the information set forth herein is based on technical data regarding the identified product that Sika believes to be reliable as of the date hereof. Prior to each use of any Sika product, the user must always read and follow the warnings and instructions on the product's current Product Data Sheet, product label and Safety Data Sheet for each Sika product, which are available at web site and/or telephone number listed in Section 1 of this SDS.

SIKA MAKES NO WARRANTIES EXPRESS OR IMPLIED AND ASSUMES NO LIABILITY ARISING FROM THIS INFORMATION OR ITS USE. SIKA SHALL NOT BE LIABLE UNDER ANY LEGAL THEORY FOR SPECIAL OR CONSEQUENTIAL DAMAGES AND SHALL NOT BE RESPONSIBLE FOR THE USE OF THIS PRODUCT IN A MANNER TO INFRINGE ON ANY PATENT OR ANY OTHER INTELLECTUAL PROPERTY RIGHTS HELD BY OTHERS.

All sales of Sika products are subject to its current terms and conditions of sale available at www.sikausa.com or 201-933-8800.

Revision Date 08/16/2022

10 / 11

Safety Data Sheet

Sikadur®-504 Aggregate



Revision Date 08/16/2022

Print Date 08/16/2022

000000606496
US / Z8

A.2. Data Sheet of Silica Fume

Construction Chemicals



MegaAdd MS(D)

Densified Microsilica

DESCRIPTION	<p>MegaAdd MS(D) is a very fine pozzolanic, ready to use high performance mineral additive for use in concrete. It acts physically to optimize particle packing of the concrete or mortar mixture and chemically as a highly reactive pozzolan.</p> <p>MegaAdd MS(D) in contact with water, goes into solution within an hour. The silica in solution forms an amorphous silica rich, calcium poor gel on the surface of the silica fume particles and agglomerates. After time the silica rich calcium poor coating dissolves and the agglomerates of silica fume react with free lime (CaOH_2) to form calcium silicate hydrates (CSH). This is the pozzolanic reaction in cementitious system.</p>
STANDARDS	ASTM C1240
USES	MegaAdd MS(D) can be used in a variety of applications such as concrete, grouts, mortars, fibre cement products, refractory, oil/gas well cements, ceramics, elastomer, polymer applications and all cement related products.
ADVANTAGES	<ul style="list-style-type: none"> • High to ultra high strength • High resistance to chlorides and sulfates • Protection against corrosion • Increased durability, longer service life for structures • Enhanced rheology, control of mixture segregation and bleed • Greater resistance to chemicals

TYPICAL PROPERTIES at 25°C

PROPERTY	TEST METHOD	VALUE
State	Amorphous	Sub-micron powder
Colour	-	Grey to medium grey powder
Specific Gravity	-	2.10 to 2.40
Bulk Density	-	500 to 700 kg/m ³
Chemical Requirements		
Silicon Dioxide (SiO_2)	-	Minimum 85%
Moisture Content (H_2O)	-	Maximum 3%
Loss on Ignition (LOI)	-	Maximum 6%
Physical Requirements		
Specific Surface Area	-	Minimum 15 m ² /g
Pozzolanic Activity Index, 7 days	-	Maximum 105% of control
Over size particles retained on 45 micron sieve	-	Maximum 10%

COMPATIBILITY	<p>MegaAdd MS(D) is suitable for use with all types of cement and cementitious materials.</p> <p>With Admixtures :</p> <p>MegaAdd MS(D) is compatible to use with all types of water reducing plasticisers / superplasticisers and poly carboxylate based superplasticiser.</p>
DOSAGE	The normal dosage of MegaAdd MS(D) is 5 - 8% by weight of cement, but it can be used up to 10%. Site trials should be carried out to establish the optimum dosage for the mix to be used as the dosage varies depending on application.

CC/MAPD808/Ver1/11/15
12 | Technical Data Sheet



MegaAdd MS(D)

BATCHING	Batch MegaAdd MS(D) into the concrete mixer and mix thoroughly with the other mixture ingredients, adopting a procedure that ensures full dispersion of the product.	
PACK SIZE	600 Kgs and 1200 Kgs Jumbo bags	
GENERAL INFORMATION	Shelf Life	12 months from date of manufacture when stored under warehouse conditions in original unopened packing. Extreme temperature / humidity may reduce shelf life.
	Cleaning	Clean all equipments and tools with water immediately after use.
HEALTH and SAFETY	PPE's	Gloves, goggles and suitable mask must be worn.
	Precautions	Contact with skin, eyes, etc. must be avoided.
	Hazard	Regarded as non-hazardous for transportation.
	Disposal	Do not reuse bags. To be disposed off as per local rules and regulations.
	Additional Information	Refer MSDS. (Available on request.)
TECHNICAL SERVICE	CONMIX Technical Services are available on request for on-site support to assist in the correct use of its products.	



MSASA
Construction Solutions for Africa

CAPE TOWN

Tel: +27 (0)87 231 0253
Unit 5 (M5 Freeway Park)
Upper Camp Rd (Midland) 7405
Cape Town - South Africa

JOHANNESBURG

Tel: +27 (0)82 786 8629
54 Maple Street (Pomona)
Kempson Park, Johannesburg 1618
South Africa

Email: info@msasa.co.za | www.msasa.co.za

Manufacturer:
CONMIX LTD.
P.O. Box 5035, Springs
United Arab Emirates
Tel: +971 6 5314185
Fax: +971 6 5314332
Email: conmix@conmix.com

Sales Office:
Tel: +971 6 5655422
Fax: +971 6 5655442
www.conmix.com



It is the customer's responsibility to satisfy themselves by checking with this company whether information is still current at the time of use. The customer must be satisfied that the product is suitable for the use intended. All products comply with the properties shown on current data sheets. However, Conmix does not warrant or guarantee the installation of the product as it does not have any control over installation or end-use of the product. All information and particularly the recommendations relating to application and end-use are given in good faith. The products are guaranteed against any manufacturing defects and are not subject to Conmix standard terms and conditions of sale.

A.3. Data Sheet of Superplasticizer



PRODUCT DATA SHEET

Sika® ViscoCrete®-180 GS

Set retarding, high range water reducing & superplasticizing admixture

DESCRIPTION

Sika® ViscoCrete®-180 GS is a Set retarding, high range water reducing & superplasticizing admixture for Concrete & Mortar utilizing Sika's 'ViscoCrete®' polycarboxylate polymer technology (3rd Generation) .

USES

1. High-performance Concrete (HPC).
2. Flowing Concrete.
3. Durable Concrete.
4. Pumped Concrete.

CHARACTERISTICS / ADVANTAGES

1. High water reduction, resulting in higher density, higher strength and reduced permeability.
2. Easier and faster pumping of concrete.
3. Increased workability and easier placeability.
4. Increased concrete durability and uniformity.
5. Reduced shrinkage and cracking.
6. Reduced rate of carbonation of the concrete.

PRODUCT INFORMATION

Composition	Aqueous solution of modified polycarboxylates
Packaging	1000 LTRs IBC 20 kg Pail
Shelf life	12 months from date of production if stored properly in undamaged unopened, original sealed packaging.
Storage conditions	In dry conditions at temperatures between +5°C and +35°C. Protect from direct sunlight. It requires recirculation when held in storage for extended periods.
Appearance and colour	Light brownish
Specific gravity	1.070 ± (0.02) g/cm3
pH-Value	4 - 6

PRODUCT DATA SHEET
Sika® ViscoCrete®-180 GS
December 2012, Version 6431
403311011000003550

TECHNICAL INFORMATION

Concreting guidance

The standard rules of good concreting practice, concerning production and placing, are to be followed. Laboratory trials shall be carried out before concreting on site, especially when using a new mix design or producing new concrete components. Fresh concrete must be cured properly and curing applied as early as possible.

APPLICATION INFORMATION

Recommended dosage

(0.5 % - 2 %) by weight of total cementitious materials.

Dispensing

Sika® ViscoCrete®-180 GS is added to the gauging water or added with it into the concrete mixer. To take advantage of the high water reduction, a wet mixing time, which is depending on the mixing conditions and mixer performance, of at least 3 mins. per cubic meter after the admixture addition is recommended. Sika® ViscoCrete®-180 GS shall not be added to dry cement.

Compatibility

Sika® ViscoCrete®-180 GS can be used in conjunction with :

1. Sika®Aer
2. Sika ViscoFlow®
3. Sika® ViscoCrete®
4. SikaPlast®
5. Sika® Retarder IQ
6. SikaFiber®
7. Sika® Plastocrete® NIQ

All admixtures must be added separately. Trials are always recommended before combining products . For additional information, please contact Sika technical personnel.

BASIS OF PRODUCT DATA

All technical data stated in this Product Data Sheet are based on laboratory tests. Actual measured data may vary due to circumstances beyond our control.

IMPORTANT CONSIDERATIONS

1. A suitable mix design has to be taken into account.
2. Do not use Sika® ViscoCrete®-180 GS with naphthalene based admixtures.
3. Over dosage of Sika® ViscoCrete®-180 GS with excess water will cause :
 - Increase in air entrainment.
 - Bleeding & Segregation.
 - Extend Initial & Final setting time.

ECOLOGY, HEALTH AND SAFETY

For information and advice on the safe handling, storage and disposal of chemical products, users shall refer to the most recent Safety Data Sheet (SDS) containing physical, ecological, toxicological and other safety-related data.

Sika Iraq (Sika Trading LLC)

Erbil / Baghdad / Basra

Tel : +96 977 938 75000

info@iq.sika.com

iq.sika.com

LOCAL RESTRICTIONS

Please note that as a result of specific local regulations the declared data for this product may vary from country to country. Please consult the local Product Data Sheet for the exact product data.

LEGAL NOTES

The information, and, in particular, the recommendations relating to the application and end-use of Sika products, are given in good faith based on Sika's current knowledge and experience of the products when properly stored, handled and applied under normal conditions in accordance with Sika's recommendations. In practice, the differences in materials, substrates and actual site conditions are such that no warranty in respect of merchantability or of fitness for a particular purpose, nor any liability arising out of any legal relationship whatsoever, can be inferred either from this information, or from any written recommendations, or from any other advice offered. The user of the product must test the product's suitability for the intended application and purpose. Sika reserves the right to change the properties of its products. The proprietary rights of third parties must be observed. All orders are accepted subject to our current terms of sale and delivery. Users must always refer to the most recent issue of the local Product Data Sheet for the product concerned, copies of which will be supplied on request.

PRODUCT DATA SHEET

Sika® ViscoCrete®-180 GS

December 2022, Version 00.01

021321011000003805



A.4. Data Sheet of CFRP



PRODUCT DATA SHEET

SikaWrap®-300 C

WOVEN UNIDIRECTIONAL CARBON FIBRE FABRIC, DESIGNED FOR STRUCTURAL STRENGTHENING APPLICATIONS AS PART OF THE SIKAR® STRENGTHENING SYSTEM.

DESCRIPTION

SikaWrap®-300 C is a unidirectional woven carbon fibre fabric with mid-range strengths, designed for installation using the dry or wet application process.

USES

SikaWrap®-300 C may only be used by experienced professionals. Structural strengthening of reinforced concrete, masonry, brickwork and timber elements or structures, to increase flexural and shear loading capacity for:

- Improved seismic performance of masonry walls
- Replacing missing steel reinforcement
- Increasing the strength and ductility of columns
- Increasing the loading capacity of structural elements
- Enabling changes in use / alterations and refurbishment
- Correcting structural design and / or construction defects
- Increasing resistance to seismic movement
- Improving service life and durability
- Structural upgrading to comply with current standards

CHARACTERISTICS / ADVANTAGES

- Multifunctional fabric for use in many different strengthening applications
- Flexible and accommodating to different surface planes and geometry (beams, columns, chimneys, piles, walls, soffits, silos etc.)
- Low density for minimal additional weight
- Extremely cost effective in comparison to traditional strengthening techniques

APPROVALS / STANDARDS

- Poland: Technical Approval ITB AT-15-5604/2011: Zestaw wyrobów Sika CarboDur do wzmacniania i napraw konstrukcji betonowych
- Poland: Technical Approval IBDM Nr AT/2008-03-0336/1 „Płaskowniki, pręty, kształtki i maty kompozytowe do wzmacniania betonu o nazwie handlowej: Zestaw materiałów Sika CarboDur® do wzmacniania konstrukcji obiektów mostowych
- USA: ACI 440.2R-08, Guide for the Design and construction of Externally Bonded FRP Systems for strengthening concrete structures, July 2008
- UK: Concrete Society Technical Report No. 55, Design guidance for strengthening concrete structures using fibre composite material, 2012.

PRODUCT INFORMATION

Construction	Fibre orientation	0° (unidirectional)	
	Warp	Black carbon fibres 99 %	
	Weft	White thermoplastic heat-set fibres 1 %	
Fibre Type	Selected mid-range strength carbon fibres		
Packaging		Fabric length per roll	Fabric width
	10 rolls in cardboard box	≥ 50 m	100 mm
	4 rolls in cardboard box	≥ 50 m	300 mm
	2 rolls in cardboard box	≥ 50 m	600 mm

Product Data Sheet
SikaWrap®-300 C
January 2013, Version 03.00
222349433010000013

Shelf life	24 months from date of production		
Storage conditions	Store in undamaged, original sealed packaging, in dry conditions at temperatures between +5 °C and +35 °C. Protect from direct sunlight.		
Dry Fibre Density	1.82 g/cm ³		
Dry Fibre Thickness	0.167 mm (based on fibre content)		
Area Density	304 g/m ² ±10 g/m ² (carbon fibres only)		
Dry Fibre Tensile Strength	4 000 N/mm ²		(ISO 10618)
Dry Fibre Modulus of Elasticity in Tension	230 000 N/mm ²		(ISO 10618)
Dry Fibre Elongation at Break	1.7 %		(ISO 10618)

TECHNICAL INFORMATION

Laminate Nominal Thickness	0.167 mm		
Laminate Nominal Cross Section	167 mm ² per m width		
Laminate Tensile Strength	Average	Characteristic	(EN 2561*)
	3 500 N/mm ²	3 200 kN/mm ²	(ASTM D 3039*)
Laminate Modulus of Elasticity in Tension	Average	Characteristic	(EN 2561*)
	225 kN/mm ²	220 kN/mm ²	
	Average	Characteristic	(ASTM D 3039*)
	220 kN/mm ²	210 kN/mm ²	
* modification: sample with 50 mm Values in the longitudinal direction of the fibres Single layer, minimum 21 samples per test series			
Laminate Elongation at Break in Tension	1.56 %		(based on EN 2561)
	1.59 %		(based on ASTM D 3039)
Tensile Resistance	Average	Characteristic	(based on EN 2561)
	585 N/mm	534 N/mm	(based on ASTM D 3039)
Tensile Stiffness	Average	Characteristic	(based on EN 2561)
	37.6 MN/m	36.7 MN/m	
	37.6 kN/m per % elongation	36.7 kN/m per % elongation	
	Average	Characteristic	(based on ASTM D 3039)
	36.7 MN/m	35.1 MN/m	
	36.7 kN/m per % elongation	35.1 kN/m per % elongation	

SYSTEM INFORMATION

System Structure	The system build-up and configuration as described must be fully complied with and may not be changed.		
	Concrete substrate adhesive primer	Sikadur®-330	
	Impregnating / laminating resin	Sikadur®-330 or Sikadur®-300	
	Structural strengthening fabric	SikaWrap®-300 C	
	For detailed information on Sikadur®-330 or Sikadur®-300, together with the resin and fabric application details, please refer to the Sikadur®-330 or Sikadur®-300 Product Data Sheet and the relevant Method Statement.		

APPLICATION INFORMATION

Consumption	Dry application with Sikadur®-330	
	First layer including primer layer	1.0–1.5 kg/m ²
	Following layers	0.8 kg/m ²
	Wet application with Sikadur®-300, primer Sikadur®-330	
	Primer layer	0.4–0.6 kg/m ²
	Fabric layers	0.6 kg/m ²
Please also refer to the relevant Method Statement for further information.		

APPLICATION INSTRUCTIONS

SUBSTRATE QUALITY

Minimum substrate tensile strength: 1.0 N/mm² or as specified in the strengthening design.
Please also refer to the relevant Method Statement for further information.

SUBSTRATE PREPARATION

Concrete must be cleaned and prepared to achieve a laitance and contaminant free, open textured surface.
Please also refer to the relevant Method Statement for further information.

APPLICATION METHOD / TOOLS

The fabric can be cut with special scissors or a Stanley knife (razor knife / box-cutter knife). Never fold the fabric.
SikaWrap®-300 C is applied using the dry or wet application process.
Please refer to the relevant Method Statement for details on the impregnating / laminating procedure.

FURTHER DOCUMENTS

Method Statements

Ref. 850 41 02: SikaWrap® manual dry application
Ref. 850 41 03: SikaWrap® manual wet application
Ref. 850 41 04: SikaWrap® machine wet application

LIMITATIONS

- SikaWrap®-300 C shall only be applied by trained and experienced professionals.
- A specialist structural engineer must be consulted for any structural strengthening design calculation.
- SikaWrap®-300 C fabric is coated to ensure maximum bond and durability with the Sikadur® adhesives / impregnating / laminating resins. To maintain and ensure full system compatibility, do not interchange different system components.
- SikaWrap®-300 C can be over coated with a cementitious overlay or other coatings for aesthetic and / or protective purposes. The over coating system selection is dependent on the exposure and the project specific requirements. For additional UV light protection in exposed areas use Sikagard®-550 W Elastic, Sikagard® ElastoColor-675 W or Sikagard®-680 S.
- Please refer to the Method Statement of SikaWrap®

manual dry application (Ref. 850 41 02), SikaWrap® manual wet application (Ref. 850 41 03) or SikaWrap® machine wet application (Ref. 850 41 04) for further information, guidelines and limitations.

BASIS OF PRODUCT DATA

All technical data stated in this Product Data Sheet are based on laboratory tests. Actual measured data may vary due to circumstances beyond our control.

LOCAL RESTRICTIONS

Please note that as a result of specific local regulations the performance of this product may vary from country to country. Please consult the local Product Data Sheet for the exact description of the application fields.

ECOLOGY, HEALTH AND SAFETY

REGULATION (EC) NO 1907/2006 - REACH

This product is an article as defined in article 3 of regulation (EC) No 1907/2006 (REACH). It contains no substances which are intended to be released from the article under normal or reasonably foreseeable conditions of use. A safety data sheet following article 31 of the same regulation is not needed to bring the product to the market, to transport or to use it. For safe use follow the instructions given in this product data sheet. Based on our current knowledge, this product does not contain SVHC (substances of very high concern) as listed in Annex XIV of the REACH regulation or on the candidate list published by the European Chemicals Agency in concentrations above 0.1 % (w/w).

LEGAL NOTES

The information, and, in particular, the recommendations relating to the application and end-use of Sika products, are given in good faith based on Sika's current knowledge and experience of the products when properly stored, handled and applied under normal conditions in accordance with Sika's recommendations. In practice, the differences in materials, substrates and actual site conditions are such that no warranty in respect of merchantability or of fitness for a particular purpose, nor any liability arising out of any legal relationship whatsoever, can be inferred either from this information, or from any written recommendations, or from any other advice offered. The

user of the product must test the product's suitability for the intended application and purpose. Sika reserves the right to change the properties of its products. The proprietary rights of third parties must be observed. All orders are accepted subject to our current terms of sale and delivery. Users must always refer to the most recent issue of the local Product Data Sheet for the product concerned, copies of which will be supplied on request. It may be necessary to adapt the above disclaimer to specific local laws and regulations. Any changes to this disclaimer may only be implemented with permission of Sika® Corporate Legal in Baar.

Sika Egypt
 Lar Industrial Zone (A)
 Section 418, Block 13035
 El DOKKI City, Egypt
 TEL: +356 44810580
 FAX: +356 44810459
www.sika.com.eg



SikaWrap-300C_en_03_2017/1.1.3.pdf

Product Data Sheet
 SikaWrap®-300 C
 January 2017, Version 03.01
 00029602003000011



A.5. Data Sheet of Sikadur®-32 LP



PRODUCT DATA SHEET

Sikadur®-32 LP

Epoxy structural bonding agent for use at high temperatures

DESCRIPTION

Sikadur®-32 LP is a 2-part, epoxy based structural bonding agent for use at high temperatures. It is moisture tolerant and can bond wet or dry materials to damp or dry substrates.
Suitable to use in hot and tropical climatic conditions.

USES

Sikadur®-32 LP may only be used by experienced professionals.

As a structural bonding agent and adhesive for bonding fresh to hardened concrete.

FEATURES

- Application temperature range +20°C to +40°C
- Thickness up to 1 mm
- Easy to mix and apply
- Suitable for dry and damp concrete substrates
- Very good adhesion to many construction materials
- Hardens without shrinkage
- Different coloured parts (for mixing control)
- No primer needed
- High initial and ultimate mechanical strengths
- Impermeable to liquids and water vapour

CERTIFICATES AND TEST REPORTS

- CE Marking and Declaration of Performance to EN 1504-4 - Structural bonding

PRODUCT INFORMATION

Composition	Epoxy resin and selected fillers	
Packaging	1 kg ready to mix unit (Parts A+B) 5 kg ready to mix unit (Parts A+B) 25 kg ready to mix unit (Parts A+B) Refer to current price list for packaging variations.	
Shelf life	24 months from date of production	
Storage conditions	The product must be stored in original, unopened and undamaged sealed packaging in dry conditions at temperatures between +5°C and +30°C. Always refer to packaging.	
Colour	Part A	white
	Part B	dark grey
	Parts A+B mixed	concrete grey
Density	Mixed resin ~1.4 ± 0.1 kg/l Value at +23°C.	

Product Data Sheet
Sikadur®-32 LP
Dikidur 32 LP, Version 02.21
00004090010000110

TECHNICAL INFORMATION

Compressive strength	Curing time	Curing temperature			(ASTM D 695-95)
		+23°C	+30°C	+40°C	
	1 day	–	~2 N/mm²	~30 N/mm²	
	3 days	~14 N/mm²	~24 N/mm²	~41 N/mm²	
	7 days	~34 N/mm²	~38 N/mm²	~52 N/mm²	
	14 days	~39 N/mm²	~43 N/mm²	~56 N/mm²	
Compressive strength at 4% elongation					
Tensile adhesion strength	Curing time	Substrate	Curing temperature	Adhesion strength	(EN 1542)
	7 days	Concrete dry	+23°C	> 3 N/mm² *	
	7 days	Concrete moist	+23°C	> 3 N/mm² *	
	*100% concrete failure				
Shear adhesion strength	≥ 10 N/mm² (at 28 days)				(ASTM C882/C882M-20)
Shrinkage	Hardens without shrinkage.				

APPLICATION INFORMATION

Mixing ratio	Part A : Part B = 2 : 1 by weight or volume			
Consumption	~1.3 kg/m ² per mm of thickness. This figure is theoretical and does not allow for any additional material due to surface porosity, surface profile, variations in level or wastage etc.			
Layer thickness	~1 mm max.			
Sag flow	Non-sag up to 1.0 mm thickness on vertical surfaces			(EN 1799)
Material temperature	+20°C min. / +40°C max.			
Ambient air temperature	+20°C min. / +40°C max.			
Dew point	Beware of condensation. Steel substrate temperature during application must be at least +3°C above dew point.			
Substrate temperature	+20°C min. / +40°C max.			
Substrate moisture content	Cementitious substrates must be dry or matt damp (no standing water). Brush the adhesive well into the substrate if matt damp.			
Pot Life	Temperature	Potlife*	Open time	(EN ISO 9514)
	+20°C	~145 minutes	~270 minutes	
	+30°C	~55 minutes	~240 minutes	
	+40°C	~35 minutes	~120 minutes	
*300 g The potlife begins when Parts A+B are mixed. It is shorter at high temperatures and longer at low temperatures. The greater the quantity mixed, the shorter the potlife. To obtain longer workability at high temperatures, the mixed adhesive may be divided into smaller quantities. Another method is to chill Parts A+B before mixing (not below +5 °C).				

BASIS OF PRODUCT DATA

All technical data stated in this Data Sheet are based on laboratory tests. Actual measured data may vary due to circumstances beyond our control.

IMPORTANT CONSIDERATIONS

- Sikadur® resins are formulated to have low creep under permanent loading. However due to the creep behaviour of all polymer materials under load, when using adhesive for structural applications, the long term structural design load must account for creep. Generally the long term structural design load must be lower than 20–25 % of the failure load. A structural engineer must be consulted for design calculations for specific structural applications.
- When using multiple units during application, do not mix the following unit until the previous one has been used in order to avoid a reduction in workability and handling time.
- For heavy components positioned vertically or overhead, provide temporary support.

ECOLOGY, HEALTH AND SAFETY

User must read the most recent corresponding Safety Data Sheets (SDS) before using any products. The SDS provides information and advice on the safe handling, storage and disposal of chemical products and contains physical, ecological, toxicological and other safety-related data.

APPLICATION INSTRUCTIONS

SUBSTRATE QUALITY

Concrete / masonry / mortar / stone

Concrete and mortar must be at least 3–6 weeks old. Substrate surfaces must be sound, clean, dry or matt damp. Free from standing water, ice, dirt, oil, grease, coatings, laitance, efflorescence, old surface treatments, all loose particles and any other surface contaminants that could affect adhesion of the bonding agent.

Steel

Surfaces must be clean, dry, free from oil, grease, coatings, rust, scale, all loose particles and any other surface contaminants that could affect adhesion of the bonding agent.

SUBSTRATE PREPARATION

Concrete / masonry / mortar / stone

Substrates must be prepared mechanically using suitable abrasive blast cleaning, needle gunning, light scabbling, bush hammering, grinding or other suitable equipment to achieve an open textured gripping surface profile.

Steel

Surfaces must be prepared mechanically using suitable abrasive blast cleaning, grinding, rotating wire brush or other suitable equipment to achieve a bright metal finish with a surface profile to satisfy the necessary tensile adhesion strength requirement. Avoid dew point conditions before and during application.

All substrates

All dust and loose material must be completely removed from all substrate surfaces before application of the product by vacuum / dust removal equipment.

MIXING

Prior to mixing all parts, mix part A (resin) briefly using a mixing spindle attached to a slow speed electric mixer (max. 300 rpm). Add part B (hardener) to part A and mix parts A+B continuously for at least 3 minutes until a uniformly coloured smooth consistency mix has been achieved. To ensure thorough mixing pour materials into a clean container and mix again for approximately 1 minute. Over mixing must be avoided to minimise air entrainment. Mix full units only. Mixing time for A+B = 4,0 minutes. Mix only the quantity which can be used within its pot life.

APPLICATION METHOD / TOOLS

Apply the mixed Sikadur®-32 LP to the prepared substrate by brush, roller, spray or trowel ensuring uniform and complete coverage.

On hardened concrete substrates mechanically prepared to receive fresh concrete, always apply by brush and work the material well into the substrate.

On damp prepared concrete substrates, always apply by brush and work the product well into the substrate.

For bonding wet fresh concrete to hardened prepared concrete, place the concrete whilst the Sikadur®-32 LP layer is still 'tacky'. If the product becomes glossy and loses 'tackiness', apply another coat of Sikadur®-32 LP and proceed to place concrete.

CLEANING OF EQUIPMENT

Clean all tools and application equipment with Sika® Colma Cleaner immediately after use. Hardened material can only be mechanically removed.

LOCAL RESTRICTIONS

Note that as a result of specific local regulations the declared data and recommended uses for this product may vary from country to country. Consult the local Product Data Sheet for exact product data and uses.

LEGAL NOTES

The information, and, in particular, the recommendations relating to the application and end-use of Sika products, are given in good faith based on Sika's current knowledge and experience of the products when properly stored, handled and applied under normal conditions in accordance with Sika's recommendations. In practice, the differences in materials, substrates and actual site conditions are such that no warranty in respect of merchantability or of fitness for a particular purpose, nor any liability arising out of any legal relationship whatsoever, can be inferred either from this information, or from any written recommendations, or from any other advice offered. The user of the product must test the product's suitability for the intended application and purpose. Sika reserves the right to change the properties of its products. The proprietary rights of third parties must be observed. All orders are accepted subject to our current terms of sale and delivery. Users must always refer to the most recent issue of the local Product Data Sheet for the product concerned, copies of which will be supplied on request.

Sika Gulf B.S.C. (c)

Tel: +973 177 36185

Email: info@sis.sika.com

Sika Kuwait Corp. Mat. & Polym. Co. W.L.

Tel: +965 22 282 295

Email: sika.kuwait@sis.sika.com

Web: gcc.sika.com

Sika UAE LLC

Sika International Chemicals LLC

Tel: +971 4 489 8100

Email: info@sis.sika.com

Web: gcc.sika.com

Sika Saudi Arabia Limited

Riyadh / Jeddah / Dammam / Rabigh

Tel: +966 11 257 8032

Email: info@sis.sika.com

Web: gcc.sika.com

Sika Oman

Tel: +968 22 828 500

Email: info@sis.sika.com

Web: gcc.sika.com



Product Data Sheet

Sika® 302 LP

October 2015, Version 02.01

100/0000000000000000

Sika® 302 LP-40 (30-302) 3-1.pdf



A.6. Data Sheet of Sikadur®-330



PRODUCT DATA SHEET

Sikadur®-330

2-component epoxy impregnation resin

DESCRIPTION

Sikadur®-330 is a 2-component, thixotropic epoxy based impregnating resin and adhesive.

USES

Sikadur®-330 may only be used by experienced professionals.

Sikadur®-330 is used as:

- Impregnation resin for SikaWrap® fabric reinforcement for the dry application method
- Primer resin for the wet application system
- Structural adhesive for bonding Sika® CarboDur® plates into slits

CHARACTERISTICS / ADVANTAGES

- Easy mix and application by trowel and impregnation roller
- Manufactured for manual saturation methods
- Excellent application behaviour to vertical and overhead surfaces
- Good adhesion to many substrates
- High mechanical properties
- No separate primer required

PRODUCT INFORMATION

Composition	Epoxy resin	
Packaging	5 kg (A+B)	Pre-batched unit
	Not pre-dosed industrial packaging:	
	Component A	24 kg pails
	Component B	6 kg pails
Colour	Component A: white paste	
	Component B: grey paste	
	Components A + B mixed: light grey paste	

PRODUCT DATA SHEET
Sikadur®-330
December 2023, Version 15.01
0000604001000004

Shelf life	24 months from date of production	
Storage conditions	Store in original, unopened, sealed and undamaged packaging in dry conditions at temperatures between +5 °C and +30 °C. Protect from direct sunlight.	
Density	1.30 ± 0.1 kg/l (component A+B mixed) (at +23 °C)	
Viscosity	Shear rate: 50 /s	
	Temperature	Viscosity
	+10 °C	~10 000 mPas
	+23 °C	~6 000 mPas
	+35 °C	~5 000 mPas

TECHNICAL INFORMATION

Modulus of elasticity in flexure	~ 3 800 N/mm ² (7 days at +23 °C)			(DIN EN 1465)
Tensile strength	~ 30 N/mm ² (7 days at +23 °C)			(ISO 527)
Modulus of elasticity in tension	~ 4 500 N/mm ² (7 days at +23 °C)			(ISO 527)
Tensile strain at break	0.9 % (7 days at +23 °C)			(ISO 527)
Tensile adhesion strength	Concrete fracture (> 4 N/mm ²) on sandblasted substrate			(EN ISO 4624)
Coefficient of thermal expansion	4.5 × 10 ⁻⁴ 1/K (Temperature range -10 °C – +40 °C)			(EN 1770)
Glass transition temperature	Curing time	Curing temperature	TG	(EN 12614)
	30 days	+30 °C	+58 °C	
Heat deflection temperature	Curing time	Curing temperature	HDT	(ASTM D 648)
	7 days	+10 °C	+36 °C	
	7 days	+23 °C	+47 °C	
	7 days	+35 °C	+53 °C	
	Resistant to continuous exposure up to +45 °C.			
Service temperature	-40 °C to +45 °C			

SYSTEMS

System structure	Substrate primer - Sikadur®-330. Impregnating / laminating resin - Sikadur®-330. Structural strengthening fabric - SikaWrap® type to suit requirements.
------------------	---

APPLICATION INFORMATION

Mixing ratio	Component A : component B = 4 : 1 by weight When using bulk material the exact mixing ratio must be safeguarded by accurately weighing and dosing each component.
Consumption	See the "Method Statement for SikaWrap® manual dry application" Ref 850 41 02. Guide: 0.7 - 1.5 kg/m ²
Ambient air temperature	+10 °C min. / +35 °C max.
Dew point	Beware of condensation. Substrate temperature during application must be at least 3 °C above dew point.
Substrate temperature	+10 °C min. / +35 °C max.

PRODUCT DATA SHEET
Sikadur®-330
December 2015, Version 88.01
0000604001000004

BUILDING TRUST



Substrate moisture content	≤ 4 % pbw		
Pot Life	Temperature	Pot life	Open time
	+10 °C	~90 minutes (5 kg)	~90 minutes
	+23 °C	~60 minutes (5 kg)	~60 minutes
	+35 °C	~30 minutes (5 kg)	~30 minutes

(EN ISO 9514)

The pot life begins when the resin and hardener are mixed. It is shorter at high temperatures and longer at low temperatures. The greater the quantity mixed, the shorter the pot life. To obtain longer workability at high temperatures, the mixed adhesive may be divided into portions. Another method is to chill components A+B before mixing them (not below +5 °C).

BASIS OF PRODUCT DATA

All technical data stated in this Product Data Sheet are based on laboratory tests. Actual measured data may vary due to circumstances beyond our control.

IMPORTANT CONSIDERATIONS

Sikadur®-330 must be protected from rain for at least 24 hours after application. Ensure placement of fabric and laminating with roller takes place within open time. At low temperatures and / or high relative humidity, a tacky residue (blush) may form on the surface of the cured Sikadur®-330 epoxy. If an additional layer of fabric or a coating is to be applied onto the cured epoxy, this residue must first be removed with warm, soapy water to ensure adequate bond. In any case, the surface must be wiped dry prior to application of the next layer or coating. For application in cold or hot conditions, pre-condition material for 24 hours in temperature controlled storage facilities to improve mixing, application and pot life limits. For further information on over coating, number of layers or creep, please consult a structural engineer for calculations and see also the "Method Statement for SikaWrap® manual dry application" Ref 850 41 02. Sikadur® resins are formulated to have low creep under permanent loading. However due to the creep behaviour of all polymer materials under load, the long term structural design load must account for creep. Generally the long term structural design load must be lower than 20-25% of the failure load. Please consult a structural engineer for load calculations for the specific application.

ECOLOGY, HEALTH AND SAFETY

For information and advice on the safe handling, storage and disposal of chemical products, users shall refer to the most recent Safety Data Sheet (SDS) containing physical, ecological, toxicological and other safety-related data.

APPLICATION INSTRUCTIONS

SUBSTRATE QUALITY

Substrate must be sound and of sufficient tensile strength to provide a minimum pull off strength of 1.0 N/mm² or as per the requirements of the design specification. See also the "Method Statement for SikaWrap® manual dry application" Ref 850 41 02.

SUBSTRATE PREPARATION

See the "Method Statement for SikaWrap® manual dry application" Ref 850 41 02.

MIXING

Pre-batched units:
Mix components A+B together for at least 3 minutes with a mixing spindle attached to a slow speed electric drill (max. 300 rpm) until the material becomes smooth in consistency and a uniform grey colour. Avoid aeration while mixing. Then, pour the whole mix into a clean container and stir again for approx. 1 more minute at low speed to keep air entrapment at a minimum. Mix only that quantity which can be used within its pot life.

Bulk packing, not pre-batched:
First, stir each component thoroughly. Add the components in the correct proportions into a suitable mixing pail and stir correctly using an electric low speed mixer as above for pre-batched units.

APPLICATION METHOD / TOOLS

See the "Method Statement for SikaWrap® manual dry application" Ref 850 41 02.

CLEANING OF EQUIPMENT

Clean all equipment immediately with Sika® Colma Cleaner. Cured material can only be removed mechanically.

LOCAL RESTRICTIONS

Please note that as a result of specific local regulations the declared data for this product may vary from country to country. Please consult the local Product Data Sheet for the exact product data.

LEGAL NOTES

The information, and, in particular, the recommendations relating to the application and end-use of Sika products, are given in good faith based on Sika's current knowledge and experience of the products when properly stored, handled and applied under normal conditions in accordance with Sika's recommendations. In practice, the differences in materials, substrates and actual site conditions are such that no warranty in respect of merchantability or of fitness for a particular purpose, nor any liability arising out of any legal relationship whatsoever, can be inferred either from this information, or from any written recommendations, or from any other advice offered. The user of the product must test the product's suitability for the intended application and purpose. Sika reserves the right to change the properties of its products. The proprietary rights of third parties must be observed. All orders are accepted subject to our current terms of sale and delivery. Users must always refer to the most recent issue of the local Product Data Sheet for the product concerned, copies of which will be supplied on request.

Sika Iraq (Sika Trading LLC)
Erbil / Baghdad / Basra
Tel: +96 077 838 75001
info@iq.sika.com
iq.sika.com

PRODUCT DATA SHEET
Sikadur®-118C
December 2025, Version 01.01
000006060100000000

4 / 4

Sikadur-118C-en-G112-2020-5-1.pdf

BUILDING TRUST



References

- [1] M. Elsayed and A. Elsayed, "Behaviour of biaxially loaded RC columns retrofitted by ferrocement jacketing," *International Research Journal of Engineering and Technology (IRJET)*, vol. 5, no. 5, pp. 55-65, 2018.
- [2] V. Kumar, "Strengthening of Axially Loaded Circular Concrete Columns using Stainless Steel Wire Mesh (SSWM)," Institute of Technology, 2017.
- [3] M. F. Belal, H. M. Mohamed, and S. A. Morad, "Behavior of reinforced concrete columns strengthened by steel jacket," *HBRC journal*, vol. 11, no. 2, pp. 201-212, 2015.
- [4] D. A. Suleman, "Strengthening of Corroded Reinforced Concrete Columns using Ultra –high Performance Concrete," Master, Civil Engineering, University of Anbar, Iraq, 2022.
- [5] A. Tarabia and H. Albakry, "Strengthening of RC columns by steel angles and strips," *Alexandria Engineering Journal*, vol. 53, no. 3, pp. 615-626, 2014.
- [6] G. Campione, F. Cannella, L. Cavaleri, M. Ferrotto, and M. Papia, "Assessment of the load carrying capacity of reinforced concrete columns strengthened by steel cages Specificità nella valutazione della capacità portante di colonne in calcestruzzo armato rinforzate con incamiciatura in acciaio," *Proceedings of Italian Concrete Days*, 2018.
- [7] R. Balamuralikrishnan, M. Al Madhani, and R. Al Madhani, "Study on retrofitting of RC column using ferrocement full and strip wrapping," *Civil Engineering Journal*, vol. 5, no. 11, pp. 2472-2485, 2019.
- [8] Ö. Mercimek, R. Ghoroubi, Ö. Anil, C. k. Çakmak, A. l. Özdemir, and Y. m. Kopraman, "Strength, ductility, and energy dissipation capacity of RC column

strengthened with CFRP strip under axial load," *Mechanics Based Design of Structures and Machines*, vol. 51, no. 2, pp. 961-979, 2023.

[9] M. Elsayed, B. A. Tayeh, M. Abou Elmaaty, and Y. Aldahshoory, "Behaviour of RC columns strengthened with Ultra-High Performance Fiber Reinforced concrete (HPFRC) under eccentric loading," *Journal of Building Engineering*, vol. 47, p. 103857, 2022.

[10] A. Gandage, "Admixtures in Concrete—A Review," in *International Conference on Construction Real Estate Infrastructure and Projects*, Pune, 2018.

[11] A. Hassan, S. Jones, and G. Mahmud, "Experimental test methods to determine the uniaxial tensile and compressive behaviour of ultra high performance fibre reinforced concrete (HPFRC)," *Construction and building materials*, vol. 37, pp. 874-882, 2012.

[12] M. B. Eide and J.-M. Hisdal, "Ultra high performance fibre reinforced concrete (HPFRC)—State of the art: FA 2 Competitive constructions: SP 2.2 Ductile high strength concrete," 2012.

[13] M. A. Al-Osta, "Exploitation of Ultrahigh-Performance Fibre-Reinforced Concrete for the Strengthening of Concrete Structural Members," *Advances in civil engineering*, vol. 2018, no. 1, p. 8678124, 2018.

[14] A. R. Lubbers, "Bond performance between ultra-high performance concrete and prestressing strands," Ohio University, 2003.

[15] I. Y. A. Hakeem, "Characterization of an ultra-high performance concrete," King Fahd University of Petroleum and Minerals (Saudi Arabia), 2011.

[16] A. J. Francis, *The cement industry 1796-1914: a history*. Newton Abbot [England]: David & Charles (in English), 1977.

-
-
- [17] B. A. Graybeal, "Material property characterization of ultra-high performance concrete. Publication no," FHWA-HRT-06-103, Federal Highway Administration, US Department of ..., 2006.
- [18] K. G. Babu and P. S. Prakash, "Efficiency of silica fume in concrete," *Cement and concrete research*, vol. 25, no. 6, pp. 1273-1283, 1995.
- [19] P. Rougeau and B. Borys, "Ultra high performance concrete with ultrafine particles other than silica fume," in *Proceedings of the International Symposium on Ultra High Performance Concrete*, 2004, vol. 32, pp. 213-225.
- [20] H. H. Bache, "Densified cement ultra-fine particle-based materials," 1981.
- [21] J. Birchall, A. Howard, and K. Kendall, "Flexural strength and porosity of cements," *Nature*, vol. 289, no. 5796, pp. 388-390, 1981.
- [22] S. Diamond, S. Sahu, and N. Thaulow, "Reaction products of densified silica fume agglomerates in concrete," *Cement and Concrete Research*, vol. 34, no. 9, pp. 1625-1632, 2004/09/01/ 2004.
- [23] R.Subakaran and S. Herath, "GPR and LiDAR Synergy: Honeycomb detection in Concrete Structures," presented at the IESL YOUNG MEMBERS' TECHNICAL CONFERENCE, The Institution of Engineers, Sri Lanka 120/15, Wijerama Mawatha, Colombo 07, 2021, ISBN 978-624-5810-02-4.
- [24] C. Völker and P. Shokouhi, "Multi sensor data fusion approach for automatic honeycomb detection in concrete," *Ndt & e International*, vol. 71, pp. 54-60, 2015.
- [25] N. Baghiee, M. R. Esfahani, and K. Moslem, "Studies on damage and FRP strengthening of reinforced concrete beams by vibration monitoring," *Engineering Structures*, vol. 31, no. 4, pp. 875-893, 2009.

-
-
- [26] V. Dawari and G. Vesmawala, "Modal curvature and modal flexibility methods for honeycomb damage identification in reinforced concrete beams," *Procedia Engineering*, vol. 51, pp. 119-124, 2013.
- [27] Jonbi1, "Repair Methods and Applications to overcome Honeycomb, Cold Joint and Cracks in Concrete," (in English), *International Journal of Technical & Scientific Research Engineering*, vol. 5, no. 5, 2022.
- [28] M. G. Marques, A. Liserre, R. Gomes, and G. N. Guimarães, "Analysis of the behavior of reinforced concrete columns strengthened with sleeve wedge bolts and a self compacting concrete layer," *Revista IBRACON de Estruturas e Materiais*, vol. 8, no. 2, pp. 88-99, 2015.
- [29] P. Cassese, C. Menna, A. Occhiuzzi, and D. Asprone, "Experimental behavior of existing RC columns strengthened with HPFRC jacket under concentric and eccentric compressive load," *Buildings*, vol. 11, no. 11, p. 521, 2021.
- [30] I.-Y. Koo and S.-G. Hong, "Strengthening RC columns with ultra high performance concrete," in *Proceedings of the 2016 Structures Congress (Structures16)*, Jeju Island, Republic of Korea, 2016, vol. 28.
- [31] M. N. Hadi, A. H. Algburi, M. N. Sheikh, and A. T. Carrigan, "Axial and flexural behaviour of circular reinforced concrete columns strengthened with reactive powder concrete jacket and fibre reinforced polymer wrapping," *Construction and Building Materials*, vol. 172, pp. 717-727, 2018.
- [32] A.-A.-S. A. M. Al-Khazragi, "Strengthening Of Uniaxial Reinforced Concrete Columns By Jacketing With (HPFRC) Ultra-High Performance Concrete And Carbon Fiber –Reinforced Polymer (CFRP)," Master, Civil Engineering, Tikrit University, Iraq, 2019.
- [33] A. H. Algburi, M. N. Sheikh, and M. N. Hadi, "New technique for strengthening square-reinforced concrete columns by the circularisation with reactive powder concrete and wrapping with fibre-reinforced polymer," *Structure and Infrastructure Engineering*, vol. 15, no. 10, pp. 1392-1403, 2019.

-
-
- [34] B. A. Tayeh, M. A. Naja, S. Shihada, and M. Arafa, "Repairing and strengthening of damaged RC columns using thin concrete jacketing," *Advances in Civil Engineering*, vol. 2019, no. 1, p. 2987412, 2019.
- [35] K. Heiza, A. Elshafey, and A. Sakr, *Structural Behavior of RC columns retrofitted by High Performance Fiber Reinforced Concrete (HPFRC)*. 2019.
- [36] S. Mashshay and A. Al-Sibahya, "Structural Behavior of Novel ECC Short Columns Subjected to Eccentric Loading. Al-Qadisiyah J," *Eng. Sci*, vol. 13, pp. 31-36, 2020.
- [37] M. A. Sakr, T. M. El Korany, and B. Osama, "Analysis of RC columns strengthened with ultra-high performance fiber reinforced concrete jackets under eccentric loading," *Engineering Structures*, vol. 220, p. 111016, 2020.
- [38] S. A. Dadvar, D. Mostofinejad, and H. Bahmani, "Strengthening of RC columns by ultra-high performance fiber reinforced concrete (HPFRC) jacketing," *Construction and Building Materials*, vol. 235, p. 117485, 2020.
- [39] M. A. Al-Osta, A. M. Sharif, A. M. Suhoothi, and S. K. Najamuddin, "Strengthening of axially and eccentrically compression loaded RC columns with UHPC jacketing system: Experimental investigation and finite element modeling," *Engineering Structures*, vol. 245, p. 112850, 2021.
- [40] R.-P. Chen, Q.-L. Ma, Y. Zhang, H.-N. Wu, Y. Liu, and L. Lu, "Experimental study on the mechanical behaviour of eccentric compression short column strengthened by ultra-high-performance fibre-reinforced concrete," in *Structures*, 2021, vol. 33: Elsevier, pp. 508-522.
- [41] P. Cassese, C. Menna, A. Occhiuzzi, and D. Asprone, "Experimental behavior of existing RC columns strengthened with HPFRC jacket under concentric and eccentric compressive load," *Buildings*, vol. 11, no. 11, p. 521, 2021.
- [42] M. Elsayed, B. A. Tayeh, M. Abou Elmaaty, and Y. Aldahshoory, "Behaviour of RC columns strengthened with Ultra-High Performance Fiber Reinforced

concrete (HPFRC) under eccentric loading," *Journal of Building Engineering*, vol. 47, p. 103857, 2022.

[43] W. Mansour, M. Sakr, A. Seleemah, B. A. Tayeh, and T. Khalifa, "Development of shear capacity equations for RC beams strengthened with HPFRC," *Computers and Concrete*, vol. 27, no. 5, pp. 473-487, 2021.

[44] D.A. Suleman, "Strengthening of Corroded Reinforced Concrete Columns using Ultra –high Performance Concrete," Master, Civil Engineering, University of Anbar, Iraq, 2022.

[45] R. M. R. Susilorini and Y. Kusumawardaningsih, "Advanced study of columns confined by ultra-high-performance concrete and ultra-high-performance fiber-reinforced concrete confinements," *Fibers*, vol. 11, no. 5, p. 44, 2023.

[46] H. Shehab, A. Eisa, A. M. Wahba, P. Sabol, and D. a. Katunský, "Strengthening of reinforced concrete columns using ultra-high performance fiber-reinforced concrete jacket," *Buildings*, vol. 13, no. 8, p. 2036, 2023.

[47] S. F. H. A. Zeyadi, "Repair of Reinforced Concrete Columns with honeycomb defect," Master, Civil Engineering, University of Al- Qadisiyah, Iraq, 2023.

[48] J. Wang, S. Lu, and J. Yang, "Behavior of eccentrically loaded rectangular RC columns wrapped with CFRP jackets under different preloading levels," *Journal of Building Engineering*, vol. 34, p. 101943, 2021.

[49] A. M. Sahi, "EXPERIMENTAL STUDY OF HOLLOW SLENDER REINFORCED CONCRETE COLUMN," Master, Civil Engineering, University of Misan, Iraq, 2021.

[50] Y. Blikharskyy, J. Selejdak, R. Vashkevych, N. Kopiika, and Z. Blikharskyy, "Strengthening RC eccentrically loaded columns by CFRP at different levels of initial load," *Engineering Structures*, vol. 280, p. 115694, 2023.

[51] F. Li, C. Chen, and Z. Xiang, "Study on Axial Compression Performance of Corroded Reinforced Concrete Columns Strengthened by Concrete Canvas and

Carbon Fiber Reinforced Plastic under Secondary Corrosion," *Buildings*, vol. 14, no. 3, p. 803, 2024.

[52] Iraqi Standard Specification, Portland cement, I. Q. S. NO. 5, 2019.

[53] Iraqi Standard Specification for the aggregation of natural resources, I. Q. S. NO.45, 2019.

[54] ASTM International, Standard Specification for Silica Fume Used in Cementitious Mixtures (ASTM C1240 - 20), ASTM International, West Conshohocken, PA, 2020.

[55] ASTM International, Standard Specification for Steel Fibers for Fiber-Reinforced Concrete (ASTM A820/A820M-16), ASTM International, West Conshohocken, PA, 2016.

[56] ASTM International, Standard Specification for Chemical Admixtures for Concrete (ASTM C494/C494M-19), ASTM International, West Conshohocken, PA, 2019.

[57] Central Organization for Standardization and Quality Control, "Iraqi Standard Specification (IQS) No.1703/1992 Water used in concrete", Baghdad, Iraq.

[58] ASTM International, Standard Test Methods and Definitions for Mechanical Testing of Steel Products (ASTM A370-17a), ASTM International, West Conshohocken, PA, 2020.

[59] M. F. Ashby, "The properties of foams and lattices," *Philosophical Transactions of the Royal Society A: Mathematical, Physical and Engineering Sciences*, vol. 364, no. 1838, pp. 15-30, 2006.

[60] C882/C882M-05e1 Standard Test Method for Bond Strength of Epoxy-Resin Systems Used With Concrete By Slant Shear, 2005, 4 pages.

-
-
- [61] M. A. Al-Osta, A. M. Sharif, A. M. Suhoothi, and S. K. Najamuddin, "Strengthening of axially and eccentrically compression loaded RC columns with UHPC jacketing system: Experimental investigation and finite element modeling," *Engineering Structures*, vol. 245, p. 112850, 2021.
- [62] R.-P. Chen, Q.-L. Ma, Y. Zhang, H.-N. Wu, Y. Liu, and L. Lu, "Experimental study on the mechanical behaviour of eccentric compression short column strengthened by ultra-high-performance fibre-reinforced concrete," in *Structures*, 2021, vol. 33: Elsevier, pp. 508-522.
- [63] T. Paulay and R. Park, *Reinforced concrete structures*. John Wiley and Sons, 1975.
- [64] T. Sullivan, G. Calvi, and M. Priestley, "Initial stiffness versus secant stiffness in displacement based design," in *13th World Conference of Earthquake Engineering (WCEE)*, 2004, vol. 65, no. 2888, pp. 581-626.
- [65] V. Kumar, M. A. Iqbal, and A. Mittal, "Energy absorption capacity of prestressed and reinforced concrete slabs subjected to multiple impacts," *Procedia Structural Integrity*, vol. 6, pp. 11-18, 2017.

الخلاصة

نتيجة الحاجة الى تدعيم وترميم المنشآت الخرسانية أدى ذلك الى ظهور العديد من أساليب وتقنيات ومواد التدعيم المختلفة مثل التدعيم والترميم بعمل قميص خرساني او معدني او التدعيم بالفيروسمنت او شرائح البوليمر المقواة بألياف الكربون.

في خلال السنوات القليلة الماضية تم استحداث طريقة لتدعيم العناصر الخرسانية باستخدام الخرسانة عالية الأداء حيث يعد هذا النوع من الخرسانة من الابتكارات الحديثة المستخدمة في العناصر الخرسانية. تمتاز هذه الخرسانة بان لها خصائص عالية في مقاومة اجتهادات الضغط والشد والانحناء بالإضافة الى تحسين المتانة والديمومة للعناصر المدعمة. وقد أجريت الكثير من الدراسات على استخدام هذه التقنية في تدعيم المنشآت الخرسانية المسلحة وكذلك دراسة خصائصها الميكانيكية.

يهدف هذا البحث الى تقديم دراسة عملية للتحقق من فعالية وجدوى استخدام الخرسانة عالية الأداء والمقواة بالألياف في تقوية الأعمدة الخرسانية المسلحة المربعة تحت تأثير الأحمال اللامركزية. وخاصة عندما يكون هناك تلف على شكل خلايا النحل في نهايات جسم العمود. ولهذا الغرض، تضمن البرنامج العملي صب ثلاثون عموداً من الخرسانة الاعتيادية مقسمة الى سبعة مجاميع وذلك حسب نسبة الفشل في العمود. حيث كانت مساحة المقطع العرضي للعينات قبل التدعيم (120 × 120) ملم بإجمالي ارتفاع 950 ملم، لكل عمود رأسان مدعمان في النهايات لغرض تسليط الأحمال اللامركزية أثناء الفحص. الغطاء الخرساني بسمك 15 ملم لجميع جوانب العمود. تم تسليح جميع الأعمدة بصورة متمثلة بالنسبة للحديد الطولي والعرضي لغرض تطبيق هذا البرنامج العملي. متغيرات الدراسة في هذا البحث هي اللامركزية (50 أو 100) ملم، وسمك غلاف التقوية (15 أو 30) ملم، وجانب التقوية (جهتين أو أربع جهات)، ونسبة الفشل في العمود عند الاطراف (35% أو 70%) من مساحة المقطع العرضي، وقد تم أخذ كل هذه العوامل في الاعتبار. في هذه الدراسة البحثية، تم تكوين الفشل في عينة العمود كنسبة من مساحة المقطع العرضي (35% أو 70%) بطول ثابت (4 / Le) ، متمثلة باستخدام شرائح من الفلين بسمك 30 ملم والخرسانة ضعيفة المقاومة، حيث تم تقسيم قطع الفلين بأداة حادة وفقاً للأبعاد المطلوبة لتمثيل نسبة الفشل. تمت دراسة تأثيرات هذه المتغيرات على قدرة تحمل العمود، والازاحة الجانبية والعمودية، والمطيلية، والجساءة، وامتصاص الطاقة للأعمدة.

أشارت نتائج البحث إلى أن خرسانة عالية الاداء هي طريقة تقوية موثوقة لتعزيز قوة وصلابة وقابلية السحب ومتانة الأعمدة الخرسانية المسلحة المعرضة لأحمال لامركزي. ترتبط الزيادة في سعة الحمل المحوري والصلابة بشكل مباشر بسمك غلاف خرسانة عالية الاداء وترتبط عكسيًا بنسبة اللامركزية للأحمال. على وجه التحديد، أثبتت طريقة التقوية من كل الجهات الأربعة بواسطة خرسانة فائقة الاداء أنها أكثر فعالية من طريقة التقوية من جهتين فقط كما هو مفصل في الفصل الرابع.



جمهورية العراق
وزارة التعليم العالي والبحث العلمي
كلية الهندسة/ جامعة ميسان
قسم الهندسة المدنية

سلوك الأعمدة الخرسانية المسلحة والمدعمة بواسطة خرسانة عالية الأداء تحت تأثير أحمال لا مركزية

اعداد الطالب

حيدر لطيف ناجي

بكالوريوس هندسة مدني 2016

رسالة

مقدمة الى كلية الهندسة في جامعة ميسان

كجزء من متطلبات الحصول على درجة الماجستير في علوم الهندسة المدنية / الانشاءات

2025